AD

USAAVLABS TECHNICAL REPORT 69-32

APPLICABILITY OF THE SOUTHWELL PLOT TO THE INTERPRETATION OF TEST DATA OBTAINED FROM STABILITY STUDIES OF ELASTIC COLUMN AND PLATE STRUCTURES

By

W. H. Horton
F. L. Cundari
R. W. Johnson

November 1971

EUSTIS DIRECTORATE
U. S. ARMY AIR MOBILITY RESEARCH AND DEVELOPMENT LABORATORY
FORT EUSTIS, VIRGINIA

CONTRACT DA 44-177-AMC-258(T)

STANFORD UNIVERSITY
STANFORD, CALIFORNIA

Approved for public release;
distribution unlimited.

DISCLAIMERS

The findings in this report are not to be construed as an official Department of the Army position unless so designated by other authorized documents.

When Government drawings, specifications, or other data are used for any purpose other than in connection with a definitely related Government procurement operation, the United States Government thereby incurs no responsibility nor any obligation whatsoever; and the fact that the Government may have formulated, furnished, or in any way supplied the said drawings, specifications, or other data is not to be regarded by implication or otherwise as in any manner licensing the holder or any other person or corporation, or conveying any rights or permission, to manufacture, use, or sell any patented invention that may in any way be related thereto.

Trade names cited in this report do not constitute an official endorsement or approval of the use of such commercial hardware or software.

DISPOSITION INSTRUCTIONS

Destroy this report when no longer needed. Do not reutrn it to the originator.

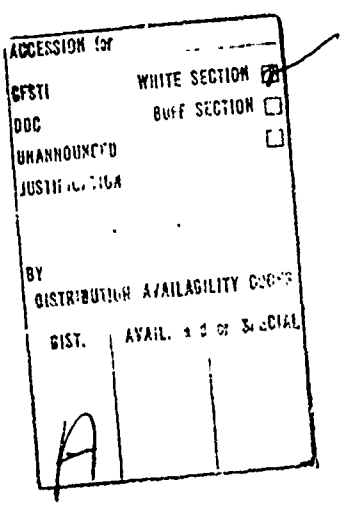

Unclassified

Security Classification

DOCUMENT CONTROL DATA - R & D

(Security classification of title, body of abstract and indexing annotation must be entered when the overall report is classified)

1. ORIGINATING ACTIVITY (Corporate author)	2a. REPORT SECURITY CLASSIFICATION
Stanford University Stanford, California	Unclassified
	2b. GROUP

3. REPORT TITLE

A REVIEW OF THE APPLICABILITY OF THE "SOUTHWELL" PLOT TO THE INTERPRETATION OF TEST DATA OBTAINED FROM STABILITY STUDIES OF ELASTIC COLUMN AND PLATE STRUCTURES

4. DESCRIPTIVE NOTES (Type of report and inclusive dates)

5. AUTHOR(S) (First name, middle initial, last name)

Horton, W. H.
Cundari, F. L.
Johnson, R. W.

6. REPORT DATE	7a. TOTAL NO. OF PAGES	7b. NO. OF REFS
November 1971	128	47

8a. CONTRACT OR GRANT NO	9a. ORIGINATOR'S REPORT NUMBER(S)
DA 44-177-AMC-258(T) b. PROJECT NO. Task 1F162204A17001 c. d.	USAAVLABS Technical Report 69-32 9b. OTHER REPORT NO(S) (Any other numbers that may be assigned this report) SUDAAR No. 296

10. DISTRIBUTION STATEMENT

Approved for public release; distribution unlimited.

11. SUPPLEMENTARY NOTES	12. SPONSORING MILITARY ACTIVITY
Supersedes AD-660584	Eustis Directorate, U.S. Army Air Mobility Research and Development Laboratory Fort Lustis, Virginia

13. ABSTRACT

Thomas Young derived in 1807 a formula which associated the applied load, the Euler critical load, the initial bow, and the elastic deformation under load for a column. Westergaard in 1922 used the Lagrangian law to derive Young's expression in a much wider context, and in so doing demonstrated its general validity in all linear instability problems. This relationship has great significance in the correlation of experimental data with linear theory. This was realized first by Ayrton and Perry in 1887. In 1932 Southwell independently redeveloped the technique and used it to discuss the classic column tests of von Kármán.

This report coordinates and extends the research made in this field during the last century and a half. It demonstrates the power and versatility of the method of expressing the given hyperbolic equation in a linear form - by change of variables - and determining the classic critical load as the slope of this line. The results show that there can be no doubt as to the applicability of the method to all linear instability problems of columns and plates. Thus, the report challenges the statements of previous researchers who have been hampered in their work by the lack of valid experiments, arising from the coarseness of measurement techniques.

DD FORM 1 NOV 68 1473

Unclassified

Security Classification

14. KEY WORDS	LINK A		LINK B		LINK C	
	ROLE	WY	ROLE	WT	ROLE	WT
Southwell Plot Stability Studies Elastic Column Plate Structures Hyperbolic Equation in a Linear Form by Change of Variables Correlation of experimental Data With Linear Theory						

DEPARTMENT OF THE ARMY
U. S. ARMY AIR MOBILITY RESEARCH & DEVELOPMENT LABORATORY
EUSTIS DIRECTORATE
FORT EUSTIS, VIRGINIA 23604

ERRATA

USAAVLABS Technical Report 69-32
TITLE: Applicability of the Southwell Plot to the Interpretation of Test Data Obtained From Stability Studies of Elastic Column and Plate Structures

Make the following change to the title on the cover:

Change the word Studied to Studies

DEPARTMENT OF THE ARMY
U. S. ARMY AIR MOBILITY RESEARCH & DEVELOPMENT LABORATORY
EUSTIS DIRECTORATE
FORT EUSTIS, VIRGINIA 23604

This program was carried out under Contract DA 44-177-AMC-258(T) with Stanford University.

The data contained in this report are the result of research conducted to apply the Southwell Plot in the interpretation of test data obtained from stability studies of elastic column and plate structures. The Southwell method was applied to test data obtained from the literature, as well as from experiments, and was found to be applicable to instability problems of plates.

The report has been reviewed by this Directorate and is considered to be technically sound. It is published for the exchange of information and the stimulation of future research.

This program was conducted under the technical management of Mr. James P. Waller, Structures Division.

Task 1F162204A17001
Contract DA 44-177-AMC-258(T)
USAAVLABS Technical Report 69-32
November 1971

APPLICABILITY OF THE SOUTHWELL PLOT TO THE INTERPRETATION OF TEST DATA OBTAINED FROM STABILITY STUDIES OF ELASTIC COLUMN AND PLATE STRUCTURES

SUDAAR 296

by

W. H. Horton
F. L. Cundari
R. W. Johnson

Prepared by

Stanford University
Department of Aeronautics and Astronautics
Stanford, California

for

EUSTIS DIRECTORATE
U.S. ARMY AIR MOBILITY RESEARCH AND DEVELOPMENT LABORATORY
FORT EUSTIS, VIRGINIA

SUMMARY

Thomas Young, medical doctor, philosopher, and Professor of Mechanical Arts at the University of Cambridge, derived in 1807 a very simple but powerful formula which associated the applied load, the Euler critical load, the initial bow, and the elastic deformation under load for a column. His hyperbolic law is in essence $w_e = (w_0 P_E/(P - P_E))$. Westergaard in 1922 used the Lagrangian law to derive this expression in a much wider context, and in so doing demonstrated its general validity in all linear instability problems.

This relationship has great significance in the correlation of experimental data with linear theory. This was realized first by Ayrton and Perry, who in 1887 published a paper on struts in which they gave a graphical interpretation of the fundamental equation, and by so doing were able to verify that the Euler load was correct for a perfect column.

Their important work was virtually ignored. However, in 1932 Southwell independently redeveloped the technique and used it to discuss the classic column tests of von Kármán. In his report, Southwell stated without proof the axiom which was so clear in Westergaard's analysis; viz, that the process should have wider use.

This report reviews these several contributions to our knowledge together with the numerous papers which have followed them. A wide range of problems is illustrated both experimentally and analytically. In those cases for which the appropriate theory or the valid experiment exists, the current results have been presented; but where gaps in reported information exist, the necessary analysis or tests were conducted and presented herein.

It is significant to record that the work covers not only normal load environments but also instabilities under thermal conditions.

Thus, we may state that the report coordinates and extends the research of some twenty engineers made in a century and a half. It demonstrates the power and versatility of the method of expressing the given hyperbolic equation in a linear form - by change of variables - and of determining the classic critical load as the slope of this line. The results obtained show that there can be no doubt as to the applicability of the method to all linear instability problems of plates. Thus, the report corrects the statement of previous researchers who have been hampered in their work by the lack of valid experiments, arising from the coarseness of measurement techniques. There is clear indication that continued study will open the door to a clearer understanding of the perplexing questions which arise in compressive elements in which curvature is present.

FOREWORD

The research reported herein was carried out under the sponsorship of the United States Air Force under Contract AF 49(638)1495 and the United States Army Aviation Materiel Laboratories under Contract DA 44-177-AMC-258(T) (Task 1F162204A17001). Their encouragement and support are gratefully acknowledged. The authors would like to thank Mr. Lawrence Wang for preparation of the figures and Mr. Bruce Willey for performing the buckling tests on the Fiberglas panels.

TABLE OF CONTENTS

LIST OF ILLUSTRATIONS

LIST OF ILLUSTRATIONS(Cont'd)

LIST OF ILLUSTRATIONS(Cont'd)

LIST OF ILLUSTRATIONS(Cont'd.)

LIST OF TABLES

LIST OF SYMBOLS

A_{mn}	general amplitude in elastic lateral deflection function for plate
a	length of side of plate
a_1	a constant equal to initial eccentricity
B_{mn}	general amplitude in initial deflection function for plate
b	length of side of plate
D	flexural stiffness $Et^3/12(1-\mu^2)$
d	displacement
E	Young's modulus
G	shear modulus = $E/2(1+\mu)$
H	sum of the normal forces
I	second moment of x-section about appropriate axis
J	polar second moment
K	A constant defining initial imperfection shape for thermally buckled plate
L	length
m	a number, 1, 2, 3, etc.
N_x	load per unit length in direction x
$N_{x_{cr}}$	critical value of N
N_y	load per unit length in direction y
N_{xy}	shear force per unit length
n	a number, 1, 2, 3, etc.
P	actual load: P_{cr} = critical instability load
P_n	n^{th} critical load
P_i	an initial value of load
q	normal force per unit area on plate
q_o	an equivalent value of q

LIST OF SYMBOLS (Cont'd)

r	radius or radial coordinate
R	applied side load to strut
t	thickness or t = time in seconds
T	temperature
T_{crit}	critical value of temperature
U	airy stress function for circular plate
v	ratio of δ/P.
w	assumed buckle shape
w'	initial deformation
W	a general displacement amplitude
W'	an initial value of W
W_o	an initial value of W
W_n	displacement amplitude of the n^{th} harmonic
$W_{n'}$	an initial value of W_n
x	a displacement along member
x, y	coordinate directions
α, β	amplitude coefficients in displacement
β_f	foundation constant for beam on elastic foundation
β_1	the effective initial angle of rotation (deep beam).
γ	a constant = $3(1-\mu^2)/8t^2$
δ	displacement at a reference station = $\sum_{n=1}^{\infty} (W_n - W_{n'})$
δ_i	an initial value of δ
ϵ	strain
ϵ_T	thermal strain

LIST OF SYMBOLS (Cont'd)

μ	Poisson's ratio
ϕ	angle of rotation - deep beam
σ_r	membrane stress in radial direction
σ_{cr}	critical compressive stress
π	constant

The subject of elastic stability is more than 200 years old. From the scientific point of view it began, in 1744, when Leonard Euler[1] made the now classic analysis of the behavior of an initially straight, perfectly elastic, centrally compressed strut. Despite his analytical achievement, there is little doubt that in the century which followed, practicing engineers still had to rely upon experience and empiricism born in experimentation.

There is no doubt, however, that researchers who were active in the field studied Euler's work very thoroughly. Indeed, Hodgkinson,[2] a foremost experimentalist, remarked in 1842 with reference to Euler:[3]

> "It appeared from the researches of this great analyst, that a pillar of any given dimensions and description of material required a certain weight to bend it, even in the slightest degree; and with less than this weight it would not be bent at all. Lagrange, in an elaborate essay in the same work, arrives at the same conclusion. The theory as deduced from this conclusion is very beautiful, and Poisson's exposition of it, in his Mecanique, 2nd edition, vol i,[4] will well repay the labour of a perusal.
>
> I have many times sought, experimentally, with great care for the weight producing incipient flexure, according to the theory of Euler; but have hitherto been unsuccessful. So far as I can see, flexure commences with weights far below those with which pillars are usually loaded in practice. It seems to be produced by weights much smaller than are sufficient to render it capable of being measured."

At the time that Hodgkinson made this remark a large quantity of experimental data was being obtained by many workers. These experimental data were, however, at variance with the predictions of Euler, and analysts thus came to regard his theory as incomplete. Now analysis according to the classic theory indicates that struts of the type already described will remain straight until a certain critical load level is reached; then the struts may suddenly bend into the form of a single bow, a shape which will be maintained with increasing load although the amplitude of the deformation will increase.

In reality, however, struts tested under axial compression have lateral deformation from the very onset of loading. It is found in practice that the load deformation curves for such bodies have the characteristic shapes given in Figure 1. When they are long, the curve tends to become asymptotic to the Euler curve, but when they are short, it does not do so. The curve for short struts is characterized by maximum values of load, as is clearly seen in the figure. It is not difficult, therefore, to arrive at the point of view that agreement between the critical load determined by Euler considerations and the buckling load as determined by experiment is a chance occurrence to be expected only in the case of very long struts. Thus, one

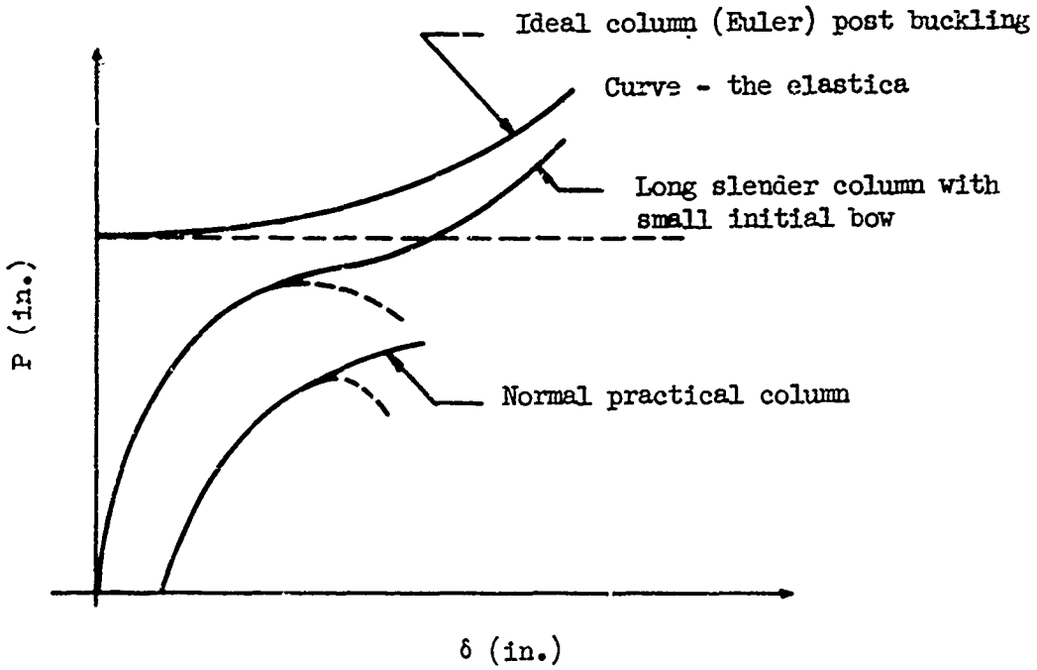

Figure 1. Behavior of Columns in Compression.

is forced to ask the question: When experimental observations give curves of the type presented in Figure 1 and the critical load is never attained, can any valid comparison of theory and experiment be made?

The first researchers to provide a substantial answer to this question were Ayrton and Perry.[5] In 1886 these two investigators published an instructive paper on struts. It is interesting to note that when they performed this work, the situation with regard to knowledge on this fundamental question was such that they commented: "We think we are right in saying that no subject connected with the strength of structures is at present regarded as being in a more vague and unscientific state than the subject of which we have undertaken the study".

As a result of their study, Ayrton and Perry[5] were among the first to realize that for a complete theory it was essential to introduce imperfections of form and loading. Their own words express this particular point and their manner of dealing with it: "The conclusion at which we have arrived is, then, that any want of axiality in placing the load, or want of straightness in the unloaded strut, or want of homogeneity in the material may be allowed for by a term C such that it may be taken as the initial deflection of a homogeneous, carefully loaded strut, and then,

$$y_1 = \frac{C}{1 - \frac{4L^2P}{EI\pi^2}} \tag{1}$$

where

y_1 = the ordinate of the strut center line in the displaced configuration

E = Young's modulus

I = second moment of cross-sectional area

L = pin center length

P = axial load."

From this expression, they deduced that the measured deflection of the midpoint from its initial value was given by

$$\delta = \frac{C \cdot P}{P_1 - P} \tag{2}$$

where P was the end load and P_1 was Euler load.

Equation (2) can be written as

$$\frac{1}{\delta} = \frac{P_1}{CP} - \frac{1}{C} = \frac{1}{C}\left[\frac{P_1}{P} - 1\right] \qquad (3)$$

If we choose new variables,

$$x = \frac{1}{\delta} \text{ and } y = \frac{1}{P}$$

then we see that equation (3) is a linear equation in these variables. Thus a plot of

$$\frac{1}{\delta} \text{ and } \frac{1}{P} \text{ is a straight line whose slope is } \frac{C}{P_1}.$$

This analytical deduction was verified from tests on Dantzic Oak and wrought iron. The appropriate data are given in Figures 2 to 5. The plots of

$$\frac{1}{\delta} \text{ and } \frac{1}{P}$$

are seen to be straight lines. Ayrton and Perry's result of equation (2) can also be expressed as

$$P_1 \frac{\delta}{P} - \delta = C = \text{effective initial deflection} \qquad (4)$$

Thus, we may choose a new variable x, such that

$$\frac{\delta}{P} = x$$

Hence, equation (4) may be written as

$$P_1 x - \delta = C = \text{constant} \qquad (5)$$

This is a linear equation in x and δ. The inverse of the slope of the line is clearly the Euler critical load, and the intercept with the δ axis is the effective initial deflection. This is shown in Figures 6 and 7.

It is strange that this equation, which gives a very elegant method of correlating theory and practice, was virtually ignored. Indeed, almost half a century passed before the method was used to any extent. Then it was independently rediscovered and presented in the second form by R. V. Southwell,[6] who published his work in the Proceedings of the Royal Society. Today the method of presentation is always referred to as a Southwell plot. Since it is this latter work to which all reference is made, the theoretical justification for the formula given in equation (2) will be derived in the Southwell manner.

Consider the strut shown in Figure 8. Let y_o denote the initial deflection,

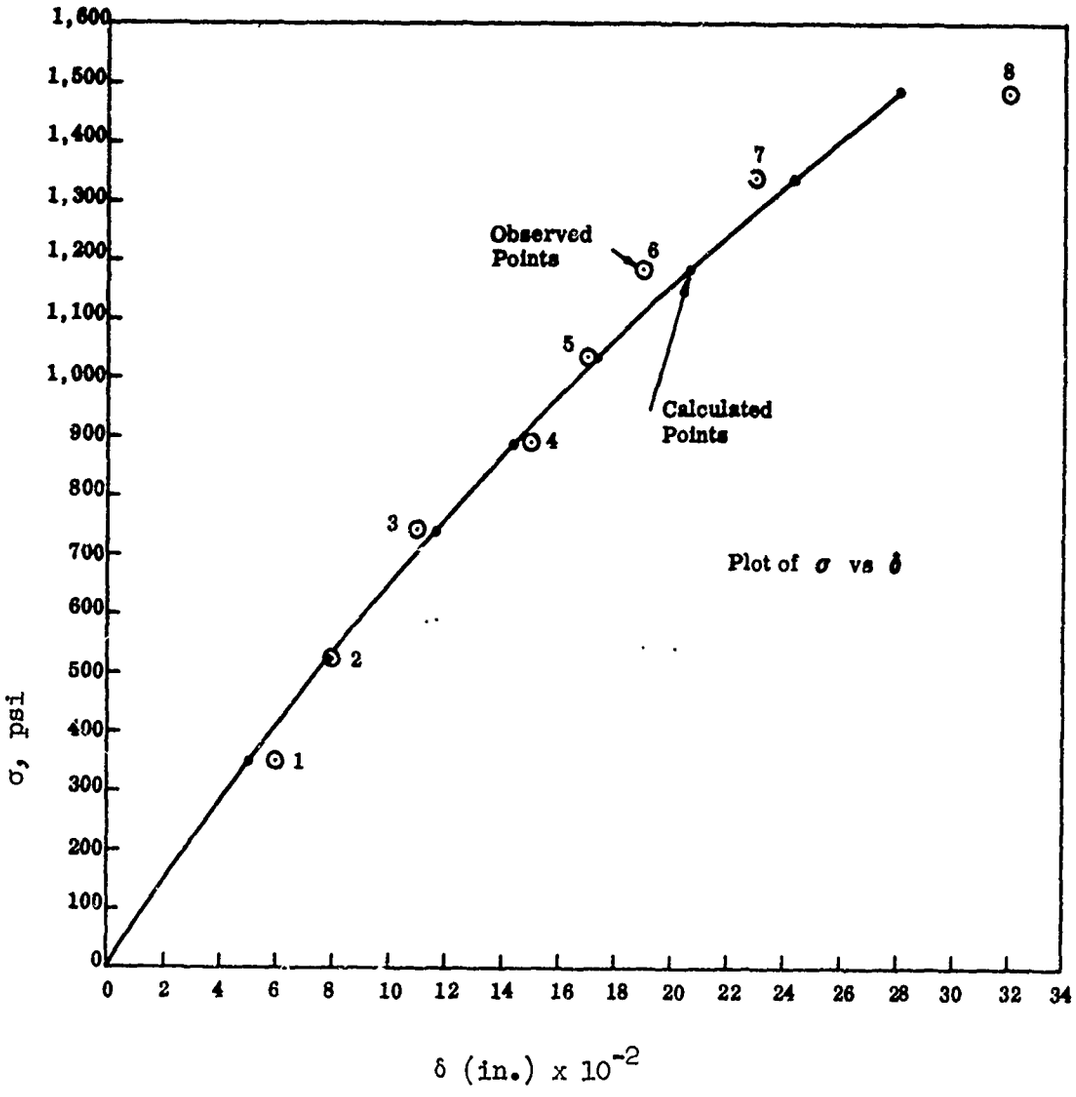

Figure 2. Stress Deflection Curve. Theoretical Calculations of Ayrton and Perry[5] Compared to Hodgkinson's Data on Dantzic Oak Strut.

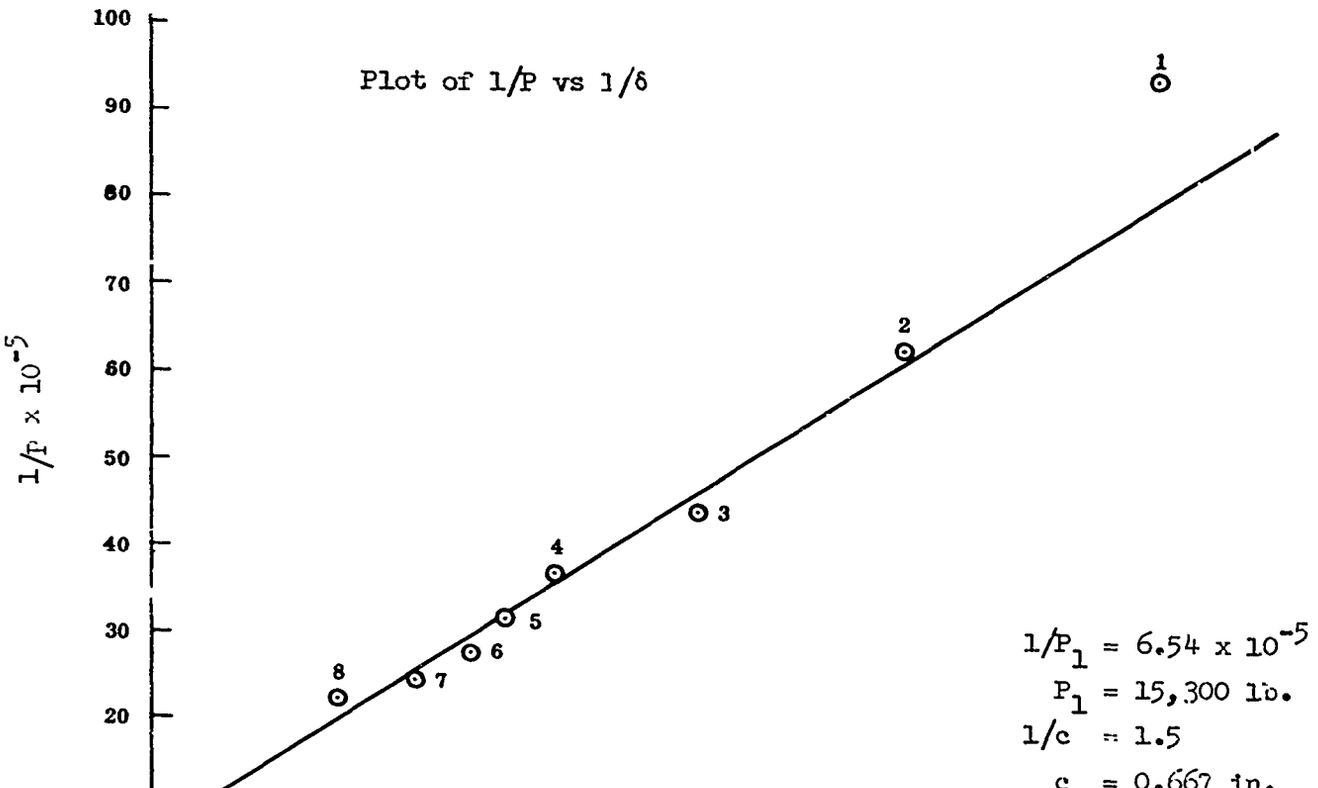

Figure 3. Hodgkinson's Data[2] on Dantzie Oak Strut Plotted in Ayrton and Perry Form.

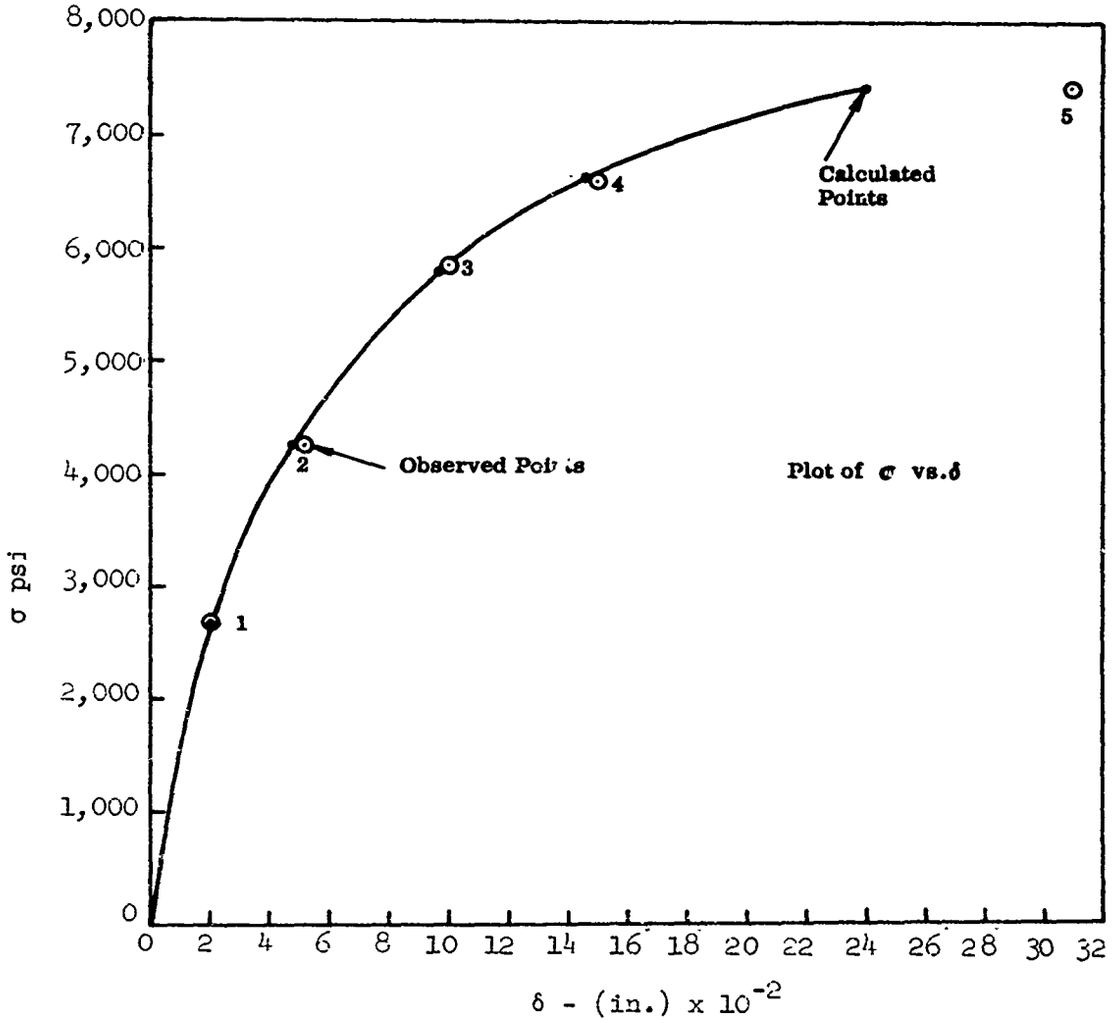

Figure 4. Stress Deflection Curve. Theoretical Calculations of Ayrton and Perry[5] on Wrought Iron Strut.

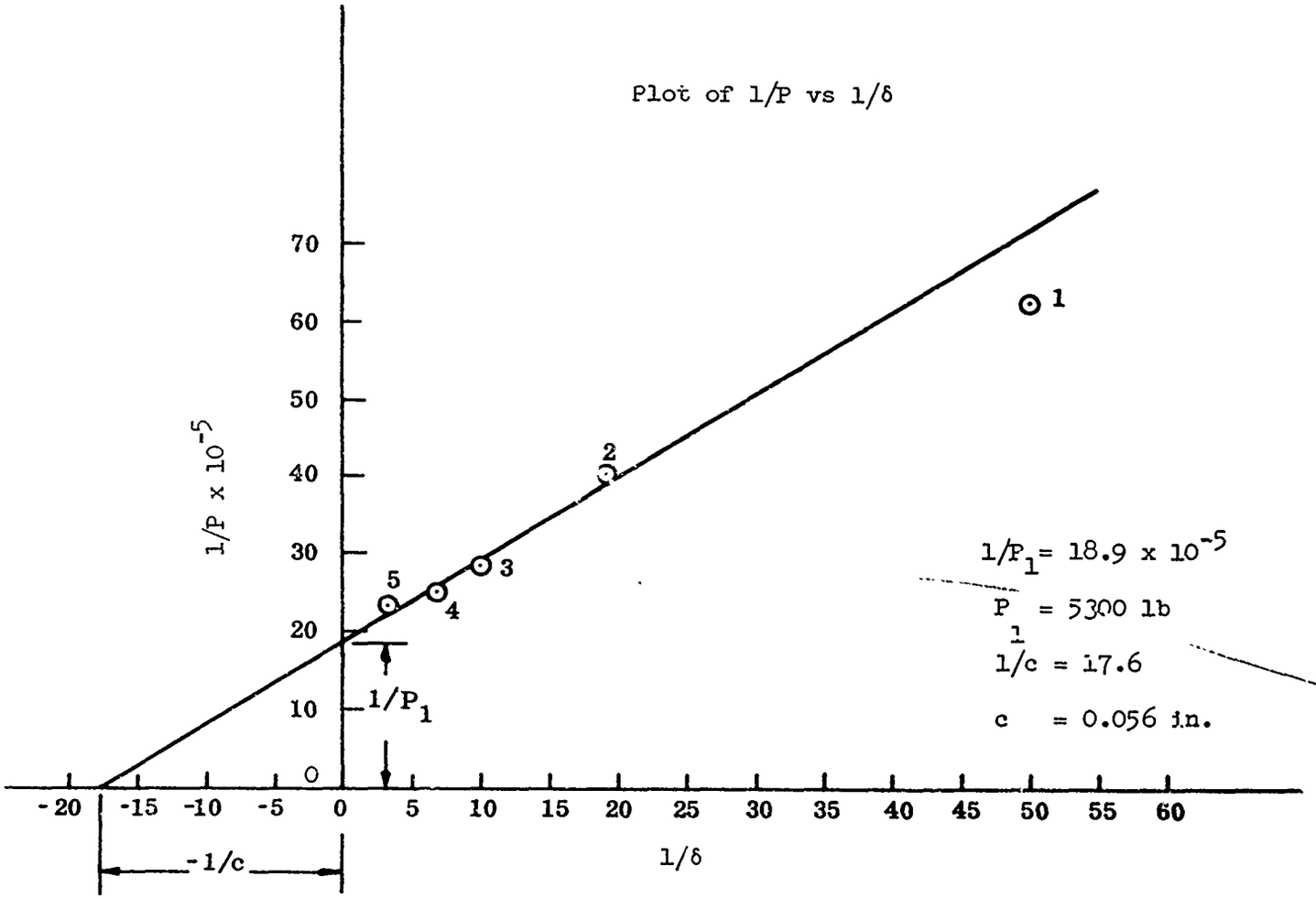

Figure 5. Hodgkinson's Data[2] on Wrought Iron Strut Plotted in Ayrton and Perry Form.

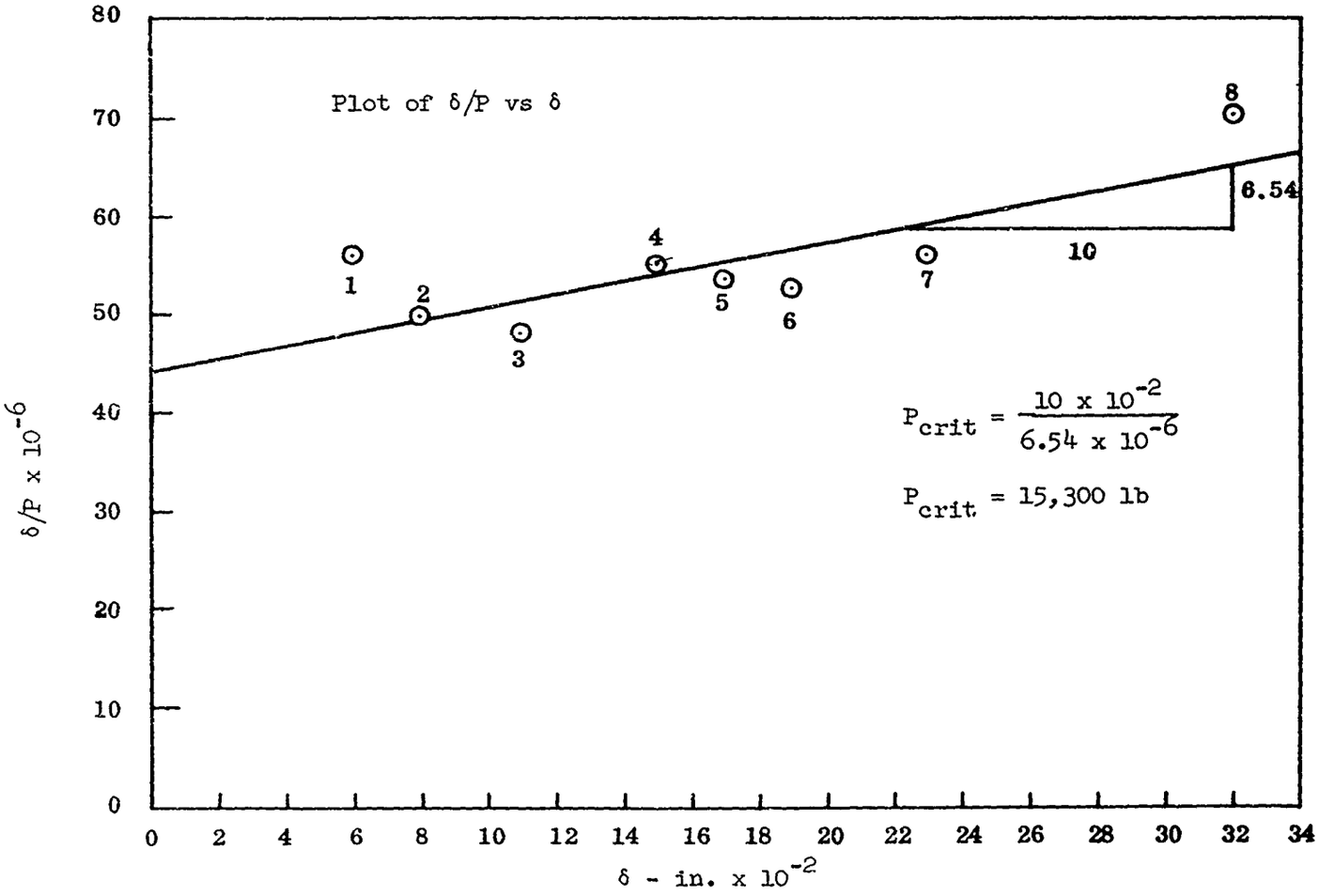

Figure 6. Hodgkinson's Data[2] on Dantzic Oak Strut Plotted in Southwell Form.

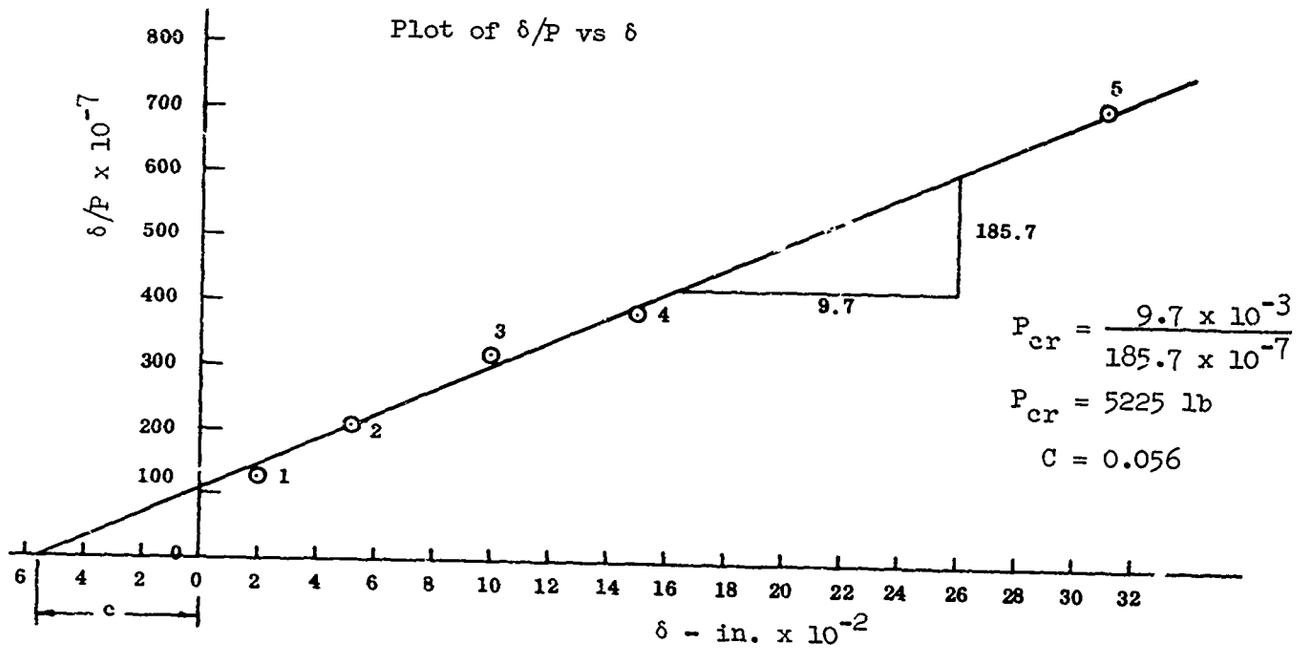

Figure 7. Hodgkinson's Data[2] on Wrought Iron Strut Plotted in Southwell Form.

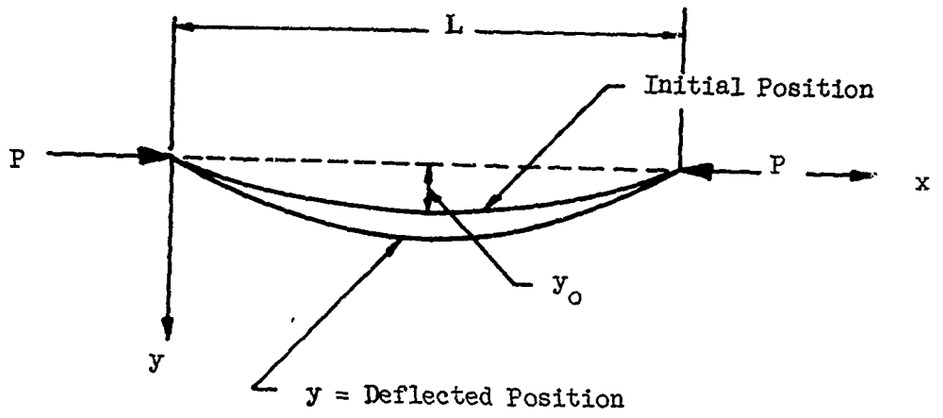

$$y_o = f(x) = \sum_{n=1}^{\infty} C_n \sin \frac{n\pi x}{L}$$

$$y = f(x) = \sum_{n=1}^{\infty} \bar{C}_n \sin \frac{n\pi x}{L}$$

Figure 8. Strut Considered by Southwell.

and let y denote the final deflection of the central line from the line of thrust. Let P be the axial load and let EI be the flexural rigidity of the body. Then the condition of equilibrium of the bent body is

$$EI(y'' - y''_o) + Py = 0 \tag{6}$$

which may be written as

$$y'' + \alpha^2 y = y''_o \tag{7}$$

Now the quantities y and y_o are both regarded as functions of x. Thus, the form of one is dependent on the other. If y_o vanishes at either end of the strut, then a general sclution of equation (7) can be obtained if y and y_o are represented by the following Fourier series:

$$y = \sum_{n=1}^{\infty} \left[C_n \sin \frac{n\pi x}{L} \right] \tag{8}$$

$$y_o = \sum_{n=1}^{\infty} \left[\overline{C}_n \sin \frac{n\pi x}{L} \right] \tag{9}$$

We find, then, that

$$C_n = \frac{\overline{C}_n}{\left(1 - \frac{\alpha^2 L^2}{n^2 \pi^2}\right)} \tag{10}$$

Thus, if P_n is the n^{th} critical load given by the Euler conditions,

$$\frac{C_n}{\overline{C}_n} = \frac{1}{1 - \frac{P}{P_n}} \tag{11}$$

Now the increase in deflection at the center of the strut (elastic deflection) is

$$d = C_1 - \overline{C}_1 - C_3 + \overline{C}_3 + \text{etc.} \tag{12}$$

and if P is a fairly considerable portion of P_1, this may be written as

$$d \doteq \frac{\bar{C}_1}{1 - \frac{P}{P_1}} - \bar{C}_1 \qquad (13)$$

Equation (13) can be rewritten as

$$d\left(\frac{P_1}{P} - 1\right) = \text{Constant} \qquad (14)$$

This equation is, of course, identical with that of Ayrton and Perry and is in fact that of a rectangular hyperbola. However, whereas Ayrton and Perry displayed it in a linear form by plotting the reciprocals of the load and the displacement, Southwell chose to plot the ratio of the displacement to the load against the displacement. There is a third way in which this equation can be expressed in a linear manner. In this alternative, the load is plotted against the ratio of the load to the displacement. This latter form was given by Donnell in his paper on the Southwell method.[7]

The differences among the Ayrton and Perry, the Southwell, and the Donnell representations are clearly shown in Figure 9.

Just as his predecessors had chosen the most accepted test data of their day to try out their approach, so did Southwell pick the well acclaimed data of von Kármán[8] (Table I).

The results are shown in Figure 10. In all cases the straight lines are good. An analysis of the critical load, as derived from the plot, and of the value given by the theoretical formula is given in Table II. The correlation is excellent.

One condition prescribed in the derivation of the formula was that the y_o should be zero at both ends of the strut. Thus, since this case is likely to be rare, it is of clear interest to know whether or not in practice the method would still work for eccentric loadings. R. V. Southwell[6] studied the problem and confirmed that small eccentricities of loading point could be accommodated. The experimental data which he used for this purpose were obtained by Robertson.

After the publication of the Southwell[6] paper, Lundquist[9] reexamined the question and generalized the result.

The formula which he developed is as follows:

$$\frac{y - y_1}{P - P_1} = \frac{y - y_1}{P_{crit} - P_1} + \frac{a_1 \sin \frac{\pi x}{L}}{P_{crit} - P_1} \qquad (15)$$

δ = elastic deflection
P = applied load
P_1 = Euler load
c = constant

δ is related, to a first approximation, to the load (P) which produces it and the Euler load (P_1) by the expression

$$\delta = \frac{cP}{P_1 - P}$$

Three possible arrangements of this form are:

Ayrton and Perry

formula $1/\delta = \left[\frac{P_1}{P} - 1\right]\frac{1}{c}$

variables $1/\delta$ and $1/P$

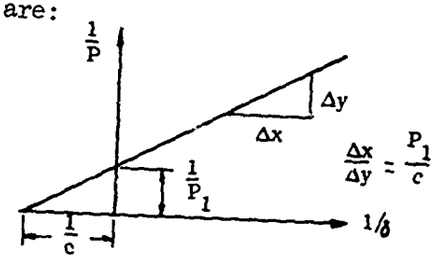

Southwell

formula $\delta\left[\frac{P_1}{P} - 1\right] = c$

variables δ/P and δ

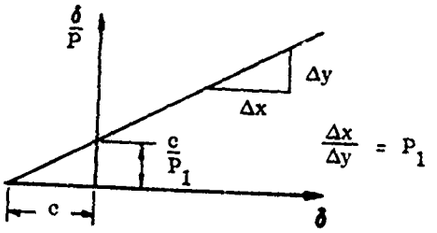

Donnell

formula $P_1 - P = c\frac{P}{\delta}$

variables P and P/δ

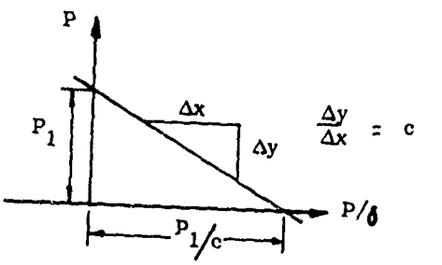

Figure 9. Linear Graphical Relationships for Columns.

TABLE I. T. VON KARMAN'S STRUTS (Ref. 8), Nos. 1, 2, 3a, 3b, 4a, 4b, 5, and 6. (MILD STEEL: E = 2, 170,000 kg/cm^2)

P = End Load in Kilograms	X = Measured Deflection in Millimeters	V = $x/P \times 10^6$
Strut No. 1---		
2260	0.01	4.43
3020	0.025	8.28
3170	0.04	12.62
3320	0.06	18.07
3470	0.09	25.94
3620	0.25	69.06
Strut No. 2---		
4520	0.02	4.43
4830	0.05	10.35
5130	0.11	21.44
5280	0.24	45.46
5430	0.25	158.38
Strut No. 3a---		
6030	0.01	1.66
7540	0.03	3.98
8290	0.11	13.27
8520	0.52	61.03
Strut No. 3b---		
*7840	0.02	2.55
8140	0.05	6.14
8290	0.07	8.44
8445	0.11	13.03
8600	0.21	24.42
Strut No. 4a---		
*9050	0.02	2.21
*9660	0.025	2.59
10260	0.03	2.92
10560	0.07	6.63
10710	0.10	9.34
10860	0.13	11.97
11010	0.25	22.71
11160	0.73	65.41
Strut No. 4b---		
*3020	0.03	9.93
*4530	0.05	11.04
*6030	0.07	11.51
*7540	0.09	11.94
*8300	0.12	14.46
9050	0.15	16.58
9805	0.23	23.46
9960	0.26	26.10
10110	0.29	28.68
10260	0.33	32.16
10410	0.41	39.39

TABLE I - Continued		
10560	0.52	49.24
10710	0.71	66.29
10860	1.46	134.44
Strut No. 5---		
*9050	0.01	1.105
*10560	0.03	2.84
10860	0.05	4.67
11160	0.07	6.27
11470	0.10	8.72
11770	0.15	12.74
12070	0.22	18.23
12370	0.30	24.25
12520	0.45	35.94
Strut No. 6---		
*10560	0.01	0.95
*12070	0.04	3.31
12370	0.06	4.85
12670	0.10	7.89
12970	0.15	11.57
13270	0.25	18.84
13430	0.34	25.32
13580	0.74	54.49

* These points were not considered amenable to the linear plot by Southwell[6] because of the lack of accuracy at the lower values of load and deflection

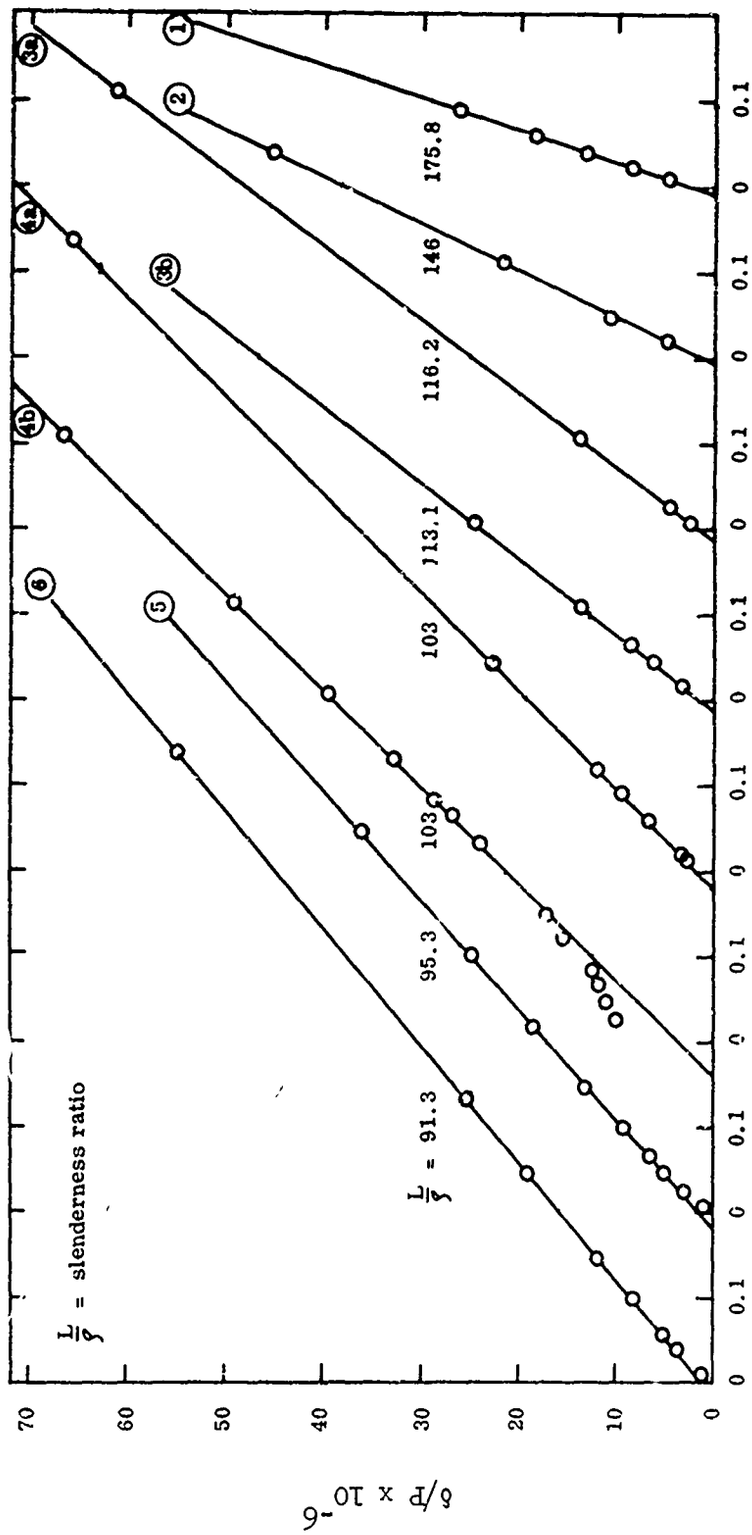

Figure 10. Von Kármán Data on Compressed Columns Plotted in the Linear Form by Southwell[6].

TABLE II. COMPARISON OF THE THEORETICAL CRITICAL LOADS WITH THE SLOPE VALUE FROM THE SOUTHWELL PLOTS (Ref. 6)

(1)	(2)	(3)	(4)	(5)
Strut No.	c deduced from best-fitting line in Figure 9 (mm)	P_1 estimated from slope of best-fitting line in Fig. 9 (kg)	P_1 as given by theoretical formula (kg)	Estimated value (Col. 3) / Theoretical value (Col. 4)
1	0.005	3712	3790	0.980
2	0.005	5453	5475	0.995
3a	0.005	8590	8645	0.994
3b	0.005	8758	8610	1.017
4a	0.003	11220	10980	1.022
4b	0.030	11090	10920	1.015
5	0.010	12815	12780	1.003
6	0.010	13750	13980	0.984

where

P and y = the load and the corresponding midpoint deflection, respectively

P_1 and y_1 = initial values of P and y, respectively

P_{crit} = the first Euler load

$a_1 \sin \frac{\pi x}{L}$ = a constant for a given reference point x.

The straight line obtained by plotting

$$\frac{y - y_1}{P - P_1}$$

as an ordinate against $y - y_1$ as an abscissa cuts the horizontal axis at the distance

$$\left[a_1 \sin \frac{\pi x}{L}\right]$$

from the origin, and the inverse slope of the line is $P_{crit} - P_1$.

With this formula he was able to analyze some of the von Kármán results which were not amenable by the original approach.

This process of analyzing experimental data was extended by Fisher[10,11] to deal with more complex conditions. The case which he considered is depicted in Figure 11. In this diagram the line AA' represents the center line of the beam. Thus, the conditions assumed for the purpose of analysis are:

1. Compressive loads P are applied at fixed points in the end cross sections of the beam.

2. The end eccentricity of P is small.

3. The center line of the beam in the unstrained case is represented by $y = n(x)$.

4. Forces proportional to P are applied to the beam in the direction O_y, and end couples proportional to P are applied in the plane O_{xy}.

5. The forces described in (4) above and their associated reactions are defined by saying that they produce in the absence of other loads a bending moment $P \cdot N(x)$ at a distance x from the origin.

6. Constant forces parallel to O_y are applied at various points along the beam, and constant end couples are applied in the plane O_{xy}.

7. The system described in (6) above is defined by saying that these

forces, together with their appropriate reactions, produce a bending moment M(x) at position x and end rotation m(x).

With these assumptions the equilibrium equation may be written as:

$$- EI \frac{d^2}{d^2x} \left\{\delta(x) + m(x)\right\} = P \left\{n(x) + m(x) + \delta(x)\right\} + M(x) + P \cdot N(x) \qquad (16)$$

or

$$\left[D^2 + \mu^2\right] \delta(x) = -\mu^2 \left\{n(x) + N(x) + m(x)\right\} = -\mu^2 H(x) \text{say} \qquad (17)$$

where

$\delta(x)$ is the added deflection due to P and its associated loads and

$$\mu^2 = \frac{P}{EI}.$$

The deflection $\delta(x)$ is determined by equation (17) and by the condition $\delta = 0$ at $x \pm L$. It is to be noted that there is an exact correspondence among y, N, and m, in that it is not these individual values which affect δ but only the sum H. Thus, we have the most important results - namely, initial bowing, end-eccentricity, transverse loads, and end couples whether proportional to P or constant, all combine to form one total equivalent eccentricity.

Fisher then proceeded with a rigorous analysis and demonstrated that Southwell's expression should be written as

$$P_1 v - \delta = H(\theta) . F_H(\theta, z) \qquad (18)$$

where

$H(\theta)$ = the sum of the normal forces on the beam

$F_H(\theta, z)$ = a function dependent upon the normal force distribution

$v = \frac{\delta}{P}$.

Now the variation of F_H as z passes from 0 to 1 is a measure of the deviation from linearity. This he demonstrated to be small in general.

A second approximation is also given to the v/δ relationship. This is in the form of a hyperbola.

$$\left(P_1 v - \delta - C_1\right)\left(P_1 v - K + C_1 - C_o\right) = -C_1\left(C_1 - C_o\right) \qquad (19)$$

where

Theoretical Conditions

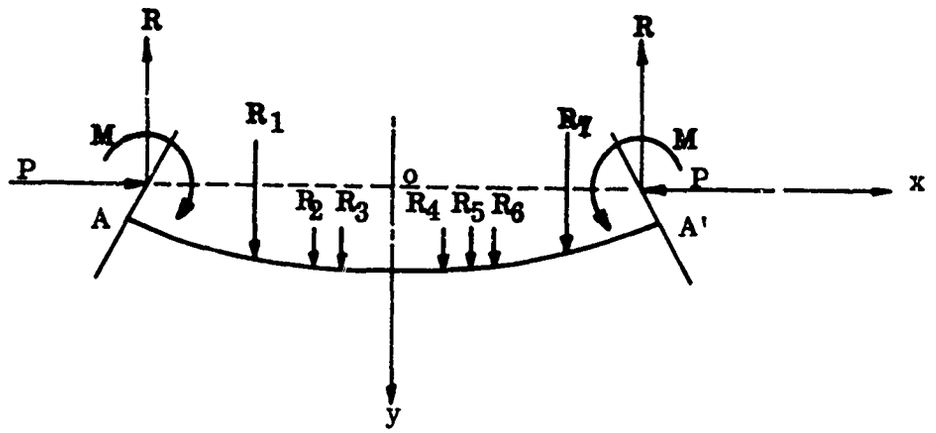

Experimental Conditions

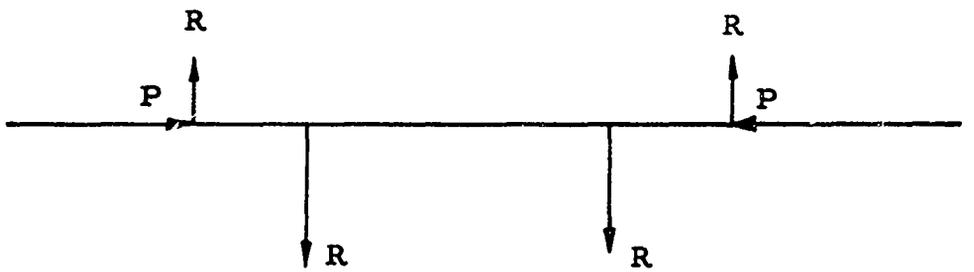

Figure 11. Various Loadings on a Spar Considered by Fisher[10].

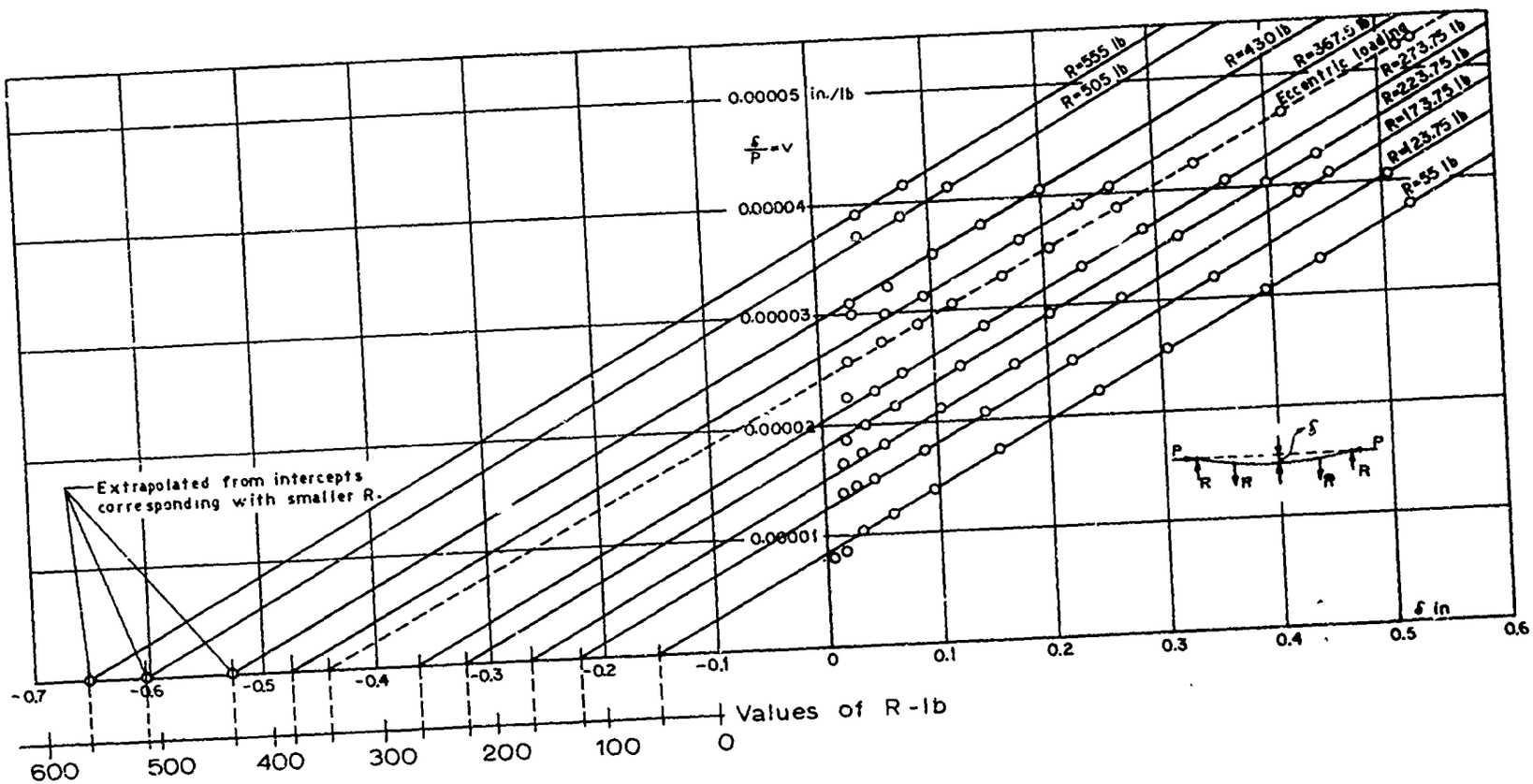

Figure 12. Southwell Plots of Fisher's[10] Data on Eccentrically Loaded Solid Rectangular Spar-.

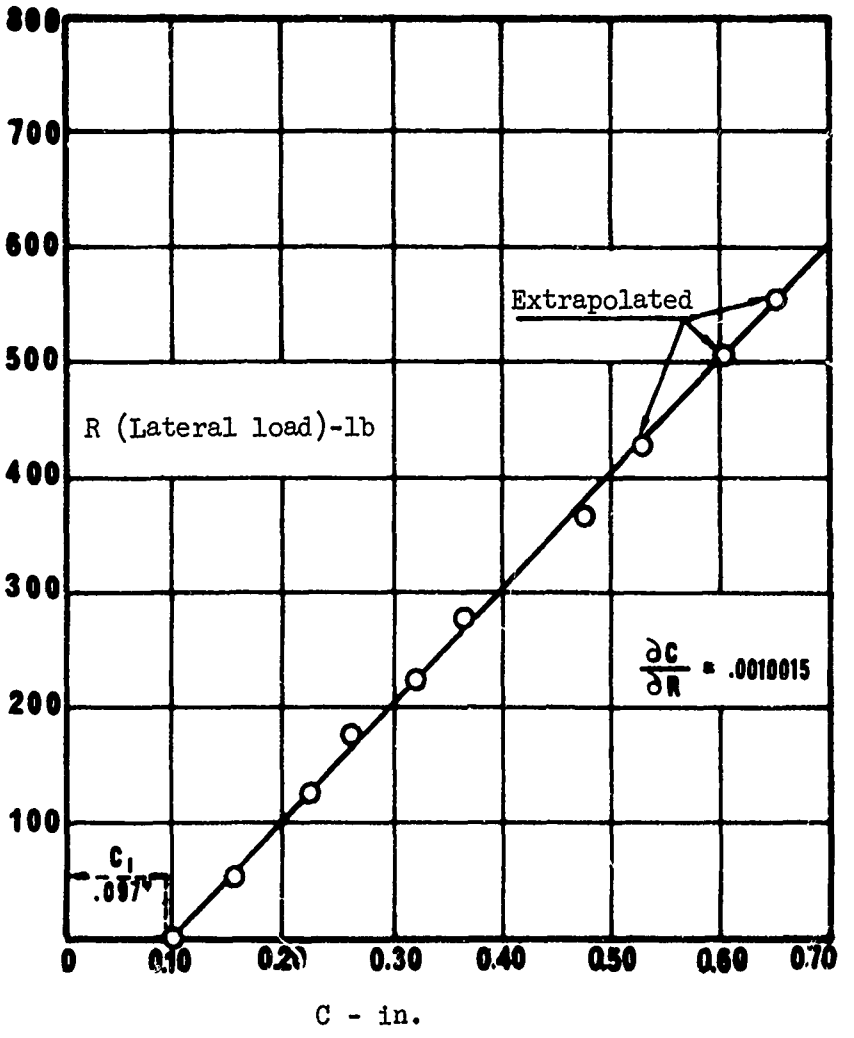

Figure 13. Plot of Lateral Load R vs Intercept Value C From Figure 12.

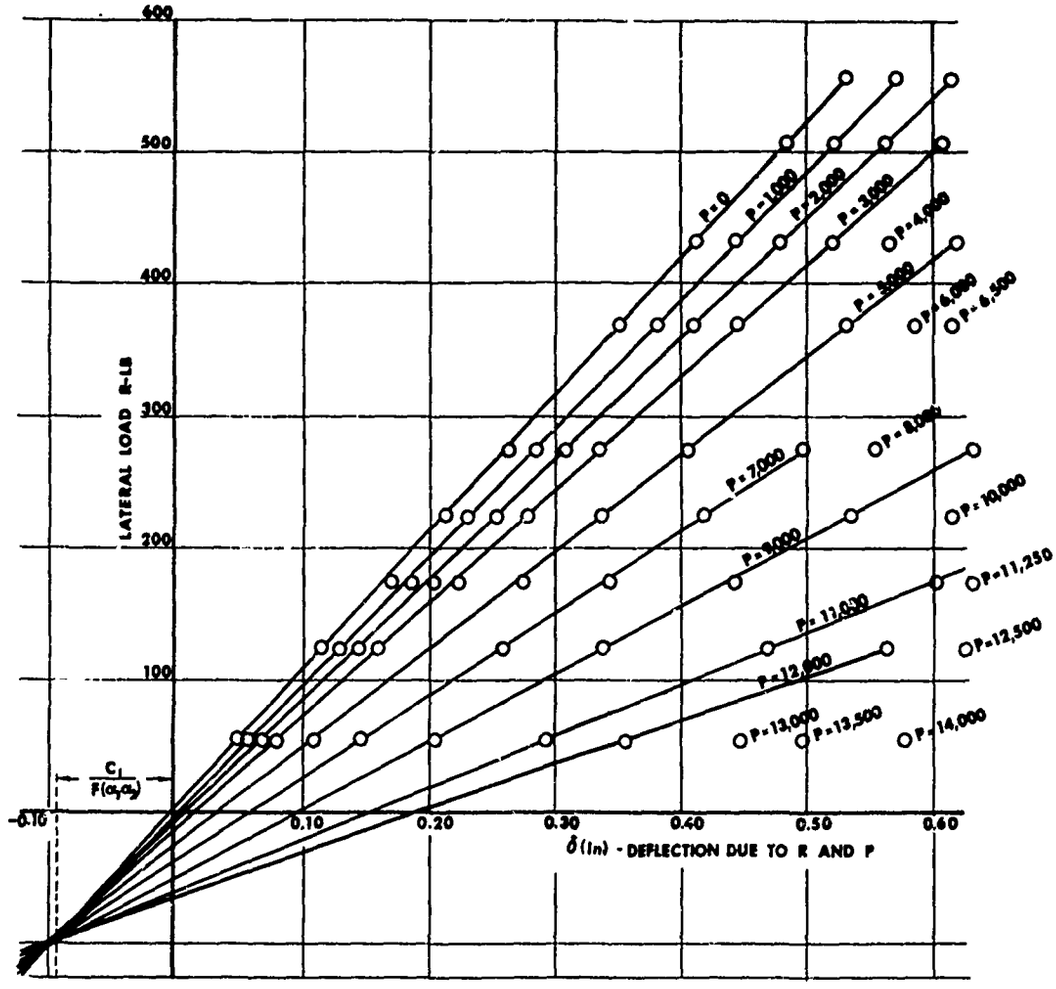

Figure 14. A Method of Representing Spar Tests. R and δ Represent Constant Values of P.

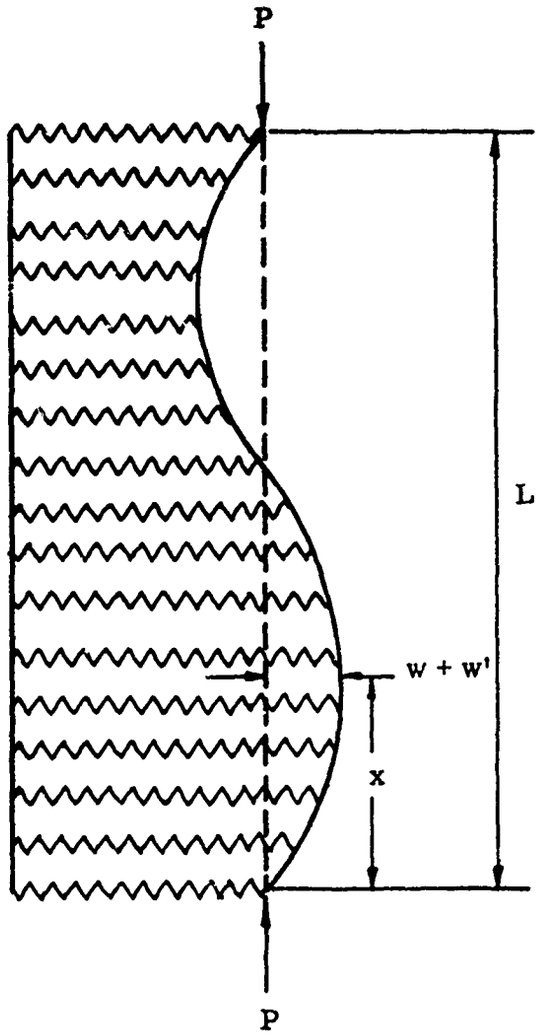

Figure 15. Initially Curved, Elastically Supported Strut Considered by Donnell[7].

P, v, and δ have the significance previously ascribed, and C_1 and C_o are constants. K has the value 0.123234.

To test his theory, Fisher performed a series of experiments. The results are portrayed in Figures 12, 13, and 14. It is seen from these figures that even large values of side force do not destroy the linearity of the δ/P versus δ curves. Thus, the tests provide substantial verification of Fisher's analysis. It is interesting to note, too, that when the Southwell eccentricities are expressed in terms of the side force values, the relationship is linear (Figure 13). This is clear evidence that the intercept with the axis has the meaning normally ascribed to it.

In his paper on the applicability of the Southwell plot, Donnell[7] also considered analytically the case of a hinged strut with continuous elastic support. This strut system is shown in Figure 15. For the purpose of his analysis he assumed an initial deformation given by

$$w' = \sum_{n=1}^{\infty} W'_n \cdot \sin \frac{n\pi x}{L} \tag{20}$$

and that the movement during buckling could be represented by

$$w = \sum_{n=1}^{\infty} W_n \cdot \sin \frac{n\pi x}{L} \tag{21}$$

Now the total energy change due to a virtual displacement dW_n must vanish, or

$$dW_n \cdot \frac{\partial}{\partial W_n} \int_o^1 \left[\frac{EI}{2}\left(\frac{d^2w}{dx^2}\right)^2 + \frac{\beta}{2} w^2\right] dx \tag{22}$$

$$= P \int_o^1 \frac{1}{2}\left\{\left[\frac{d}{dx}(w'+w+dW_n \cdot \sin \frac{n\pi x}{L})\right]^2 - \left[\frac{d}{dx}(w'+w)\right]^2\right\} dx$$

where

EI = the bending rigidity

β = the modulus of the elastic support.

Thus, it can be shown that

$$P = \frac{W_n}{W'_n + W_n}\left(\frac{n^2\pi^2 EI}{L^2} + \frac{L^2\beta}{n^2\pi^2}\right) = \frac{W_n}{W'_n + W_n} \cdot P_n \tag{23}$$

This equation can be written in the form

$$W_n = \frac{W'_n}{\frac{P_n}{P} - 1} \tag{24}$$

where

Pn = the classical critical loads for a perfect strut having a continuous elastic support.

Once again the relationship between the elastic deformation and the applied load reveals a form similar to the Southwell representation for the strut. Of course, in a problem of this type, which may easily exhibit modal shapes having harmonics higher than the fundamental one, it is important to observe and record adequately the buckling shape as well as the load and deflection parameters.

Hayashi and Kihira[12] in a report recently presented to the Japan Congress on Testing Materials provide some experimental results for this problem. The test setup which they used is depicted in Figure 16, while their results are portrayed in Figures 17, 18, and 19.

Just as a restraining spring located along the length of a column causes an increase in the critical load reflected by a change in slope of the Southwell line (as the above referenced tests show), so does a point of local stiffness reduction caused by slight yielding of the material in a local area cause a change in the apparent critical load. This situation is clearly seen in the test data of Fisher given in Figure 20. This is an important facet since such local yielding is not always readily apparent from the load displacement curve.

The discussion, so far, has centered around uniform pin-ended columns and their fundamental critical loads. Such restrictions, however, are not necessary. The process applies for all end conditions, as has been demonstrated analytically by Ariaratnam[13] and experimentally by Hill.[14] The question of critical loads beyond the first was treated by Donnell.[7] This analysis was perhaps his most important contribution to the column problem.

In the normal Southwell derivation, as in Donnell's, the total displacement at any point is the algebraic sum of the various harmonic components of the deformation at that point. If three of these are considered, as depicted in Figure 21, then the overall deflection δ at the 1/3 and 2/3 positions is related to the harmonic amplitudes as follows:

$$\delta_{1/3} = 0.866(W_1 + W_2) \tag{25}$$

$$\delta_{2/3} = 0.866(W_1 - W_2) \tag{26}$$

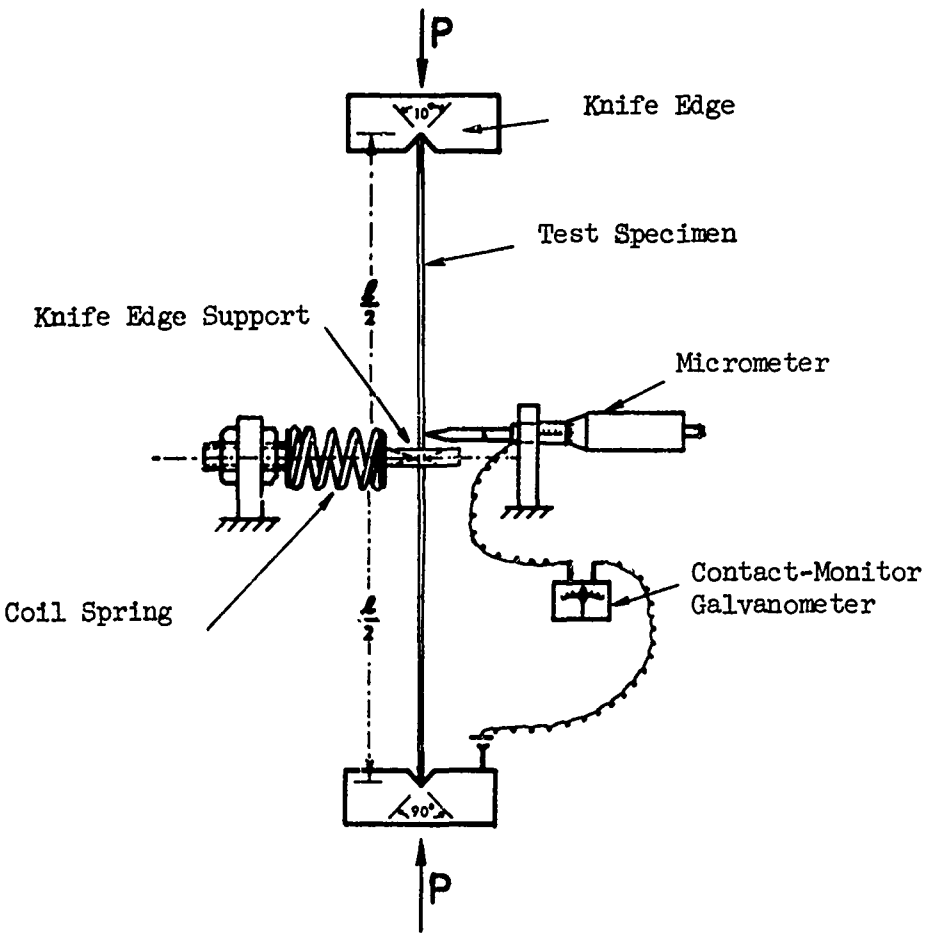

Figure 16. Experimental Test Setup for Column Testing (from Reference 12).

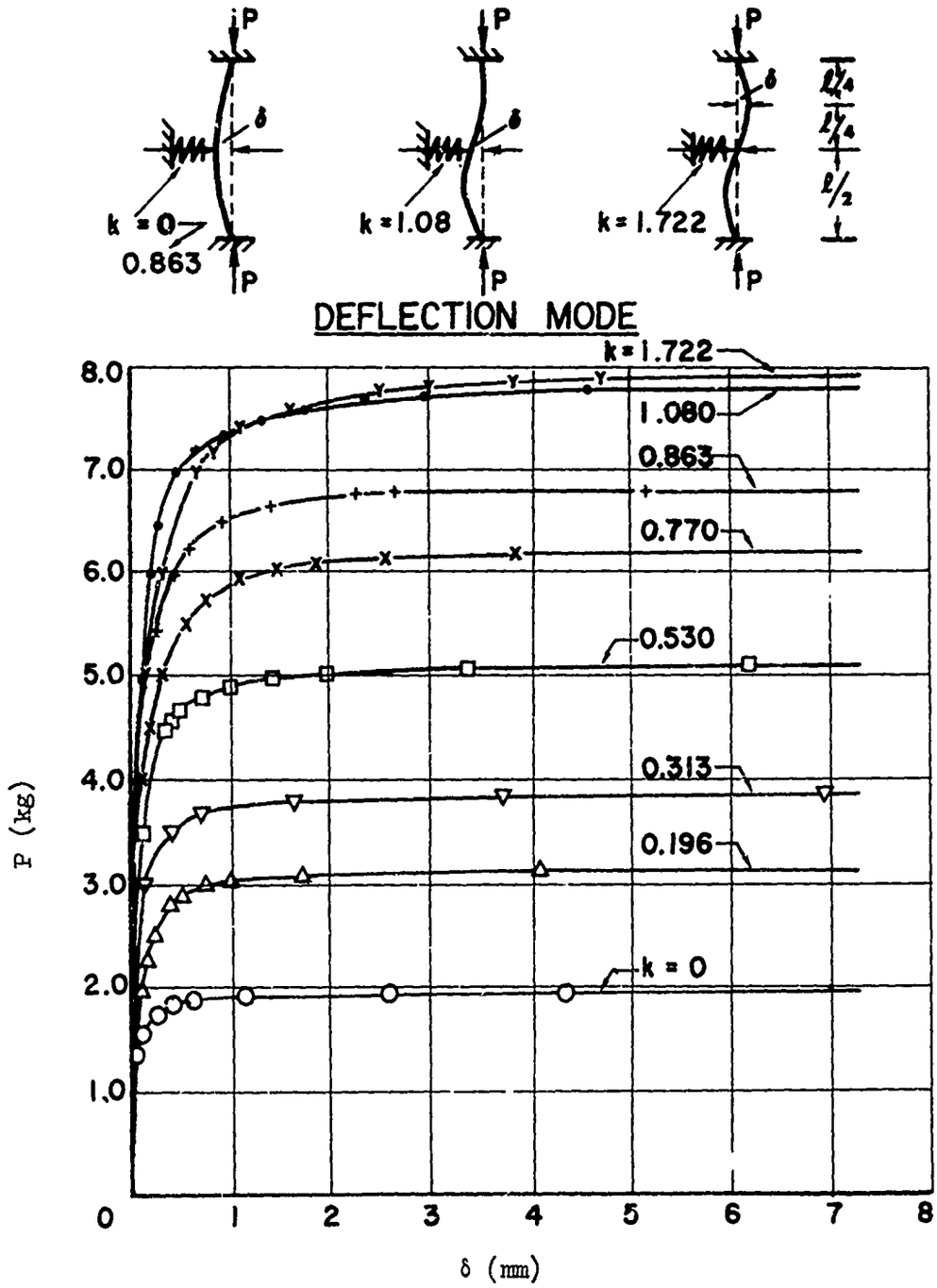

Figure 17. Plots of P vs δ for the Buckling of Elastically Supported Columns.

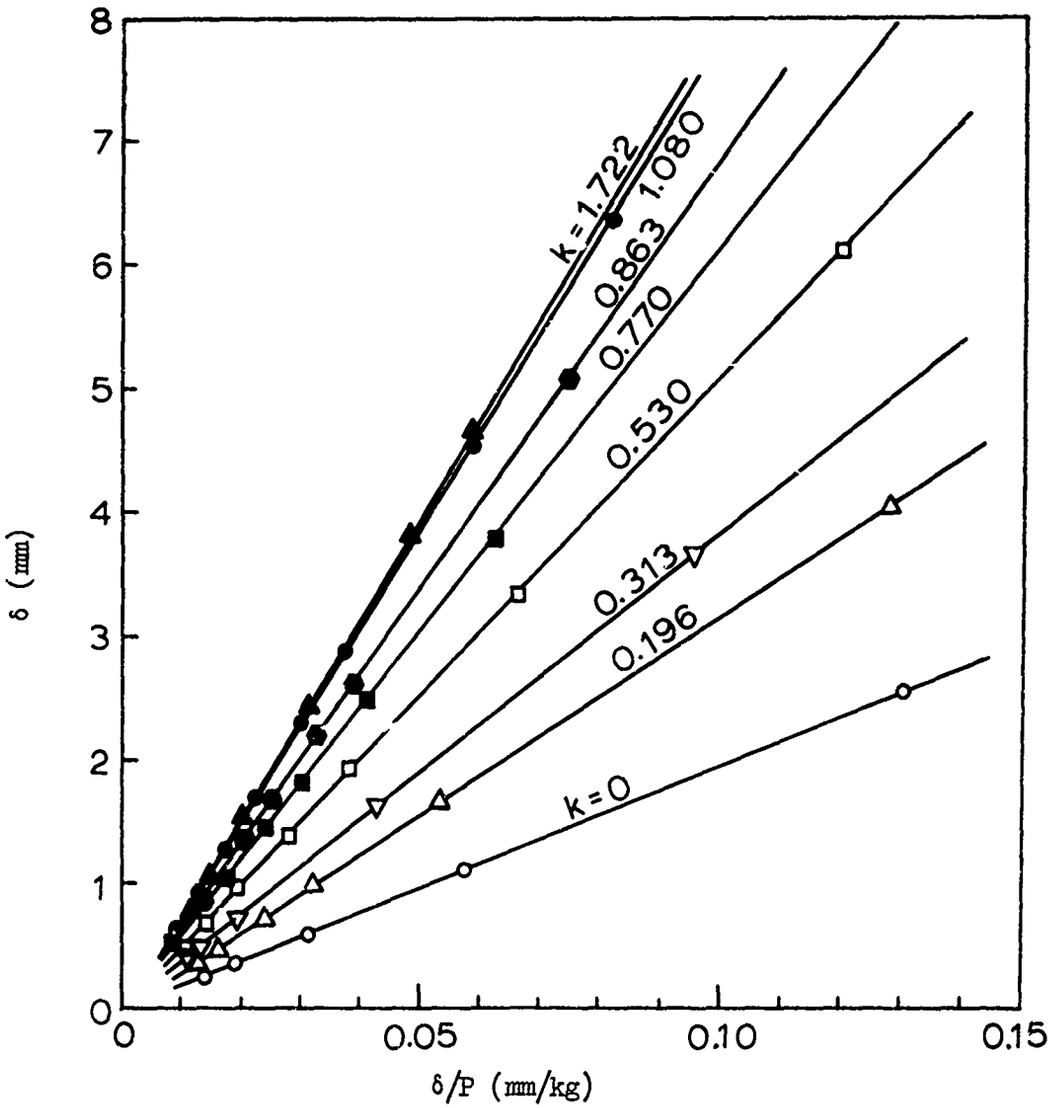

Figure 18. Plots of δ vs δ/P From Data Shown in Fig. 17 (from Reference 12).

$\frac{P_{CR}}{P_E}$

k (kg/mm)		0	0.196	0.313	0.530	0.770	0.863	1.080	1.722
P_{CR} (kg)	Exp	20.0	32.1	38.7	51.3	62.5	68.5	78.7	80.0
	Cal	20.9	33.0	39.9	52.3	65.4	70.6	81.7	83.6

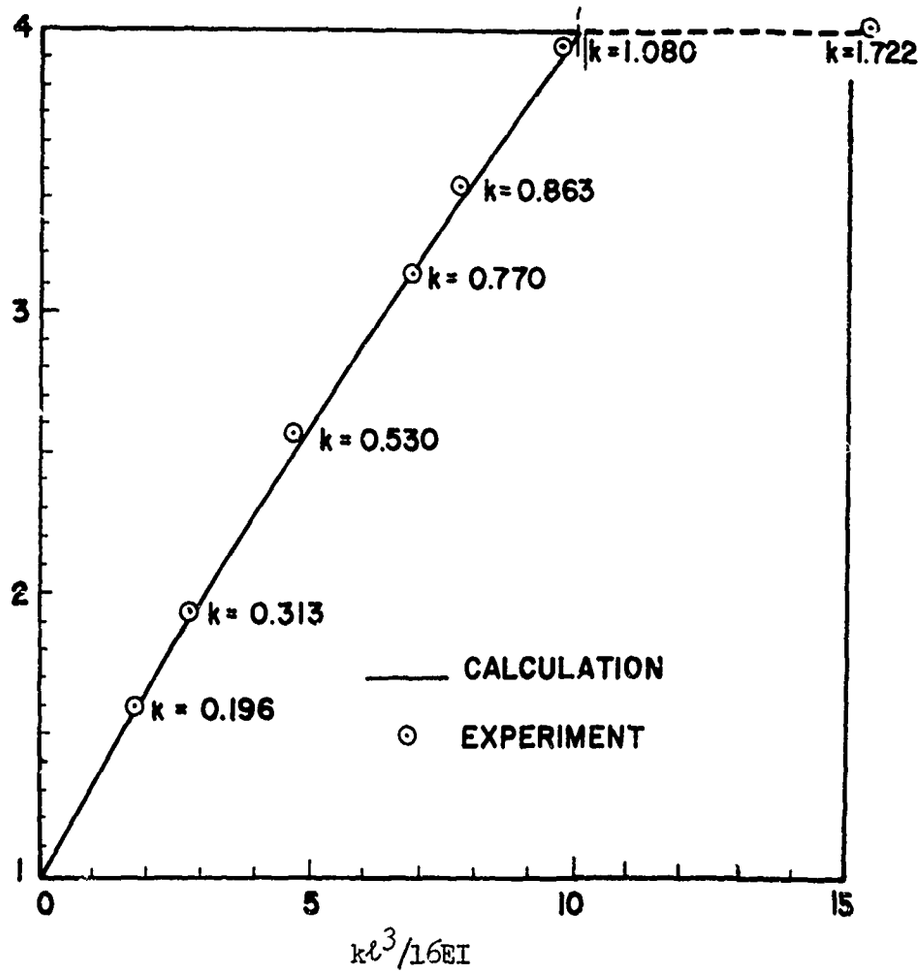

Figure 19. Comparison of Experiments and Theory Data From Figure 18 (from Reference 12).

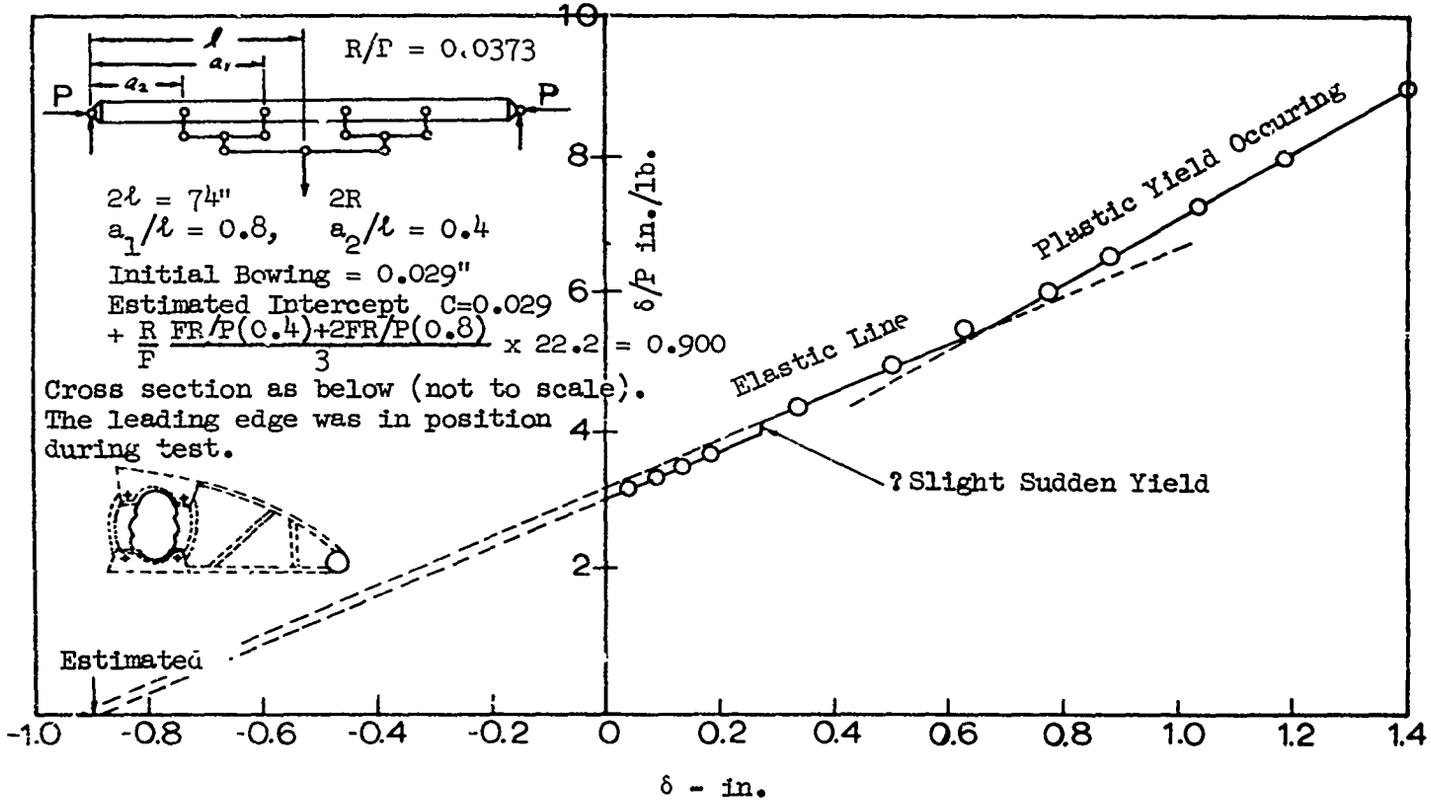

Figure 20. Southwell Plot of Data Obtained on an Aeroplane Spar Showing Plasticity Effects (from Reference 11).

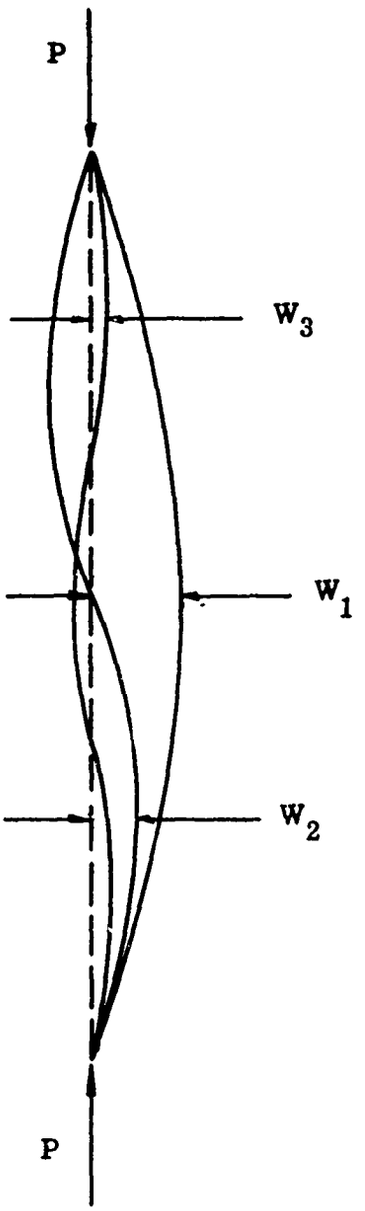

Figure 21. Harmonic Components of Deflection of a Compressed Column.

whence

$$W_1 = 0.58\,[\delta_{1/3} + \delta_{2/3}] \tag{27}$$

Such an expression for W_1 is clearly more accurate than the normal Southwellian approximation which gives

$$W_1 = \delta_{1/2} \tag{28}$$

in which expression there is an error of W_3 and higher harmonics; whereas in the second approximation formula given above, equation (28), the error is W_4 and higher harmonics.

It is clear that in cases in which a large number of harmonics are concerned, the use of the many simultaneous equations would add greatly to the data processing as well as to the acquisition. But by using the principles of Harmonic Analysis, it can be shown that if

$$\delta_{1/m},\ \delta_{2/m},\ \text{---}\ \delta_{(m\,-\,1/m)}$$

are deflections at points dividing the length into m aliquot parts,

$$W_n \doteq \frac{2}{m}\left[\delta_{(1/m)}\sin\frac{n\pi}{m} + \delta_{(2/m)}\sin\frac{2n\pi}{m} + \text{---}\right.$$

$$\left.\delta_{(m\,-\,1/m)}\sin\,(m-1)\,\frac{n\pi}{m}\right] \tag{29}$$

Donnell remarked that it was unfortunate that no experimental evidence existed on this question. However, in a report published in the Journal of Research of the National Bureau of Standards, Tuckerman[15] examined the Southwell plot from the point of view of the Westergaard[16] general theory, and produced data to verify the harmonic theory. This experimental work was performed by McPherson and Levy. From this laboratory study, he was able to determine first and second critical loads for one column tested and first and third for another.

The experimental results are presented in Table III, and the final curves are given in Figure 22 for the first and second mode problem. The theoretical critical load levels are compared with the experimentally determined values in Table IV.

The corresponding data with respect to the determination of the first and third critical levels are given in Tables V and VI and in Figures 23 and 24.

It should be noted that in each case, the agreement between the first critical load and the Euler load is good (3 percent), but the agreement between the second and third values and their corresponding theoretical counterparts is poorer (11 percent and 12 percent).

TABLE III. CRITICAL LOAD OF 13.5-BY-1/4-BY-1/2-INCH COLD-ROLLED STEEL COLUMN WITH EQUAL AND OPPOSITE ECCENTRICITIES AT THE ENDS*

Load	ΔT**	ΔM**	ΔB**	P_1	$\frac{1}{2}d_1$***	$\frac{\frac{1}{2}d_1}{P_1}$***	d_2***	$\frac{d_2}{P_1}$***
lb	10^{-4}	10^{-4}	10^{-4}	lb	10^{-4}	$\frac{10^{-4}}{lb}$	10^{-4}	$\frac{10^{-4}}{lb}$
790--	0	0	0	0	0	-	0	-
750--	-1.02	-0.73	0.01	-40	-0.37	.00912	-0.51	.01288
710--	-1.93	-1.20	0.13	-80	-0.60	.00750	-1.03	.01288
670--	-2.73	-1.63	0.33	-120	-0.81	.00679	-1.53	.01275
630--	-3.40	-1.93	0.54	-160	-0.96	.00602	-1.97	.01231
590--	-4.10	-2.19	0.91	-200	-1.09	.00548	-2.50	.01252
550--	-4.67	-2.34	1.21	-240	-1.17	.00488	-2.94	.01225
510--	-5.23	-2.53	1.52	-280	-1.26	.00452	-3.38	.01205
470--	-5.73	-2.66	1.82	-320	-1.33	.00416	-3.78	.01179
430--	-6.29	-2.78	2.19	-360	-1.39	.00386	-4.24	.01178
390--	-6.74	-2.87	2.52	-400	-1.44	.00359	-4.63	.01158
350--	-7.22	-3.01	2.83	-440	-1.50	.00342	-5.02	.01142
310--	-7.69	-3.05	3.14	-480	-1.52	.00318	-5.42	.01130
270--	-8.14	-3.13	3.47	-520	-1.56	.00301	-5.80	.01115
230--	-8.53	-3.19	3.79	-560	-1.60	.00285	-6.16	.01100
190--	-9.01	-3.26	4.08	-600	-1.63	.00272	-6.55	.01090
150--	-9.40	-3.35	4.40	-640	-1.68	.00262	-6.90	.01080
110--	-9.78	-3.36	4.71	-680	-1.68	.00247	-7.24	.01065

* This table reproduced from Reference 15.

** Δ is the difference in strain on opposite sides of the specimen (bending strain) arranged to be zero at the arbitrary "zero load" for computations of 790 lb.

*** d_1 and d_2 are the bending strains corresponding to the first and second critical loads, respectively.

$\frac{1}{2}d_1 = \left(\frac{\Delta M}{2}\right)$, $d_2 = \left(\frac{\Delta T - \Delta B}{2}\right)$.

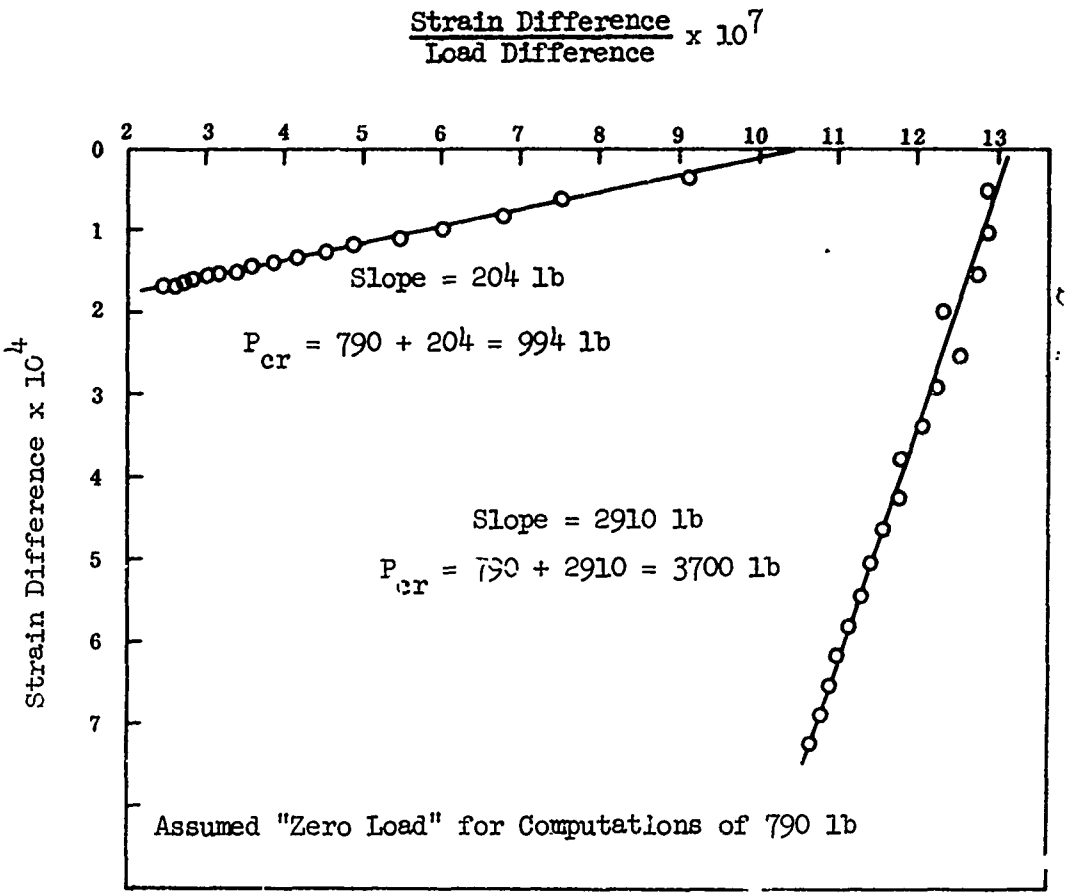

Figure 22. Lundquist-Type Plots for First and Second Modes of an Axially Compressed Column (from Reference 15).

TABLE IV. CRITICAL LOAD OF 13.5-BY-1/4-BY-1/2-INCH COLD-ROLLED STEEL COLUMN WITH EQUAL AND OPPOSITE ECCENTRICITIES AT THE ENDS*

FIRST CRITICAL LOAD	
From strain at middle	994 lb
From strain at quarter points	1,015 lb
Theoretical $\frac{\pi^2 EI}{L^2}$ (Assumed E - 29 x 10^6 lb/in.^{2})	1,020 lb

SECOND CRITICAL LOAD	
From strain at quarter points	3,700 lb
Theoretical $\frac{4\pi^2 EI}{L^2}$ (Assumed E - 29 x 10^6 lb/in.^{2})	4,100 lb

* This table reproduced from Reference 15.

TABLE V. CRITICAL LOAD OF 27.7-BY-3/8-BY-3/4-INCH COLD-ROLLED STEEL COLUMN WITH EQUAL ECCENTRICITIES AT THE ENDS*

P	ΔT**	ΔM**	ΔB**	d_1***	P_1**	a_1***	ΔT****	ΔM****	ΔB****	d_3***	P_3****	$\frac{d_3}{P^3}$***
lb	10^{-4}	10^{-4}	10^{-4}	10^{-4}	lb	$\frac{10^{-4}}{lb}$	10^{-4}	10^{-4}	10^{-4}	10^{-4}	lb	$\frac{10^{-4}}{lb}$
100	1.81	-6.03	1.16	-3.03	-900	.00337	0	0	-	0	0	-
200	1.53	-5.60	0.96	-2.90	-800	.00363	-1.10	1.32	-1.59	1.43	100	.01337
300	1.22	-5.24	0.74	-2.84	-700	.00406	-2.55	2.57	-3.07	2.73	200	.01365
400	0.92	-4.81	0.51	-2.73	-600	.00455	-3.81	3.96	-4.60	4.12	300	.01373
500	0.66	-4.31	0.31	-2.55	-500	.00510	-5.13	5.34	-6.21	5.56	400	.01390
600	0.41	-3.78	0.10	-2.35	-400	.00587	-6.44	6.75	-7.80	7.00	500	.01399
700	0.17	-3.20	-0.06	-2.10	-300	.00699	-7.87	8.23	-9.55	8.55	600	.01425
800	0.01	-2.40	-0.17	-1.65	-200	.00960	-9.26	9.77	-11.25	10.09	700	.01442
900	-0.11	-1.49	-0.20	-1.10	-100	.01097	-10.70	11.35	-13.01	11.69	800	.01461
1000	0	0	0	0	0	-	-12.09	12.79	-14.75	13.21	900	.01469

* This table reporduced from Reference 15.

** Δ is the difference in strain on opposite sides of the specimen (bending strain) arranged to be zero at the arbitrary "zero load" for computations of 1,000 lb.

*** d_1 and d_3 are the bending strains corresponding to the first and third critical loads, respectively.

**** For these readings the column was bent, as shown in Figure 21, to emphasize the third harmonic. For these the arbitrary "zero load" for computations is 100 lb.

$$d_1 = \left(\frac{2\Delta M + \Delta B + \Delta T}{3}\right), \quad d_3 = \left(\frac{\Delta M - \Delta T - \Delta B}{3}\right)$$

TABLE VI. CRITICAL LOAD OF A 27.7-BY-3/8-BY-3/4-INCH COLD-ROLLED STEEL COLUMN*

FIRST CRITICAL LOAD	
From strain gages	1,251 lb
Theoretical $\frac{\pi^2 EI}{L^2}$	1,240 lb
(Assumed, $E = 29 \times 10^6$ lb/in.^{2})	

THIRD CRITICAL LOAD	
From strain gages	9,825 lb
Theoretical $\frac{9\pi^2 EI}{L^2}$	11,100 lb
(Assumed, $E = 29 \times 10^6$ lb/in.^{2})	

* This table reproduced from Reference 15.

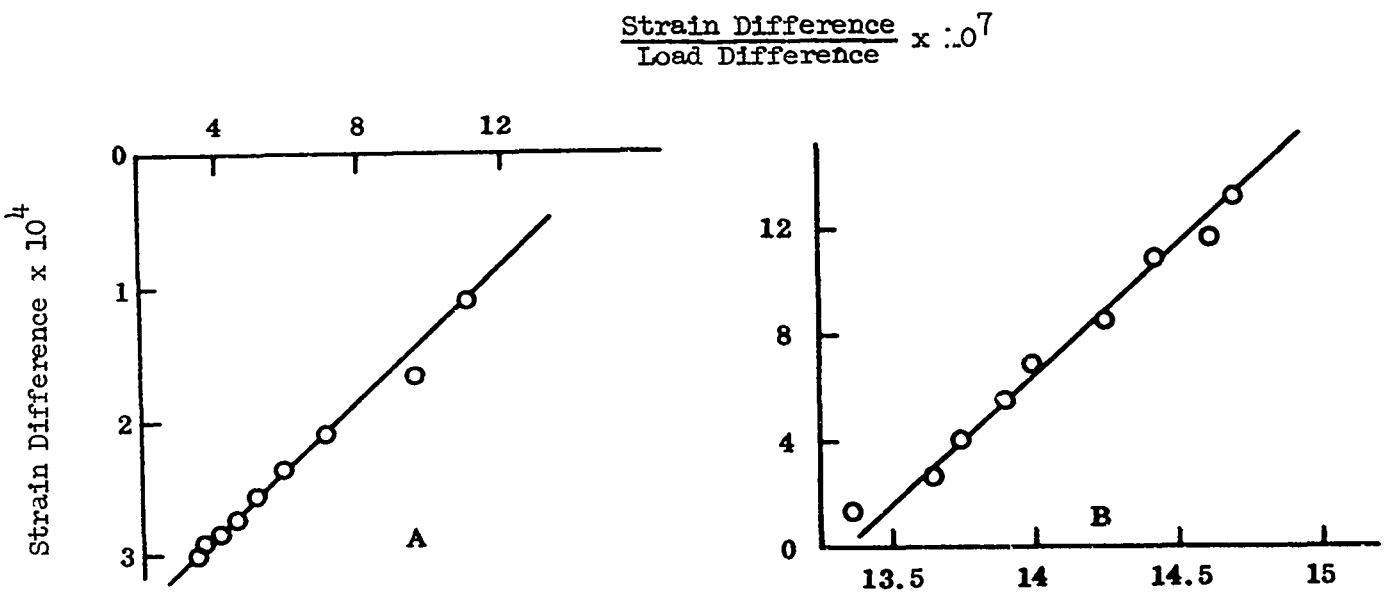

Slope = 251 lb

P_{cr} = 1000 + 251 = 1251 lb

Figure 23. Lundquist Plot of First Mode for an Axially Compressed Column (from Reference 15).

Slope = 9725 lb

P_{cr} = 100 + 9725 = 9725 lb

Figure 24. Lundquist Plot of Third Mode for an Axially Compressed Column (from Reference 15).

The next application of interest appears in the study reported by Bridget, Jerome, and Vosseller.[17] This work was concerned with the stability of angle struts. The instability mode for such structures is markedly dependent on the width of the flanges. When the flanges are narrow, the mode is of the Euler Column type, but when they are wide, local or torsional instability can occur. It was found in the investigation that the Southwell plot was applicable irrespective of mode. The overall results of the study are given in Figure 25. A typical Southwell plot is shown in Figure 26.

These experiments were conducted under the guidance of Donnell,[7] who provided theoretical justification for the procedure in a report published in 1938. He analyzed the stability of a compressed flat panel hinged on three sides and free on the fourth, as shown in Figure 27. Because the deformed shape of such a body is, to a fair approximation, a developable surface, extensional stresses can be neglected in the internal energy, and the initial deformation of the panel can be represented by

$$w' = \frac{s}{b} \sum_n W_n' \sin \frac{n\pi x}{L}$$

and the additional deflection can be represented by

$$w = \frac{s}{b} \sum_n W_n \sin \frac{n\pi x}{L} \tag{30}$$

Then the condition where the energy change due to a virtual displacement dW_n vanishes is

$$dW_n \frac{\partial}{\partial W_n} \frac{Et^3}{12(1-\mu^2)} \int_0^b \int_0^L \frac{1}{2}\left[\left(\frac{\partial^2 w}{\partial x^2}\right)^2 + \left(\frac{\partial^2 w}{\partial s^2}\right)^2 + 2(1-\mu)\left(\frac{\partial^2 w}{\partial x \partial s}\right)^2 + 2\mu \frac{\partial^2 w}{\partial x^2}\frac{\partial^2 w}{\partial s^2}\right] dx\, ds = \frac{P}{b} \int_0^b \int_0^L \frac{1}{2}\left\{\left[\frac{\partial}{\partial x}\left(w' + w + dW_n \frac{s}{b} \sin \frac{n\pi x}{L}\right)\right]^2 - \frac{\partial}{\partial x}\left[(w' + w)\right]^2\right\} dx\, ds \ldots\ldots\ldots \tag{31}$$

where E, μ, and t are the elastic modulus, Poisson's ratio, and thickness, respectively.

Substituting equation (30) into (31), we obtain

$$P \frac{W_n}{W_n' + W_n} \left[\frac{Et^3 b}{12(1-\mu^2)}\right]\left(\frac{n^2\pi^2}{L^2} + \frac{6(1-\mu)}{b^2}\right) = \frac{W_n}{W_n' + W_n} P_n \tag{32}$$

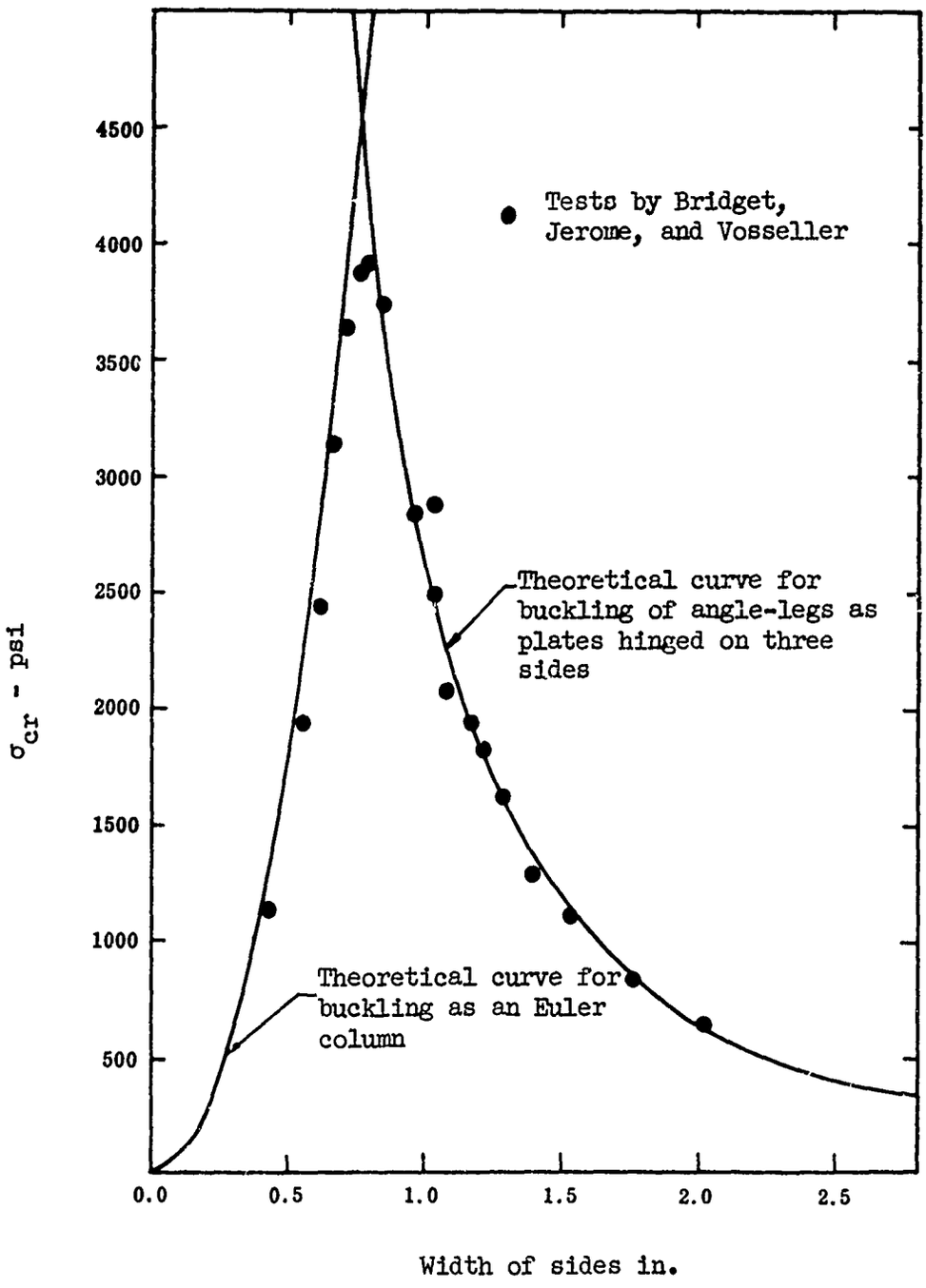

Figure 25. Correlation of Theoretical Curves With Results of Bridget, Jerome, and Vosseller as Determined From Southwell Plots of Compressed Duralumin Angles (from Reference 17).

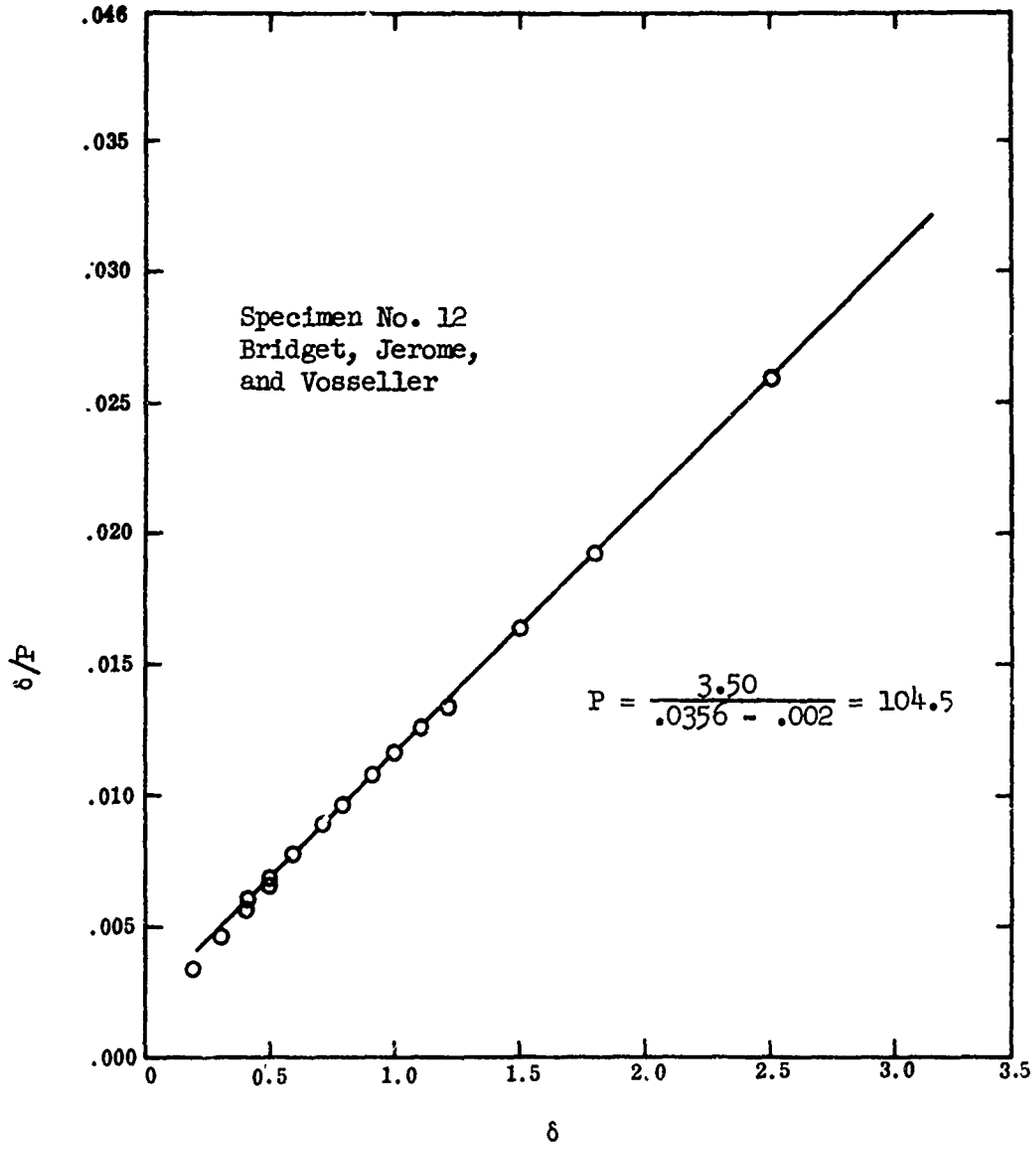

Figure 26. Southwell Plot of Bridget, Jerome, and Vosseller's Data on Compressed Angles (from Reference 17).

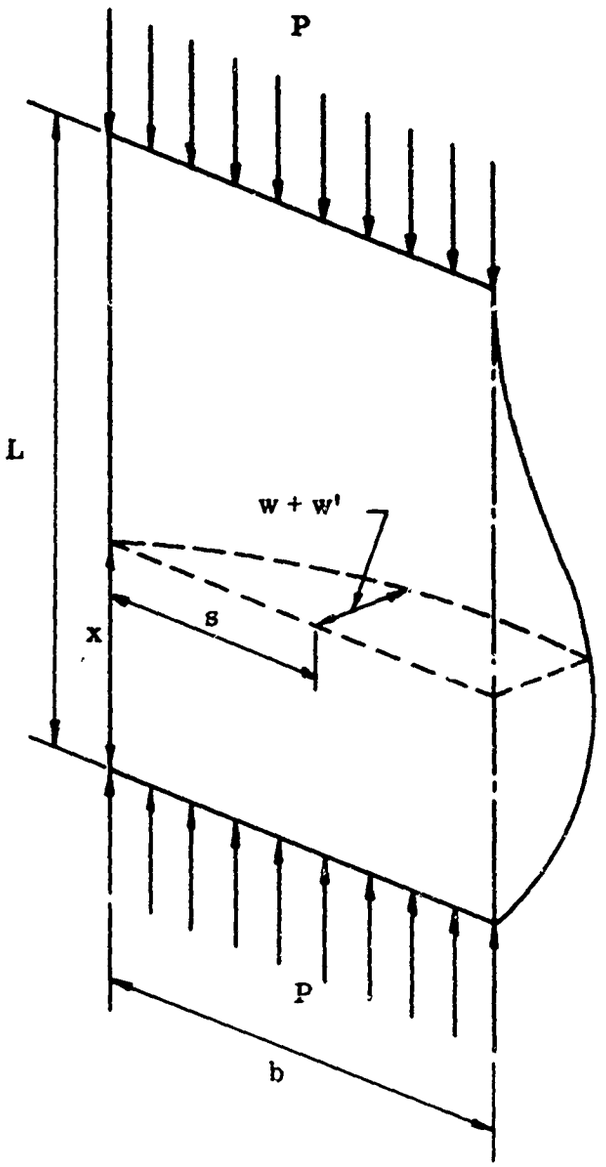

Figure 27. Panel Hinged on Three Sides Having an Initial Deviation From Flatness.

where P_n is the n^{th} critical load. This expression if clearly identical in form to that derived by Southwell[6] and suggested by Ayrton and Perry.[5]

If the linear plot method (Southwell Plot) described had significance merely with regard to the strut, then, without question, it would merit discussion. But the value of the technique is much wider. We shall deal with various successful applications of the procedure in chronological order.

In 1933 Gough and Cox[18] made experiments on the shear buckling of plates with a view to checking the analytical studies of Southwell and Skan.[19] In the first series of tests which they made, the buckling loads were determined by distortion of images reflected in the surface of the strip. The results of this approach were very positive. In all cases, there was a serious discrepancy between theory and experiment. The "critical loads" determined as described were found to be representable by an expression which differed from the theoretical not only in magnitude but also in form.

As a consequence, the interpretation of the tests was made on the basis of the Southwell[6] argument, which proceeds as follows.

If initial irregularities are present in the plane of the sheet, there will be a component of the wave form corresponding to the first critical load, as defined by theory. If the amplitude of this component is W_o, the effect of a shear load S is to multiply this amplitude in the ratio $S/(S_o - S)$, S_o being the critical load. Thus, the corresponding values of S and W (elastic deflection) should satisfy the relationship.

$$W = SW_o / (S_o - S) \tag{33}$$

i.e.,
$$W \left[\frac{S_o}{S} - 1\right] = \text{constant} \tag{34}$$

an equation of precisely the same form as equation (14).

Thus, the plot of W versus W/S should be linear, and the slope should correspond to the first critical load for a perfect plate, since the intercept is clearly the value of the effective imperfection.

The results of this approach are portrayed in Figure 28. Good linear relationships are obtained. The comparison of the theoretical loads and the values estimated from experiment is given in Table VII.

The application of the same techniques for the interpretation of the instability results of flat plates is also feasible. Timoshenko and Gere[20] determined a linear relationship similar to equation (14) for plates in which there is no midplane stretching. The initial deflection must be small in comparison to the plate thickness. The fourth-order differential equation of equilibrium is

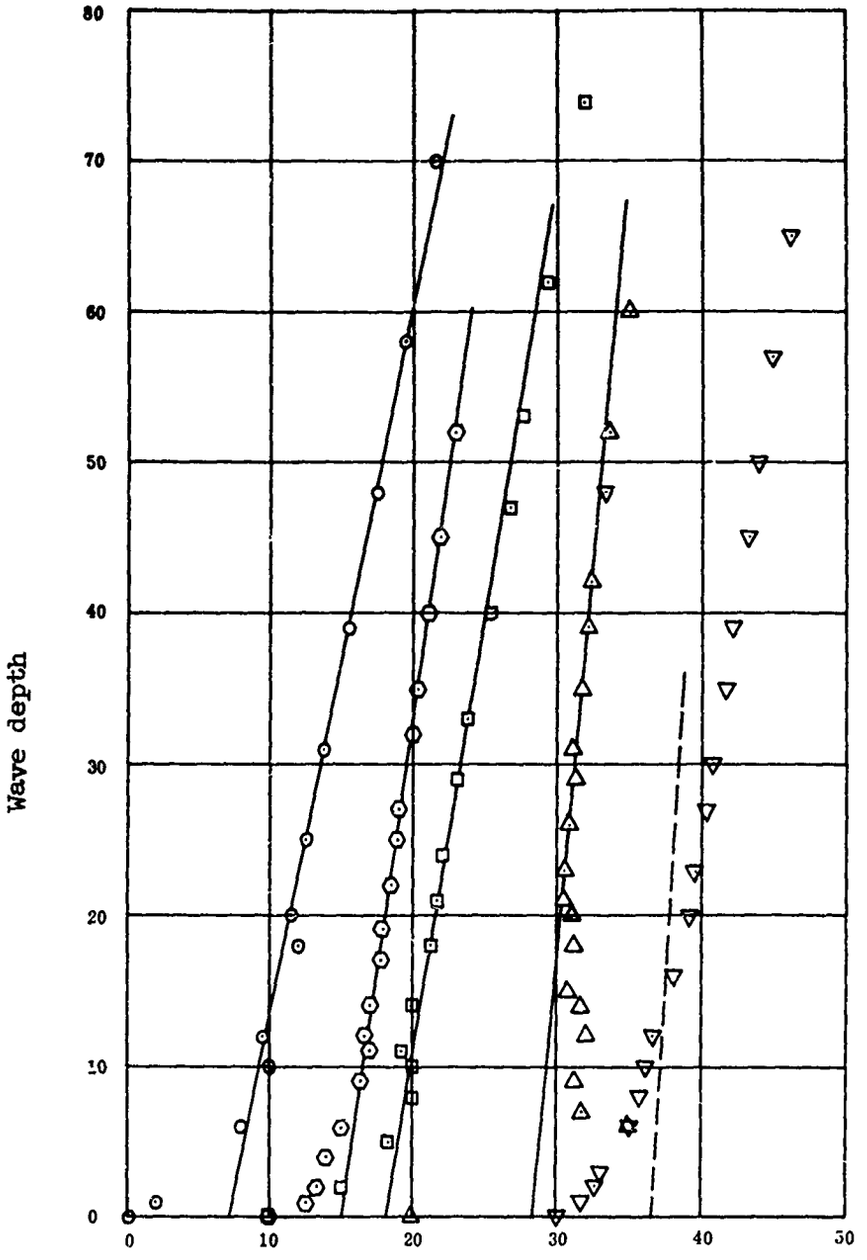

Strip DGLI, 150 - 1-1/2-in. width (w/S plotted from 0 as zero).
Strip DGLI, 157 - 1-1/4-in. width (w/S plotted from 10 as zero).
Strip DGLI, 156 - 1-in. width (w/S plotted from 10 as zero).
Strip DGLI, 155 - 3/4-in. width (w/S plotted from 20 as zero).
Strip DGLI, 154 - 1/2-in. width (w/S plotted from 30 as zero).

Figure 28. Determination of Critical Load From Gough and Cox Data on Thin Strips Under Shear (from Reference 18).

TABLE VII. DETAILS OF STRIPS TESTED AND MEASURED VALUES OF WAVE DEPTH*

Reference mark of strip	DGLI 154	DGLI 155	DGLI 156	DGLI 157	DGLI 150
Width (in.)	1/2	3/4	1	1 1/4	1 1/2
Length (in.)	10	15	20	25	30
Thickness (in.)	0.0126	0.0126	0.0126	0.0126	0.0126
Theoretical buckling load (tons)	16.3	10.9	8.2	6.5	5.4
Buckling load estimated from wave-depth readings (tons)	-	11.4	6.65	6.86	5.29
$\frac{S_e}{S_o} = \frac{\text{estimated buckling load}}{\text{theoretical buckling load}}$	-	1.045	.81	1.055	.98
Shear load (tons)	Wave-Depth (deflection meter reading)*				
0.2	0	0	0	0	-
0.25	-	-	-	-	0
0.4	0	6	2	1	-
0.5	-	-	-	-	1
0.6	1	7	5	2	-
0.75	-	-	-	-	6
0.8	2	9	8	3	-
1.0	3	12	10	4	10
1.2	6	14	11	6	-
1.25	-	-	-	-	12
1.4	8	15	14	9	-
1.5	-	-	-	-	18
1.6	10	18	18	11	-
1.75	-	-	-	-	20
1.8	12	20	21	12	-
2.0	16	21	24	14	25

TABLE VII - Continued					
2.2	20	23	29	17	-
2.25	-	-	-	-	31
2.4	23	26	33	19	-
2.5	-	-	-	-	39
2.6	27	29	40	22	-
2.75	-	-	-	-	48
2.8	30	31	47	25	-
3.0	35	35	53	27	58
3.2	39	39	62	32	-
3.25	-	-	-	-	70
3.4	45	42	74	35	-
3.5	-	-	-	-	90
3.6	50	48	89	40	-
3.75	-	-	-	-	115
3.8	57	52	104	45	-
4.0	65	60	127	52	150
4.25	-	-	-	-	195
4.5	-	-	-	-	252
4.75	-	-	-	-	323
5.0	-	-	-	-	401

* Data repooduced from Gough and Cox Reference 18.

** The values of deflection readings used for determining the critical loads are those included between the horizontal lines marked in the table.

$$D \nabla^4 w = q - \left[N_x \frac{\partial^2 (w_o + w)}{\partial x^2} + 2N_{xy} \frac{\partial^2 (w_o + w)}{\partial x \partial y} + N_y \frac{\partial^2 (w_o + w)}{\partial y^2} \right] \tag{35}$$

where

w = elastic lateral displacement of the median surface

w_o = initial lateral deformation of the median surface

D = flexural stiffness

q = transverse loading

and the in-plane stresses are

$$\sigma_x = \frac{N_x}{t}$$

$$\sigma_y = \frac{N_y}{t} \tag{36}$$

$$\sigma_{xy} = \frac{N_{xy}}{t}$$

being positive in compression. From the equation above, it was shown by Timoshenko and Gere that an initial curvature produces a deflection identical to that given by a lateral load of intensity.

$$q_o = N_x \frac{\partial^2 w_o}{\partial x^2} + 2N_{xy} \frac{\partial^2 w_o}{\partial x \partial y} + N_y \frac{\partial^2 w_o}{\partial y^2} \tag{37}$$

This mathematical identity is true only as long as w_o is so small that the principle of superposition is not invalidated. This result is a particular example of the general case derived by Fisher in Reference 10. (See also Figure 36.)

For this linear plate theory under the restriction of a uniaxial load with simply supported edges, Figure 29, the elastic lateral deflection may be taken as

$$w = \sum_{m=1}^{\infty} \sum_{n=1}^{\infty} B_{mn} \sin \frac{m\pi x}{a} \sin \frac{n\pi y}{b} \tag{38}$$

and then the initial deflection is defined as

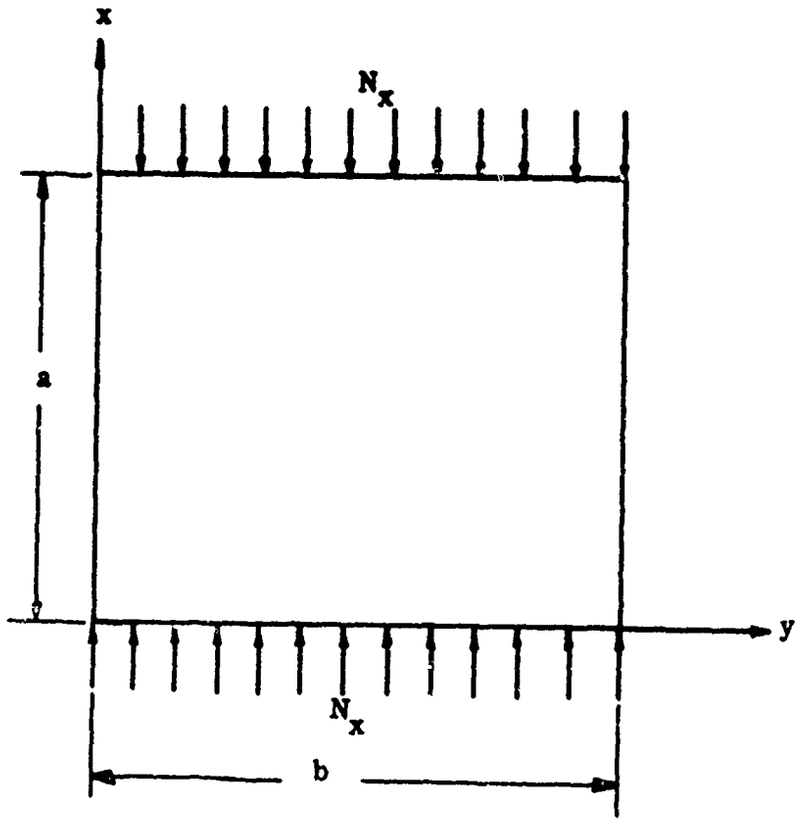

Figure 29. Rectangular Plate With Uniaxial In-plane Loading.

$$w_o = \sum_{m=1}^{\infty} \sum_{n=1}^{\infty} A_{mn} \sin \frac{m\pi x}{a} \sin \frac{n\pi y}{b} \tag{39}$$

Substitution of these Fourier relationships into equation (37) results in

$$B_{mn} \left[\left(\frac{m}{a}\right)^2 + \left(\frac{n}{b}\right)^2 \right] \pi^4 = \frac{1}{D} \left[N_x B_{mn} \left(\frac{m\pi}{a}\right)^2 + N_x A_{mn} \left(\frac{m\pi}{a}\right)^2 \right] \tag{40}$$

Thus,

$$B_{mn} = \frac{A_{mn} N_x}{\frac{\pi^2 D}{m^2 a^2} \left[m^2 + \left(\frac{na}{b}\right)^2 \right]^2 - N_x} \tag{41}$$

for

$$m = 1, 2, \ldots\ldots$$
$$n = 1, 2, \ldots\ldots$$

For a perfect flat plate with ideal boundaries, the critical uniaxial loads per unit length are well established. They are

$$N'_x = N_{x_{cr}} \Big|_{m,n} = \frac{\pi^2 D}{m^2 a^2} \left[m^2 + \left(\frac{na}{b}\right)^2 \right]^2 \tag{42}$$

for

$$m = 1, 2, \ldots\ldots$$
$$n = 1, 2, \ldots\ldots$$

Therefore, equation (41) becomes

$$B_{mn} = \frac{A_{mn}}{\frac{N'_x}{N_x} - 1} \tag{43}$$

This can also be rewritten as

$$B_{mn} \left[\frac{N'_x}{N_x} - 1 \right] = A_{mn} \tag{44}$$

for

$$m = 1, 2, 3, \ldots\ldots$$
$$n = 1, 2, 3, \ldots\ldots$$

Clearly this result is in a one-to-one correspondence with that established by Southwell for the case of the column.

If we consider a realistic square plate under normal test conditions, all experimental evidence indicates that the deflection is of the first modal shape at the commencement of buckling, and equations (42) and (44) become

$$N'_x = N_{x_{cr}} = \frac{\pi^2 D 4}{a^2} \tag{45}$$

$$\delta \left[\frac{N_{x_{cr}}}{N_x} - 1 \right] = B_{11} \left[\frac{N_{x_{cr}}}{N_x} - 1 \right] = A_{11} \tag{46}$$

Equation (46) is identical to equation (14). Therefore, the Southwell Plot is also applicable in this case.

As buckling develops, however, modal changes may occur, and then consideration must be given to the effects of further terms which result from the higher harmonics. Thus, for interpretation of test data appropriate to these cases, it is clearly necessary for the observer to describe and record accurately the modal behavior of the test vehicle and to realize the need for careful positioning of the displacement sensor. In general, for a square plate the deformations are sinusoidal, and the modes higher than the first do not normally occur. Hence, in practice, the elastic deflection δ may be measured at almost any position on the plate. Of course, for maximum sensitivity the center point should be chosen.

In his 1938 paper, Donnell[7] applied the finite displacement theory, which he had previously derived in 1934[21] for thin-walled cylindrical shells, to a panel, and so permitted edge restraint and allowed for in-plane stretching of the plate. On this basis, if Φ is the usually defined stress function, he found that

$$\frac{1}{Et} \nabla^4 \Phi = \frac{1}{r} \frac{\partial^2 w}{\partial x^2} + K \left[\left(\frac{\partial^2 w}{\partial x \partial s} \right)^2 - \frac{\partial^2 w}{\partial x^2} \frac{\partial^2 w}{\partial s^2} \right] \tag{47}$$

where r is the radius of curvature and x and s are longitudinal and circumferential coordinates. If Φ and w are harmonic functions of x and s, the internal strain energy is

$$v = \iint \frac{1}{2} \left[\frac{Et^3}{12(1 - \mu^2)} \left(\nabla^2 w \right)^2 + \frac{1}{Et} \left(\nabla^2 \Phi \right)^2 \right] dx ds \tag{48}$$

In the case of a flat panel, the added midplane extensional terms are those of the first order squared. These are due to the elemental rotations

as shown in Reference 21. Let the initial curvature and the elastic movement of the square "flat" panel, hinged on four sides and shown in Figure 30, be respectively

$$w' = W' \sin \frac{\pi x}{L} \sin \frac{\pi x}{L}$$
$$w = W \sin \frac{\pi x}{L} \sin \frac{\pi x}{L} \tag{49}$$

Setting $1/r = 0$ shows that equation (47) is similar to the compatibility equation for the flat plate "large displacement" theory derived in 1910 by von Kármán.[22] Now further substituting

$$K = \left(1 + 2 \frac{W'}{W}\right)$$

and equation (49) into equation (46) results in

$$\nabla^4 \Phi = \frac{Et\pi^4}{L^4} \left(1 + 2\frac{W'}{W}\right) W^2 \left(\cos^2 \frac{\pi x}{L} \cos^2 \frac{\pi s}{L} - \sin^2 \frac{\pi x}{L} \sin^2 \frac{\pi s}{L}\right)$$

$$= \frac{Et\pi^4}{2L^4} (W + 2W')W \left(\cos \frac{2\pi x}{L} + \cos \frac{2\pi s}{L}\right) \tag{50}$$

When possible conditions for displacements in the plane of the plate at the edges are neglected, equilibrium in the plane of the plate is evidently satisfied if

$$\nabla^2 \Phi = \frac{Et\pi^2}{8L^2} (W + 2W')W\left(\cos \frac{2\pi x}{L} + \cos \frac{2\pi s}{L}\right) \tag{51}$$

The condition that the total work due to a virtual displacement dW vanishes is

$$dW \frac{\partial V}{\partial W} = \frac{P}{L} \int_0^L \int_0^L \frac{1}{2}\left\{\left[\frac{\partial}{\partial x}\left(w' + w + dW \sin \frac{\pi x}{L} \sin \frac{\pi s}{L}\right)\right]^2\right.$$

$$\left. - \left[\frac{\partial}{\partial x} (w' + w)\right]^2\right\} dxds \tag{52}$$

Substituting equations (48), (49), and (51) into equation (52) results in

$$P = \frac{W}{W' + W} \left[\frac{\pi^2 Et^3}{3(1 - \mu^2) L}\right]\left[1 + \frac{3(1 - \mu^2)}{8t^2} (W + 2W')(W + W')\right]$$

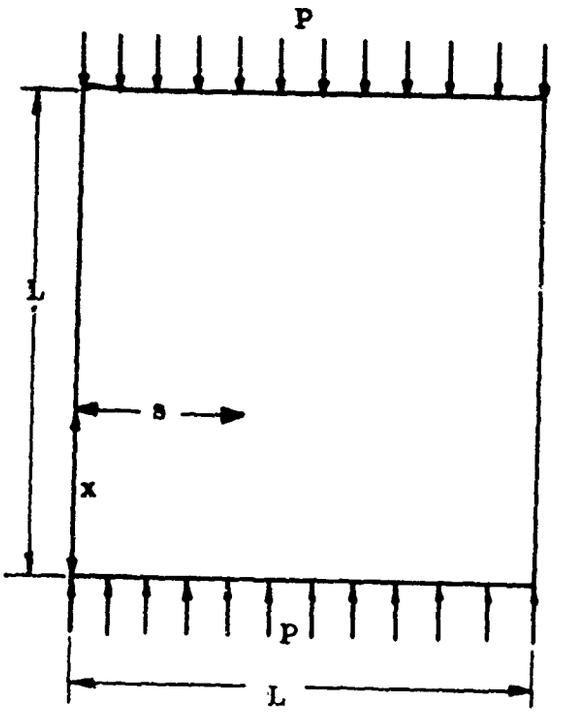

Figure 30. Square Panel Hinged on Four Sides as Considered by Donnell[7].

$$= \frac{W}{W' + W} P_c \left[1 + \frac{3(1 - \mu^2)}{8t^2} (W + 2W')(W + W')\right] \quad (53)$$

where P_c is the critical load without initial curvature.

It is clear from equation (53) that if W' and W are very small in relation to the plate thickness, then the expression

$$\Psi = \frac{3(1 - \mu^2)}{8t^2} \left[(W + 2W')(W + W')\right] \quad (54)$$

is negligible and for all practical purposes the Southwell approximation is valid. However, as the ratios of W'/t and/or W/t increase, the Southwell condition is violated. Nevertheless, if the ratio of W'/W is small, equation (53) can be written as

$$P = P_c \left[1 - \left(\frac{W'}{W}\right) + \gamma W^2\left(1 + \frac{2W'}{W}\right)\right] \quad (55)$$

where

$$\gamma = \frac{3(1 - \mu^2)}{8t^2}$$

which may be further approximated, with little error, to the expression

$$P = P_c \left[1 + \gamma W^2\right] \quad (56)$$

Thus, if a new variable is chosen such as $Z = W^2$, equation (56) may be written as

$$P = P_c(1 + \gamma z) \quad (57)$$

which, of course, is a linear equation in the variables P and z. This result is similar in form to that published by Yoshiki et al.[23,24,25] and also bears a remarkable similarity to Queinec's[38] results which are discussed later in this report. It can be visualized easily that if a graphical representation of equation (57) is made for the variables P and z, then the straight line will intercept the load axis at a value of P which corresponds to the theoretical critical load value P_c.

At this stage it is interesting to determine the bounds of applicability of the Southwell approximation in terms of the amplitude of permitted motion. For this, the important term in Donnell's equation, equation (53), is of course the expression for Ψ, equation (54). Thus, if a valid Southwell condition is to exist, this coefficient Ψ must be very small in comparison

to unity. In general, the upper bound of applicability for equation (53) would appear to occur when the square of the measured displacement is

$$(W)^2 \doteq \left[\frac{8t^2}{3(1 - \mu^2)}\right] \tag{58}$$

where $\Psi \lll 1$.

Equation (53) can be rewritten similar to the Southwell form as

$$\frac{P}{P_c}\left[\frac{W' + W}{W}\right] = 1 + \Psi$$

or

$$\left[\frac{(1 + \Psi)P_c}{P} - 1\right] W = W' \tag{59}$$

Hence, it is obvious that the numerical value of Ψ is the measure of the precision with which the Southwell Plot will predict the classical critical load. In other words, the coefficient Ψ is the error introduced into the evaluation if no bounds, other than the limitations of the original "large displacement" derivation, are placed on W (or W/t). For example, if the error is to be limited to 1 percent, then $\Psi = .01$; therefore, the upper bound placed on W is given from equation (58) as

$$(W)^2 \leq \frac{8t^2}{3(1 - \mu^2)}(.01) \tag{60}$$

Experiments conducted in the Aeronautical Structures Laboratory at Stanford University have demonstrated the validity of the Southwell approximation for plates with restrained loaded edges and simply supported unloaded edges. These results are shown in Table VIII and Table IX and in Figures 31, 32, 33, 34, and 35. They have shown that imperfection magnitude and side rail clearance are linearly related, as are imperfection values and the intensity of a central normal force. This result matches that of Fisher[10] for a column.

If further justification of the Southwell[6] linear approach for flat plates is needed, it can be obtained by reevaluation of the analytical work of Coan[26] and the experimental results of Hoff, Boley, and Coan.[27] Coan analytically investigated the buckling of rectangular isotropic plates having small initial curvature, simply supported loaded edges, and simply supported unloaded edges which were free to warp. The initial curvature was restricted to be small. The theoretical curve relating

$$\bar{P}_x/P_{cr}$$

TABLE VIII. BEHAVIOR OF A COMPRESSED 4-PLY FIBERGLAS PANEL OF 181 CLOTH - 6-IN.-BY-6-IN. LOADED EDGES CLAMPED AND UNLOADED EDGES SIMPLY SUPPORTED WITH VARIOUS SIDE RAIL CLEARANCES.

Load (lb)	Strain μ in./in.		
20	20	20	20
30	23	23	55
40	30	30	67
50	38	38	85
60	48	48	108
70	62	70	137
80	83	102	185
90	115	140	250
100	158	192	339
110	219	278	445
120	300	393	570
130	400	528	676
140	508	648	775
150	615	748	892
160	720	853	960
170	818	958	1092
180	900	1054	1175
Side Edge Clearance (in.)	0.0015	0.002	0.004

Tests conducted at Aeronautical Structures Laboratory, Stanford University.

TABLE IX. BEHAVIOR OF A COMPRESSED 4-PLY FIBERGLAS PANEL OF 181 CLOTH - 6-IN.-BY-6-IN. LOADED EDGES CLAMPED AND UNLOADED EDGES SIMPLY SUPPORTED WITH VARIOUS NORMAL FORCES APPLIED AT CENTER OF PANEL

Load (lb)	Strain Units				
0	0	0	0	0	0
20	0.40	0.80	0.80	0.80	0.80
40	0.95	1.40	1.60	1.80	2.05
60	1.50	2.15	2.50	3.10	3.55
80	2.25	3.25	3.80	4.85	5.35
100	3.30	4.60	5.45	7.20	7.75
120	4.80	6.55	7.65	10.15	10.90
140	6.95	9.25	10.80	14.20	15.00
160	10.40	13.20	15.30	19.60	20.30
180	16.20	19.30	21.40	26.40	26.90
200	25.40	27.40	29.20	34.30	34.30
Normal Force (gm)	Test 1 / 0	Test 2 / 75	Test 3 / 130	Test 4 / 190	Test 5 / 250

Tests conducted at Aeronautical Structures Laboratory, Stanford University.

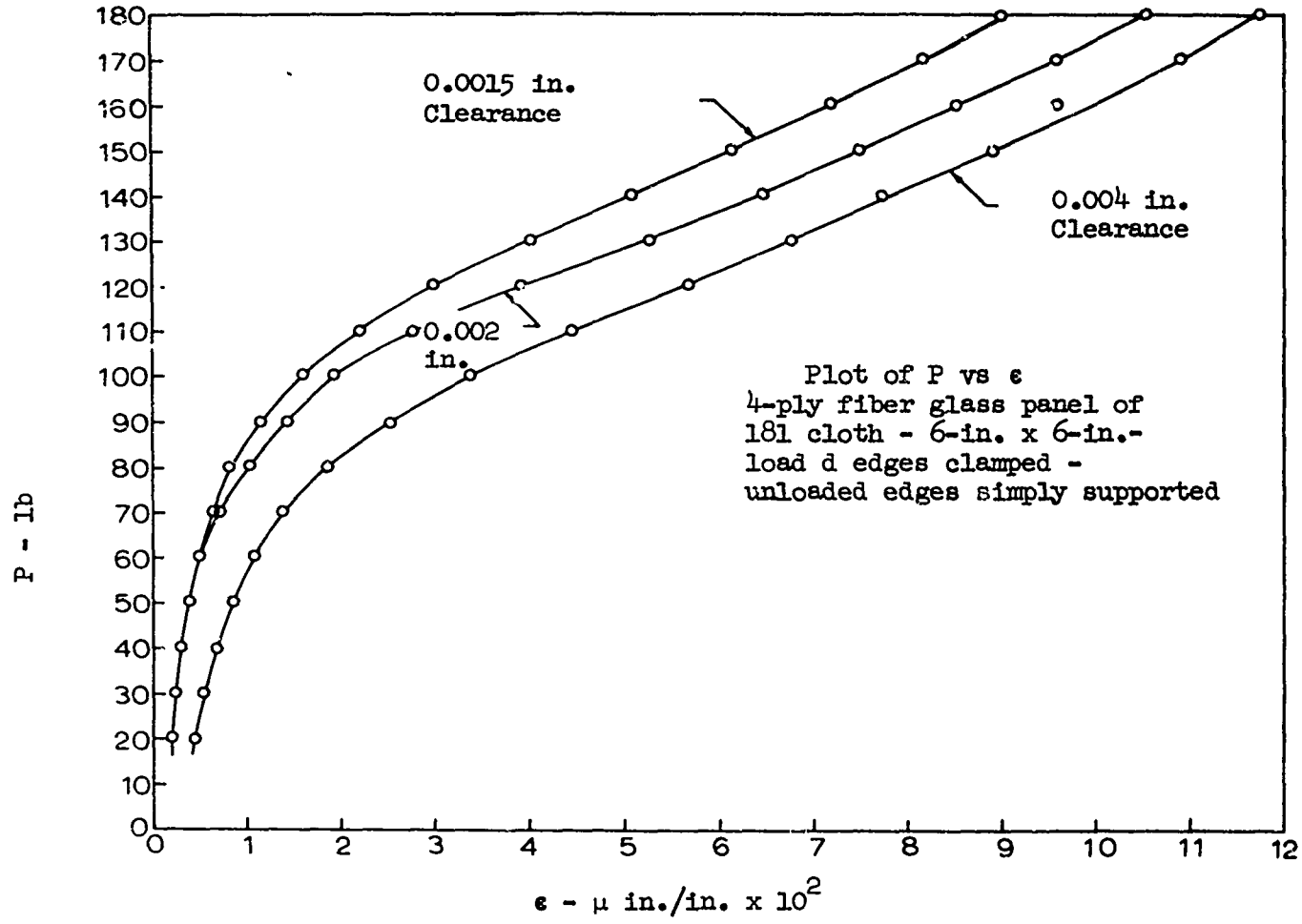

Figure 31. Buckling Tests of Fiber Glass Panels Conducted at Stanford University With Various Side Edge Clearances.

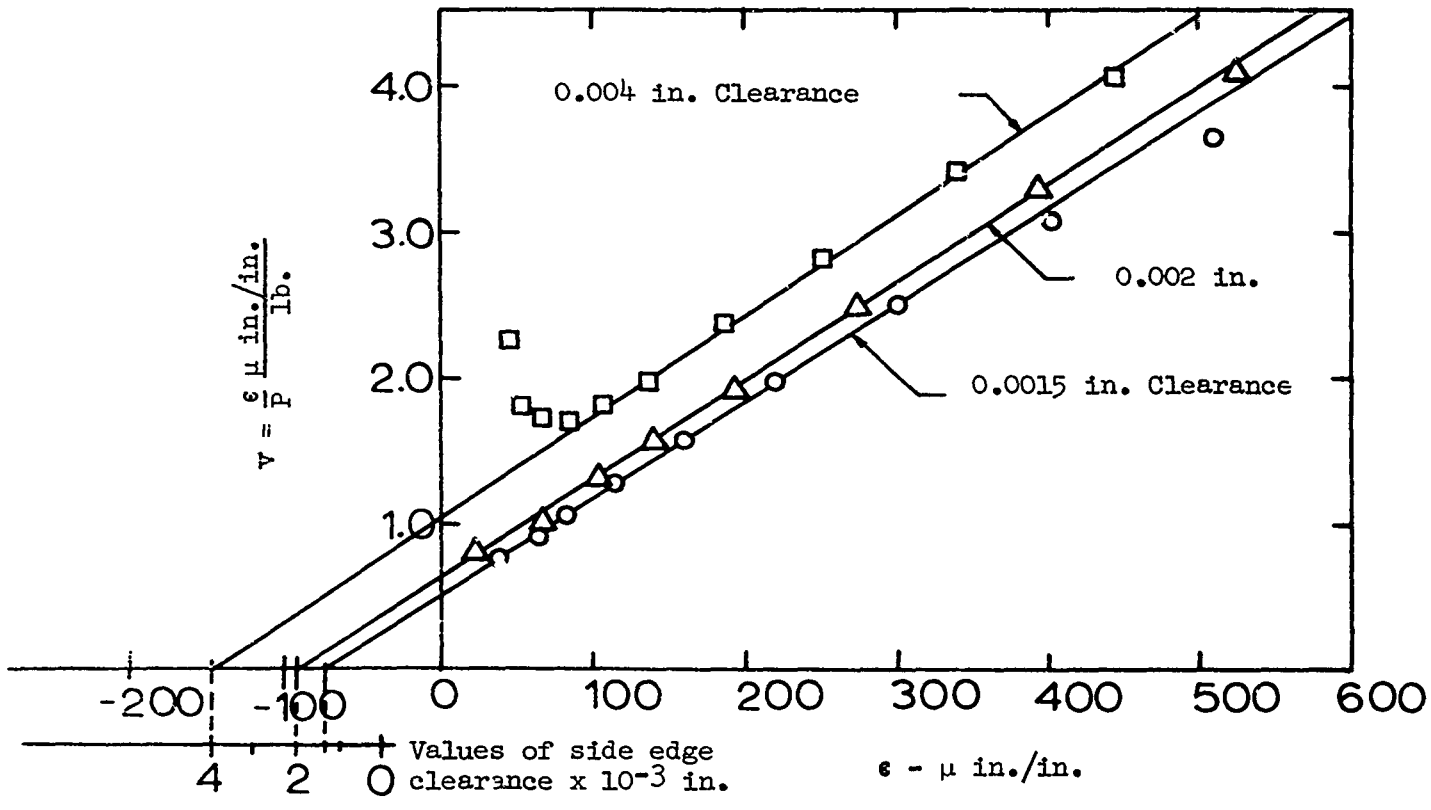

Figure 32. Southwell Plots of Data Shown in Figure 31.

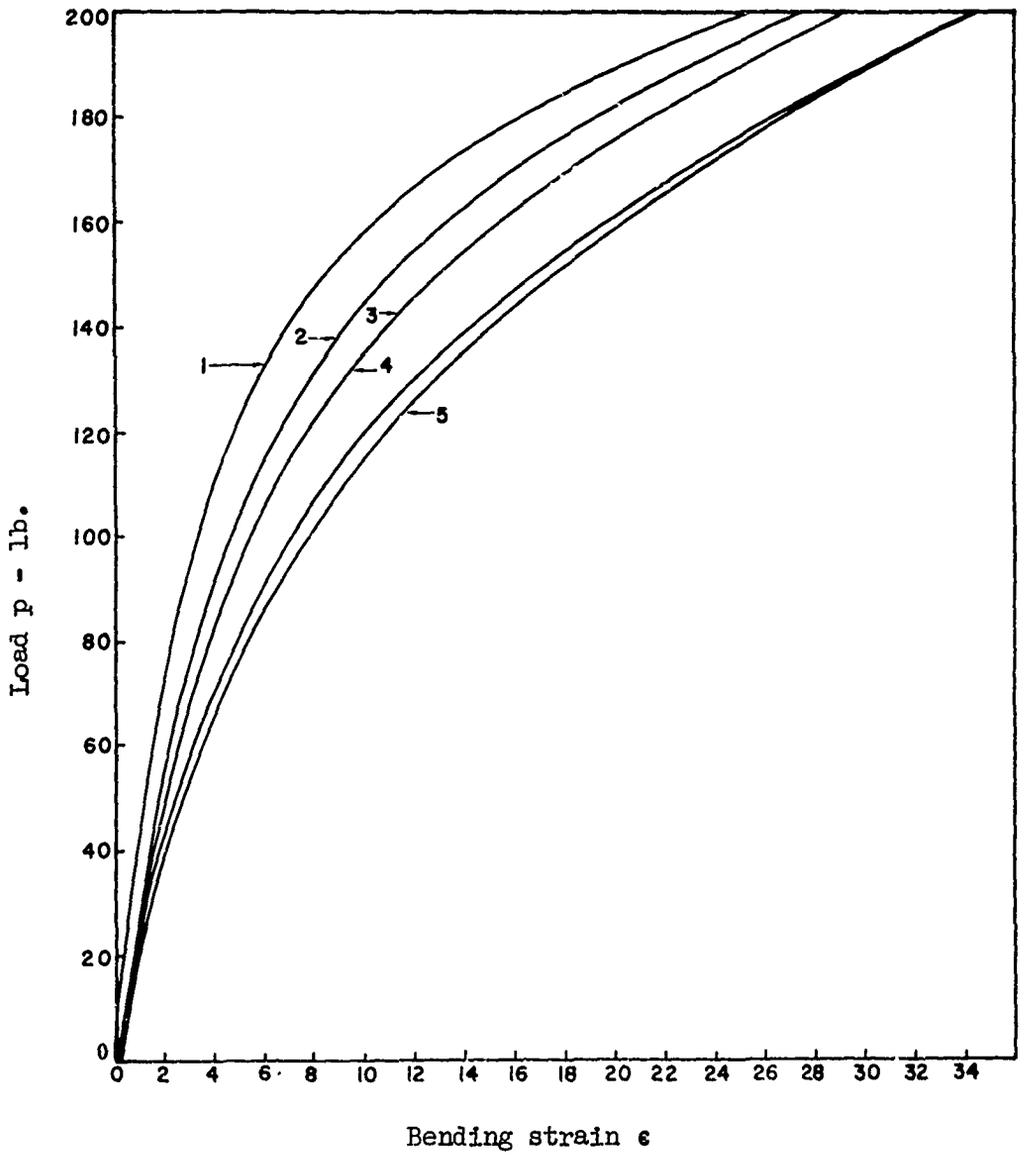

Figure 33. Buckling Tests of Fiberglas Panels With Various Values of Normal Force Conducted at Stanford University.

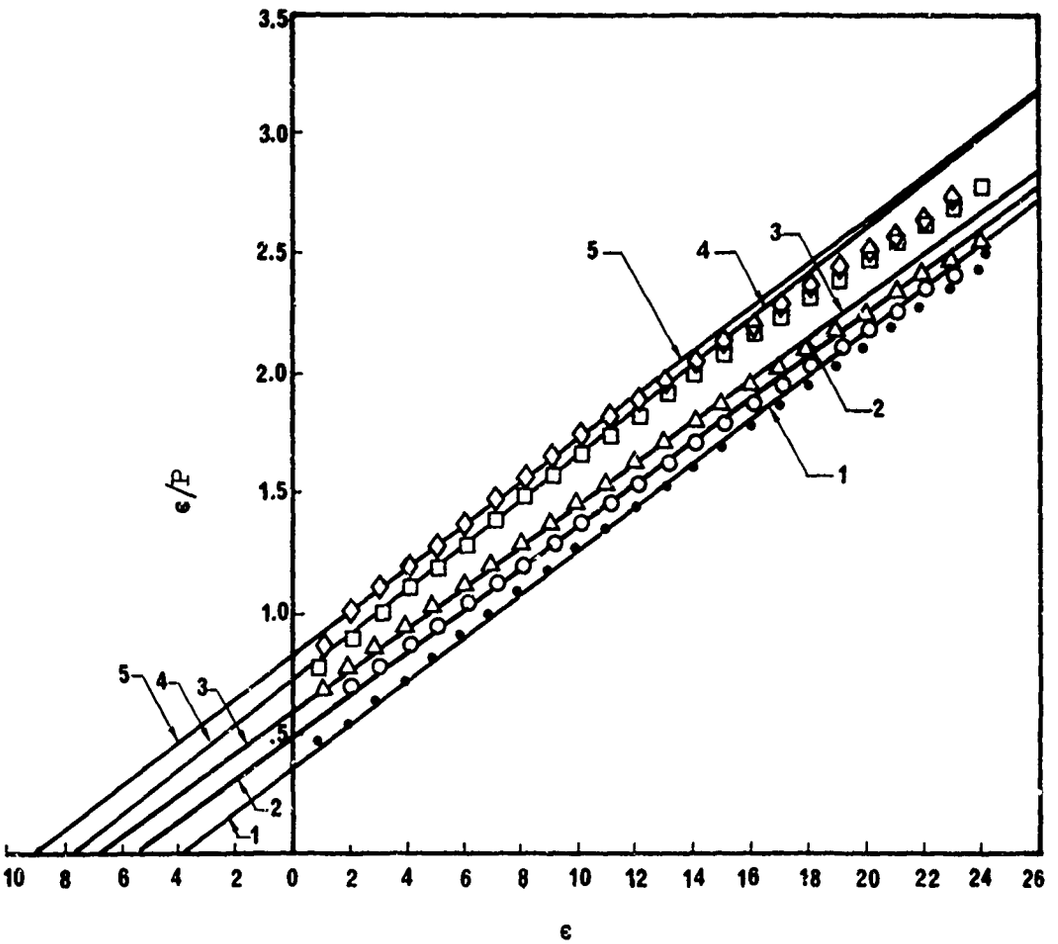

Figure 34. Southwell Plots of Data Shown in Figure 33.

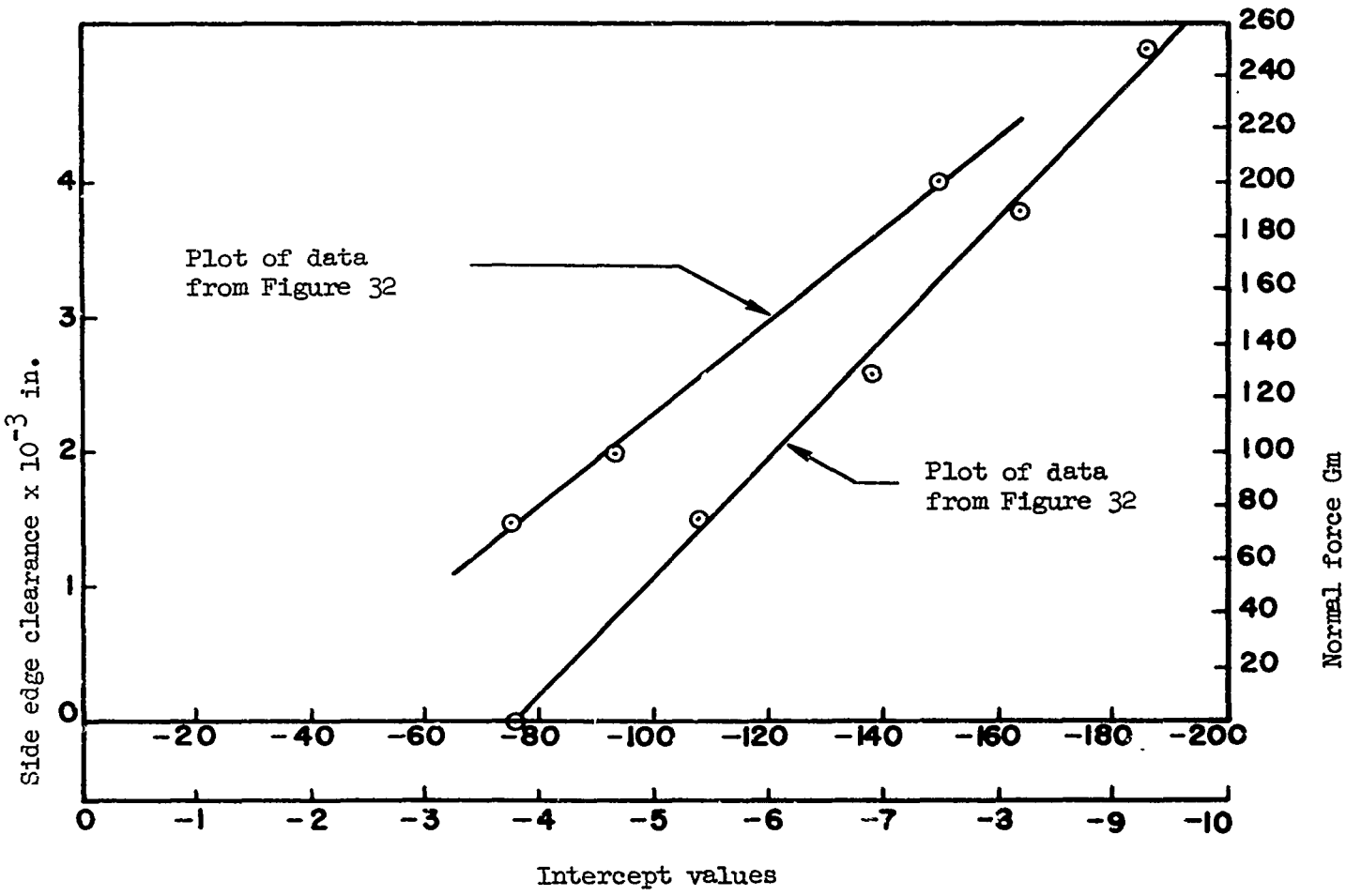

Figure 35. Plot of Side Edge Clearance and Normal Force vs Intercept Values From Figures 32 and 34.

and K_c, Figure 4 or Reference 26, where

$\bar{P}_x$ = average compressive load

P_{cr} = critical load for a perfect plate

K_c = elastic deformation at the plate center divided by the plate thickness,

was used to obtain the data listed in Table X. This information has been plotted in the Southwell manner and is shown in this form in Figure 36. The resulting straight line has an inverse slope of

$$\frac{\frac{K_c}{K_c}}{\rho} = \rho = \frac{\bar{P}_x}{P_{cr}} = 0.96 \tag{61}$$

which is within 4 percent of the classical relationship.

In the experimental work of Hoff, Boley, and Coan,[27] "flat" fiberglass plates were buckled. Lateral deflections and strains of the plates were measured and load-deflection curves as well as load-strain curves were shown. Some of the data from Figures 6, 7, 9, and 10 of the report are shown in Tables XI and XII. These data were recast in the Southwell manner and plotted in Figures 37, 38, and 39.

This technique can be applied also to the case of a biaxially loaded plate. The dimensions and coordinates are shown in Figure 40. The equilibrium equation which holds true under the assumption of a Hookean homogeneous, isotropic, and perfectly flat plate is

$$D\nabla^4 w = - N_x \frac{\partial^2 w}{\partial x^2} - N_y \frac{\partial^2 w}{\partial y^2} \tag{62}$$

when the effect of an initial deformation, w_o, is included, this equation becomes

$$D\nabla^4 w = - N_x \left[\frac{\partial^2 w}{\partial x^2} + \frac{\partial^2 w_o}{\partial x^2}\right] - N_y \left[\frac{\partial^2 w}{\partial y^2} + \frac{\partial^2 w_o}{\partial y^2}\right] \tag{63}$$

For a simply supported plate where the biaxial forces N_x and N_y are uniformly applied in the plane of the middle surface, the appropriate elastic deflection is

$$w = \sum_{m=1}^{\infty} \sum_{n=1}^{\infty} B_{mn} \sin \frac{m\pi x}{a} \sin \frac{n\pi y}{b} \tag{64}$$

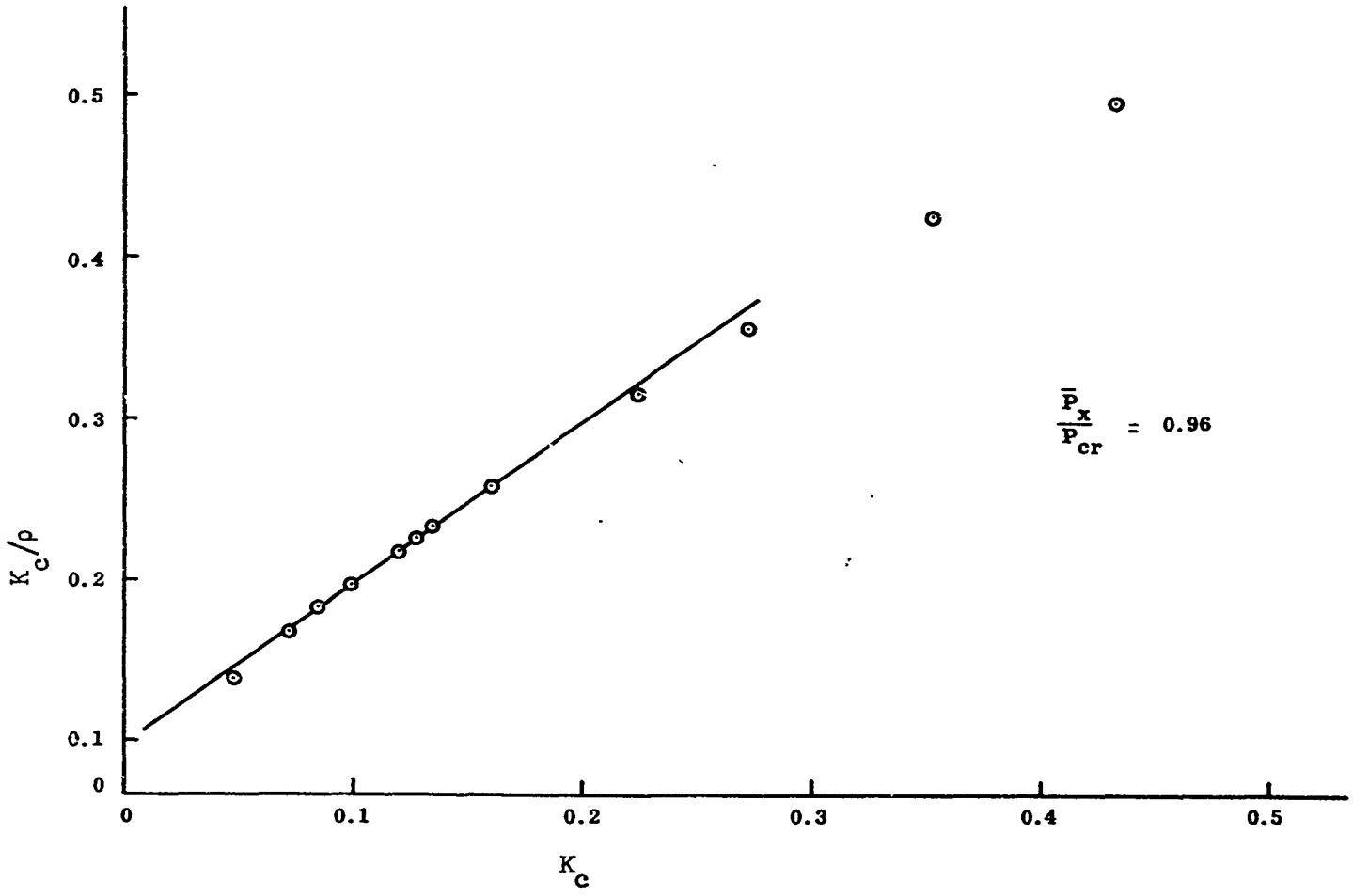

Figure 36. Southwell-Type Plot of Square Plate Buckling Theory Including Small Initial Curvature. Data Obtained From Figure 4 of Coan[26].

TABLE X. DEFLECTION BEHAVIOR OF A SIMPLY SUPPORTED SQUARE PLATE WITH SMALL INITIAL CURVATURE LOADED IN EDGE COMPRESSION, UNIFORMLY DISPLACED LOADING EDGES AND STRESS-FREE SUPPORTED EDGES

$\frac{\bar{P}_x}{P_{cr}}$	K_c	$\frac{K_c}{\frac{\bar{P}_x}{P_{cr}}}$
0	0	0
0.347	.048	0.1380
0.533	.072	0.1680
0.459	.0848	0.1850
0.500	.0983	0.1966
0.553	.1200	0.2170
0.569	.1280	0.2250
0.597	.1380	0.2310
0.621	.1600	0.2580
0.710	.2240	0.3150
0.766	.2720	0.3550
0.826	.3520	0.4260
0.871	.4320	0.4960
0.903	.5040	0.5580
0.992	.606	0.6110

Data obtained from theoretical curve, case 1, Figure 4 of Coan.[26]

TABLE XI. LOAD DISPLACEMENT DATA FOR BUCKLING TESTS ON SQUARE FIBERGLAS PANELS

P lb x 10^3	δ in.	$\overline{P - P_o}$	$\overline{\delta - \delta_o}$	$\overline{\delta - \delta_o}/\overline{P - P_o}$ $\frac{\text{in.}}{\text{lb}} \times 10^{-6}$
Panel (28a + 4c), (Data obtained from Fig. 9, Ref. 27)				
3.36	.0167	0	0	-
3.79	.0222	0.43	.0055	.0128
4.07	.0278	0.70	.0111	.01585
4.31	.0333	0.95	.0166	.0175
4.55	.0431	1.19	.0250	.0210
4.78	.0514	1.42	.0347	.0245
4.96	.0625	1.60	.0458	.0286
5.21	.0833	1.85	.0666	.0360
5.40	.1028	2.04	.0816	.0422
5.57	.1223	2.21	.1056	.0477
5.76	.1528	2.40	.1361	.0567
Panel (24d/4c), (Data obtained from Fig. 7, Ref. 27)				
4.52	.00190	0	0	-
4.83	.00240	0.31	.0005	.00160
5.31	.00344	0.79	.00154	.00195
5.86	.00495	1.34	.00305	.00177
6.38	.00715	1.86	.00525	.00282
6.83	.00990	2.31	.00800	.00346
6.92	.01070	2.40	.00880	.00366
7.07	.01237	2.55	.01047	.00412
7.32	.01430	2.80	.01240	.00443
7.65	.01730	3.13	.01540	.00492
8.07	.02090	3.55	.01900	.00535
8.52	.02450	4.00	.02260	.00565
Panel (28a + 4c), snug side edge clearance, (Data obtained from Fig. 10, Ref. 27) Test one.				
5.00	0.0227	0	0	-
5.24	.0253	0.24	.0026	.0108
5.49	.0293	0.49	.0066	.0135
5.64	.0347	0.64	.0120	.0187
5.78	.0373	0.78	.0146	.0187
5.90	.0427	0.90	.0200	.0222
6.07	.0520	1.07	.0293	.0274
6.20	.0627	1.20	.0400	.0333
6.35	.0800	1.35	.0573	.0424
6.51	.0973	1.51	.0746	.0494
6.68	.1213	1.68	.0986	.0587
6.82	.1427	1.82	.1200	.0660

TABLE XI - Continued

Test two				
5.00	.0280	0	0	-
5.24	.0333	0.24	.0053	.0221
5.49	.0387	0.49	.0107	.0218
5.64	.0440	0.64	.0160	.0250
5.78	.0507	0.78	.0227	.0291
5.90	.0587	0.90	.0307	.0341
6.07	.0747	1.07	.0467	.0436
6.20	.0933	1.20	.0653	.0544
6.35	.1175	1.35	.0895	.0663
6.51	.1440	1.51	.116	.0768
Panel (28a + 4c), approx 0.010-in. side edge clearance. Test one				
4.17	.0160	0	0	-
4.32	.0187	0.15	.0027	.0180
4.55	.0213	0.38	.0053	.0140
4.75	.0266	0.58	.0106	.0183
4.89	.0293	0.72	.0133	.0185
5.07	.0373	0.90	.0213	.0237
5.25	.0453	1.08	.0293	.0271
5.38	.0560	1.21	.0400	.0331
5.49	.0707	1.32	.0547	.0414
5.65	.092	1.48	.0760	.0513
5.78	.112	1.61	.0960	.0597
5.91	.128	1.74	.1120	.0644
Test two				
4.17	.0280	0	0	-
4.32	.0320	0.15	.0040	.0267
4.55	.0373	0.38	.0093	.0245
4.75	.0453	0.58	.0173	.0298
4.89	.0520	0.72	.0240	.0333
5.07	.0640	0.90	.0360	.0400
5.25	.0827	1.08	.0547	.0507
5.38	.0973	1.21	.0693	.0573
5.49	.116	1.32	.0880	.0667
5.65	.1373	1.48	.1093	.0738

Deflections measured at panel center.

TABLE XII. LOAD BENDING STRAIN DATA FOR BUCKLING TESTS ON SQUARE FIBERGLAS PANELS

Panel (24d/4c) (Data obtained from Fig. 6, Ref. 27)

P lb x 10^3	ϵ $\frac{in.}{in.}$ x 10^{-6}	$P - P_o$	$\epsilon - \epsilon_o$	$\frac{\epsilon - \epsilon_o}{P - P_o}$ $\frac{in.}{lb}$ x 10^{-9}
2.93	71.4	0	0	0
3.43	91.0	0.50	19.6	39.2
3.88	116.9	0.95	45.5	47.9
4.30	149.4	1.37	78.0	56.9
4.72	194.8	1.79	123.4	69.0
5.08	233.6	2.15	162.4	75.6
5.41	279.2	2.48	207.8	83.8
5.80	350.6	2.87	279.2	97.2
6.06	422.0	3.13	350.6	112.0
6.42	526.0	3.49	454.6	130.2
6.71	669.0	3.78	597.6	158.1
7.03	890.0	4.10	818.6	199.6
7.33	1078.0	4.40	1006.6	228.8
7.69	1280.0	4.76	1208.6	254.0
7.98	1448.0	5.05	1376.6	273.0

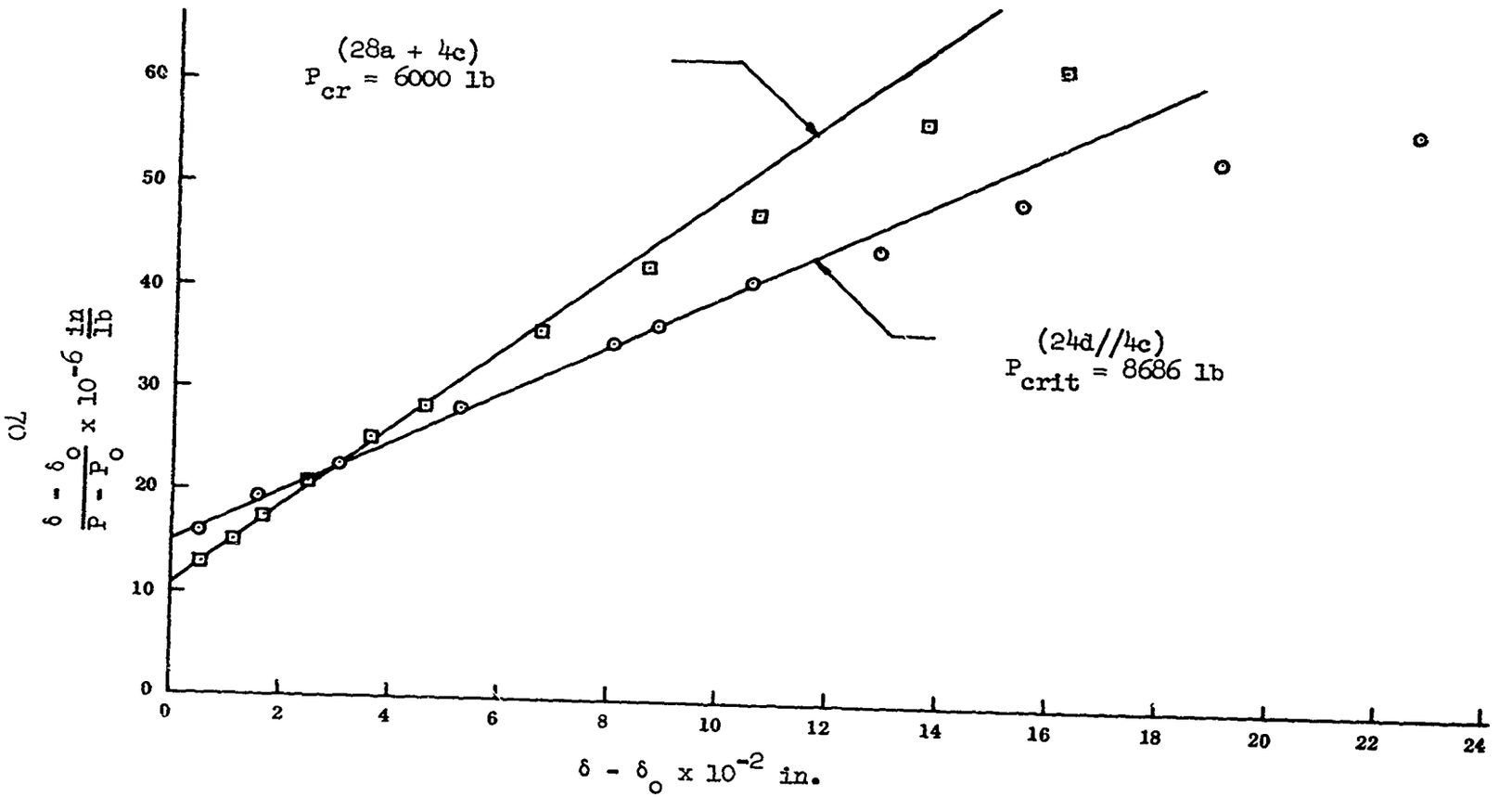

Figure 37. Southwell-Type Plot of Square Fiberglas Panels. Data Obtained From Figures 7 and 9 of Reference 27.

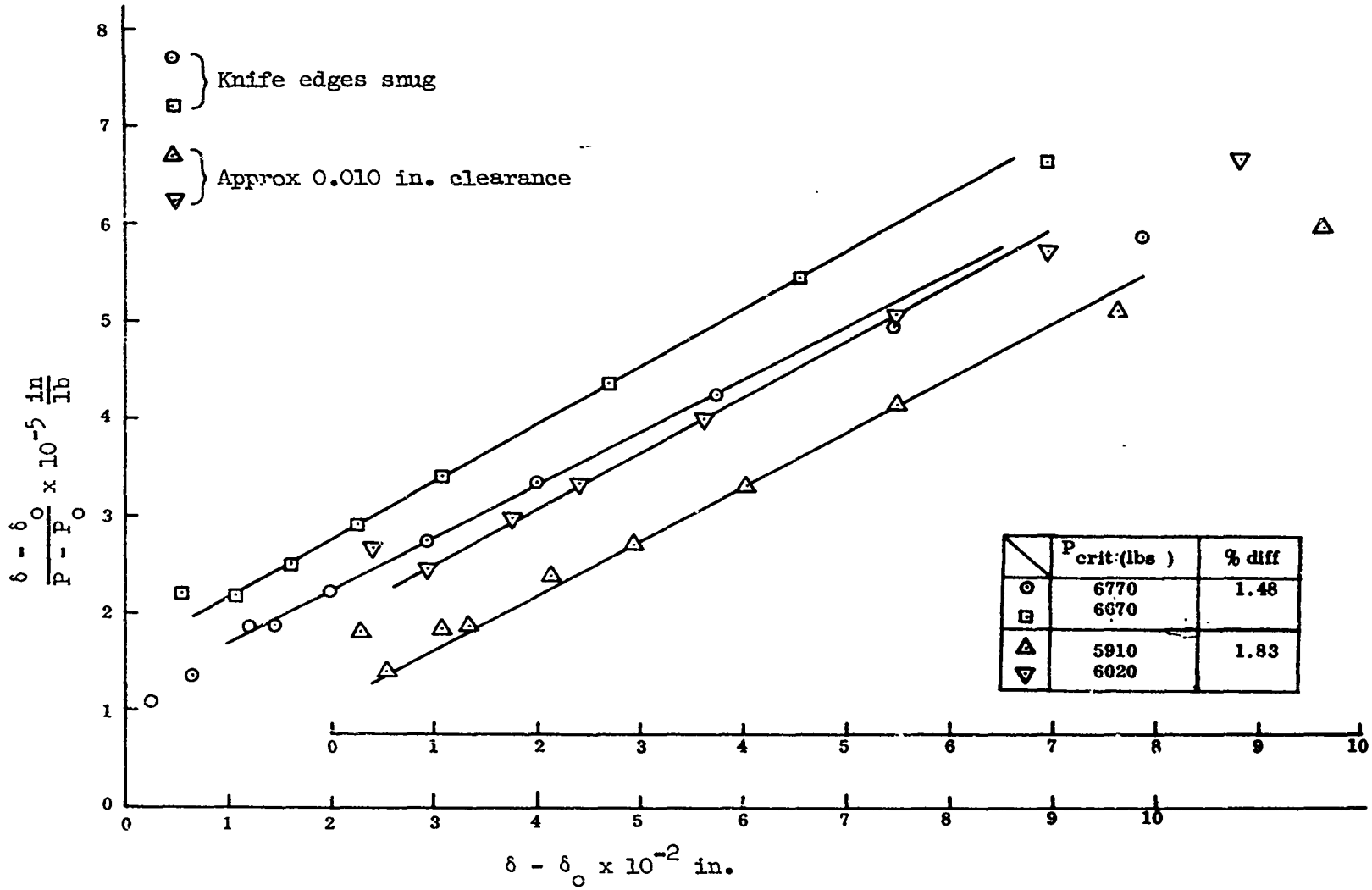

Figure 38. Southwell-Type Plots of a Square Fiberglas Panel (28a + 4c) for Different Side Edge Clearances. Data Obtained From Figure 10.

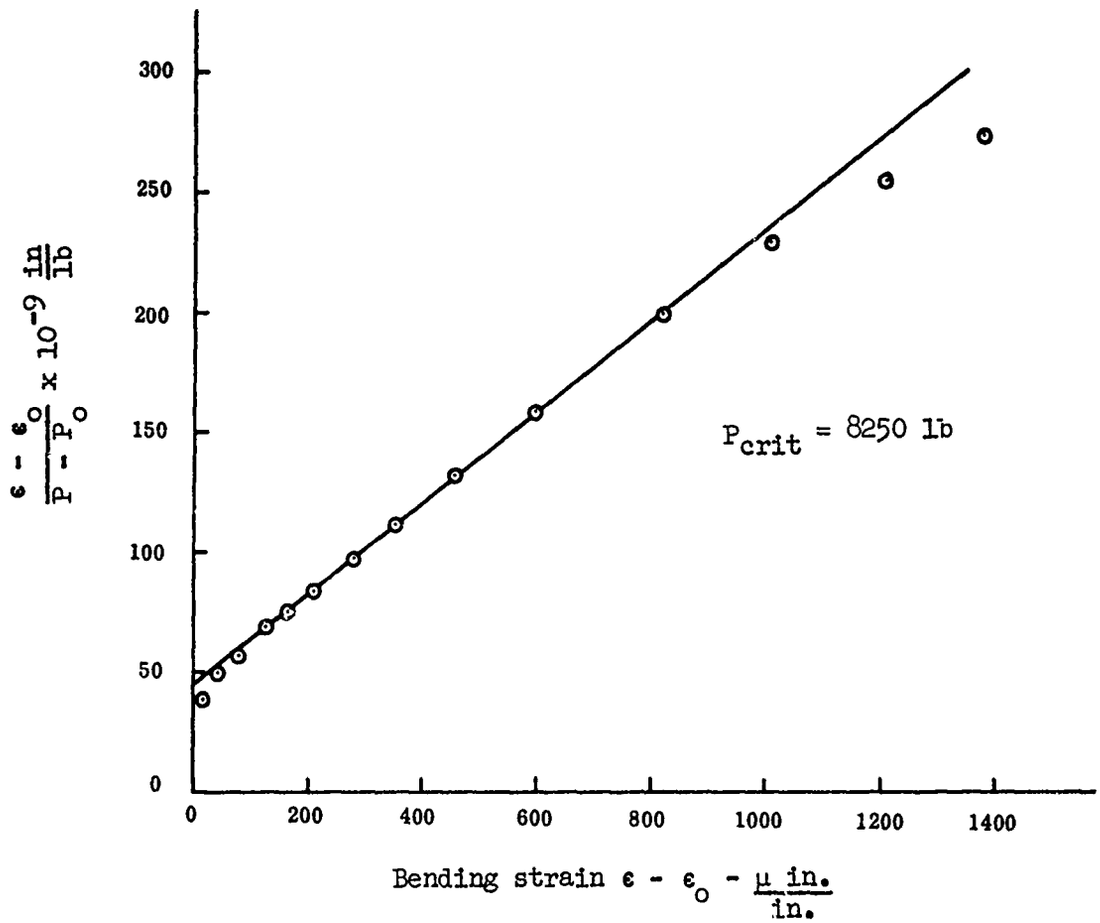

Figure 39. Southwell-Type Plot for a Square Fiberglas Panel (24d + 4c). Data Obtained From Figure 6 of Reference 27.

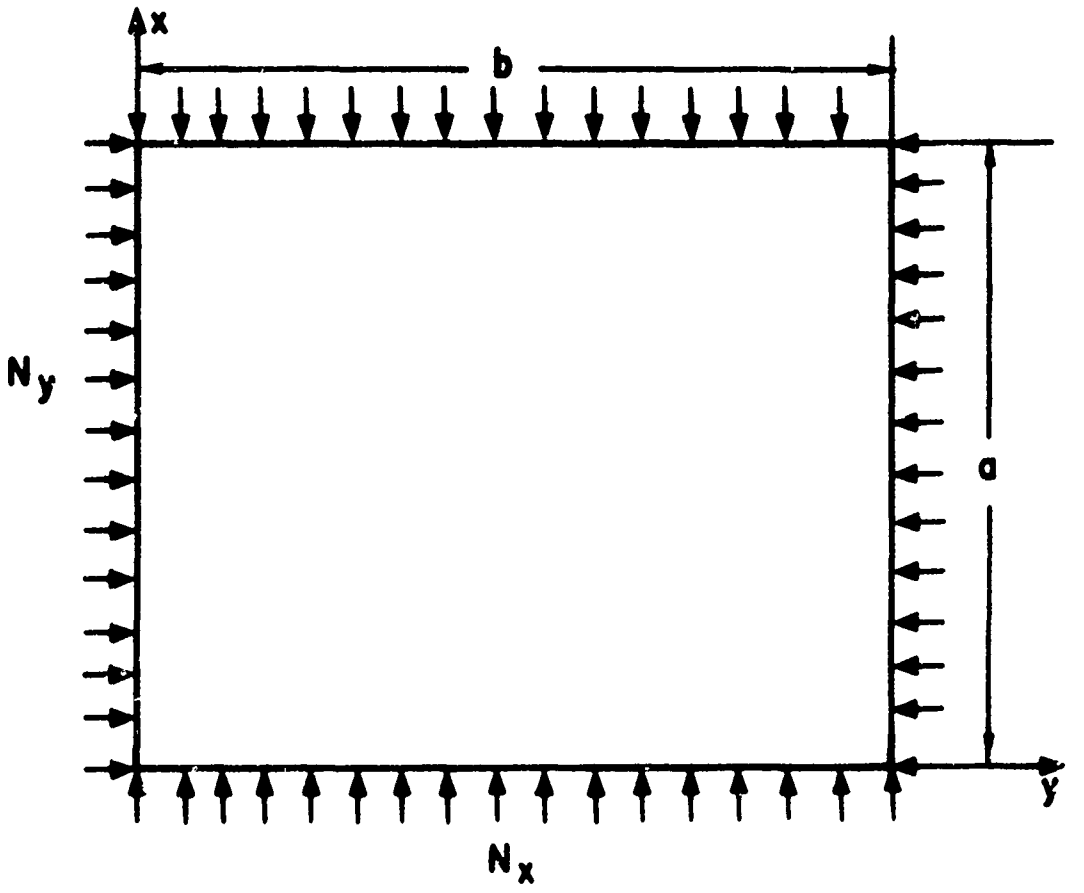

Figure 40. Rectangular Plate With Biaxial In-plane Loading.

Thus, the initial deformation is assumed to be

$$w_o = \sum_{m=1}^{\infty} \sum_{n=1}^{\infty} A_{mn} \sin \frac{m\pi x}{a} \sin \frac{n\pi y}{b} \tag{65}$$

where m and n represent the number of buckles or the number of half waves in the x and y coordinate directions, respectively. Substituting these Fourier relationships into equation (63) leads to

$$B_{mn}\left[\left(\frac{m}{a}\right)^2 + \left(\frac{n}{b}\right)^2\right]^2 \pi^4 D = \left\{N_x\left[B_{mn}\left(\frac{m\pi}{a}\right)^2 + A_{mn}\left(\frac{m\pi}{a}\right)^2\right] + N_y\left[B_{mn}\left(\frac{n\pi}{b}\right)^2 + A_{mn}\left(\frac{n\pi}{b}\right)^2\right]\right\} \tag{66}$$

This reduces to

$$B_{mn} = \frac{A_{mn}}{\dfrac{D\pi^2\left[\left(\frac{m}{a}\right)^2 + \left(\frac{n}{b}\right)^2\right]^2}{\left[N_x\left(\frac{m}{a}\right)^2 + N_y\left(\frac{n}{b}\right)^2\right]} - 1} \tag{67}$$

for

$$m = 1, 2, \ldots\ldots$$

$$n = 1, 2, \ldots\ldots$$

This equation (67), relating the amplitude of the elastic deformation, the amplitude of the assumed imperfection (a constant), the classical critical loading, and the biaxial loads, is similar in type to equation (41) for the uniaxial loading case.

For the perfect flat plate with ideal boundaries, the critical biaxial loads are directly dependent upon the aspect ratio of the plate, $\frac{a}{b}$, and are determined from the relation

$$N_x m^2 + N_y\left(\frac{a}{b}\right)^2 n^2 = \frac{D\pi^2}{a^2}\left[m^2 + \left(\frac{a}{b}\, n\right)^2\right]^2 \tag{68}$$

The critical combinations for N_x and N_y for any particular value of a/b are determined by minimization of equation (68) with respect to m and n. The usual interaction curve clearly outlining the stability bounds for an a/b = 1.0 is shown in Figure 41.

If a square plate is considered, the aspect ratio will have a value of unity, a/b = 1.0. Therefore, equation (68) becomes

$$N_x m^2 + N_y n^2 = \frac{D\pi^2}{a^2}\left[m^2 + n^2\right]^2 \tag{69}$$

The interaction for this particular case having the nondimensional form of coordinate axes of

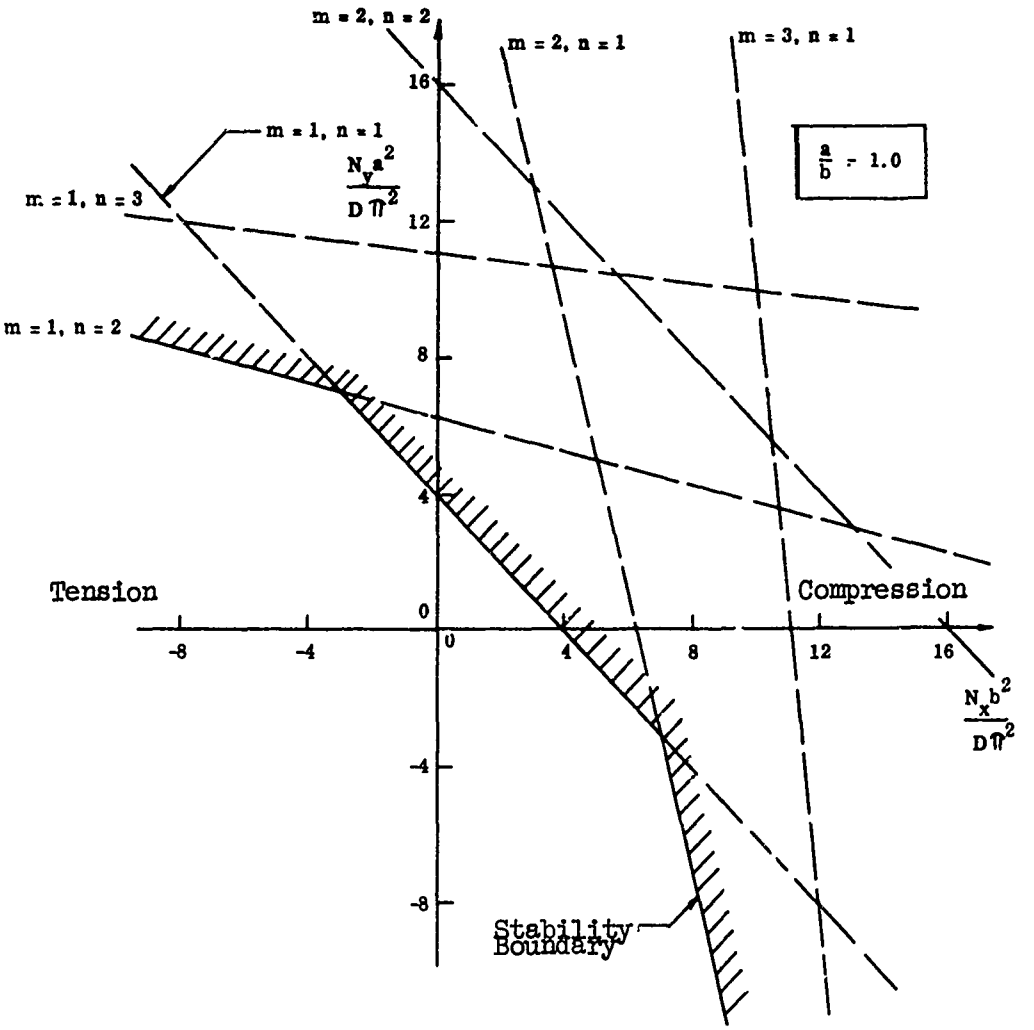

Figure 41. Interaction Curve for Determination of Stability Boundary for Biaxially Loaded Plate With Aspect Ratio a/b = 1.0.

$$\frac{N_x a^2}{D\pi^2} \quad \text{and} \quad \frac{N_y a^2}{D\pi^2}$$

is shown in Figure 41. From this graph, the classical critical loads can be determined for particular biaxial load ratios. Thus, if the loading ratio

$$K = \frac{N_x}{N_y}$$

is substituted into equation (69), the critical loading for a perfect plate would become

$$\bar{N}_{cr} = N_{x_{cr}} = \frac{D\pi^2}{a^2} \frac{[m^2 + n^2]^2}{[m^2 + \frac{1}{K} n^2]} = \frac{D\pi^2}{a^2} \frac{n^2[(\frac{m}{n})^2 + 1]}{[(\frac{m}{n})^2 + \frac{1}{K}]} \tag{70}$$

After substitution of this expression into equation (67), the elastic deflection is

$$A_{mn} = \frac{A_{mn}}{\frac{\bar{N}_{cr}}{\bar{N}} - 1} \tag{71}$$

where $\bar{N} = N_x \quad KN_y$. This implies that the loading rate in the two directions will maintain a constant proportionality. Transposing equation (71) results in

$$B_{mn}\left[\frac{\bar{N}_{cr}}{\bar{N}} - 1\right] = A_{mn} \tag{72}$$

for the particular m and n which correspond to $\bar{N}_{cr}$ obtained from Figure 41. If the values of the total in-plane loads

$$P_x = N_x a$$

$$P_y = N_y a$$

are substituted into equation (72), we obtain

$$B_{mn}\left[\frac{\bar{P}_{cr}}{\bar{P}} - 1\right] = A_{mn} \tag{73}$$

Thus, once again the relationship between the variables of the elastic deformation and the load shows a direct correspondence to the Southwell equation (14). The experimental work to check this derivation should

be completed in the very near future.

In the analysis performed above, the imperfection of the plate was considered to be an initial deformation whose shape was similar to the expected buckle mode. An alternate manner in which to consider the imperfection is to suppose that an additional transverse load is applied at some point on the plate. This technique has received attention by Loo and Evan-Iwanowski[28] in the experimental study of instability of spherical caps. Their work is discussed in our paper on shells.[29] It is, of course, validated by the tests of Fisher and by the tests reported here on panels.

Turner, Martin, and Weikel[30,31] numerically examined a biaxially loaded plate with such an added normal force. Their computer results are listed in Table XIII and depicted graphically in Figure 42. These computed points are essentially collinear. This result tends to give credence to the suggestion that a knowledge of the nature of the basic imperfection is not of importance if it is desired merely to confirm the theory for perfect bodies. It is obviously of importance in the compilation of data designed to help in the formulation of practical theories of real structures.

Real structures, of course, are very rarely subjected to uniformly distributed loadings or restrained in the simple manner considered so far. Walker[32] has made a substantial effort to consider flat plates under conditions which more closely approximate those encountered in actuality. His study has been directed toward the establishment of a stability theory for plates axially compressed by nonuniformly distributed load. In the analysis performed, a wide range of possible boundary conditions was taken into account. The theoretical treatment was evaluated in the laboratory. The tests which were performed and reported in the given reference appear to be very thorough, well conducted tests. In the analysis of the data derived, Walker demonstrated that a linear relationship existed between δ and δ/P, but he offered no analysis to confirm that this was so. Typical results are given in Figure 43. In presenting the results, the author pointed out that the correlation of the theoretical critical load value and the instability level predicted from the analysis of the test is very good. This can be seen from the graphs in Figure 44.

However, it must be admitted that while flat plates do play an important part in everyday structures, generally, conditions are more complex. In aeronautics, combinations of plate and column (Usually called a stringer in this application) are frequently met. The testing of components of this type is fraught with all the difficulties of the simpler cases. Ramberg, McPherson, and Levy[33] have carried out an experimental study of this problem. In their analysis of the test data, they applied a Southwell-type plot. They demonstrated, as is clearly seen in Figures 45 through 48, that it gave good results for stringers attached to sheets, irrespective of their failing mode. They were unable to apply the process to the sheet between stringers due to the lack of appropriate data prior to the instability value.

TABLE XIII. COMPUTER RESULTS - RECTANGULAR PLATE STABILITY PROBLEM

Step	$\Delta\sigma$, psi	$\sigma=\sum\Delta\sigma$	Δw at $x = y = 0$	$\sum\Delta w$	$w^* = \sum\Delta w - 0.00575$	$\frac{w^*}{\sigma} \times 10^6$
1	0	0	0.00575	0.00575	0	
2	100	100	0.000587	0.006337	0.00059	5.9
3	100	200	0.000736	0.007073	0.00132	6.6
4	100	300	0.000951	0.008042	0.00227	7.6
5	100	400	0.001287	0.009311	0.00356	8.9
6	100	500	0.001836	0.011147	0.00540	10.8
7	100	600	0.002823	0.013970	0.00822	13.7
8	100	700	0.004922	0.018892	0.01314	18.7
9	100	800	0.010558	0.029450	0.02370	29.6

* Reference 31

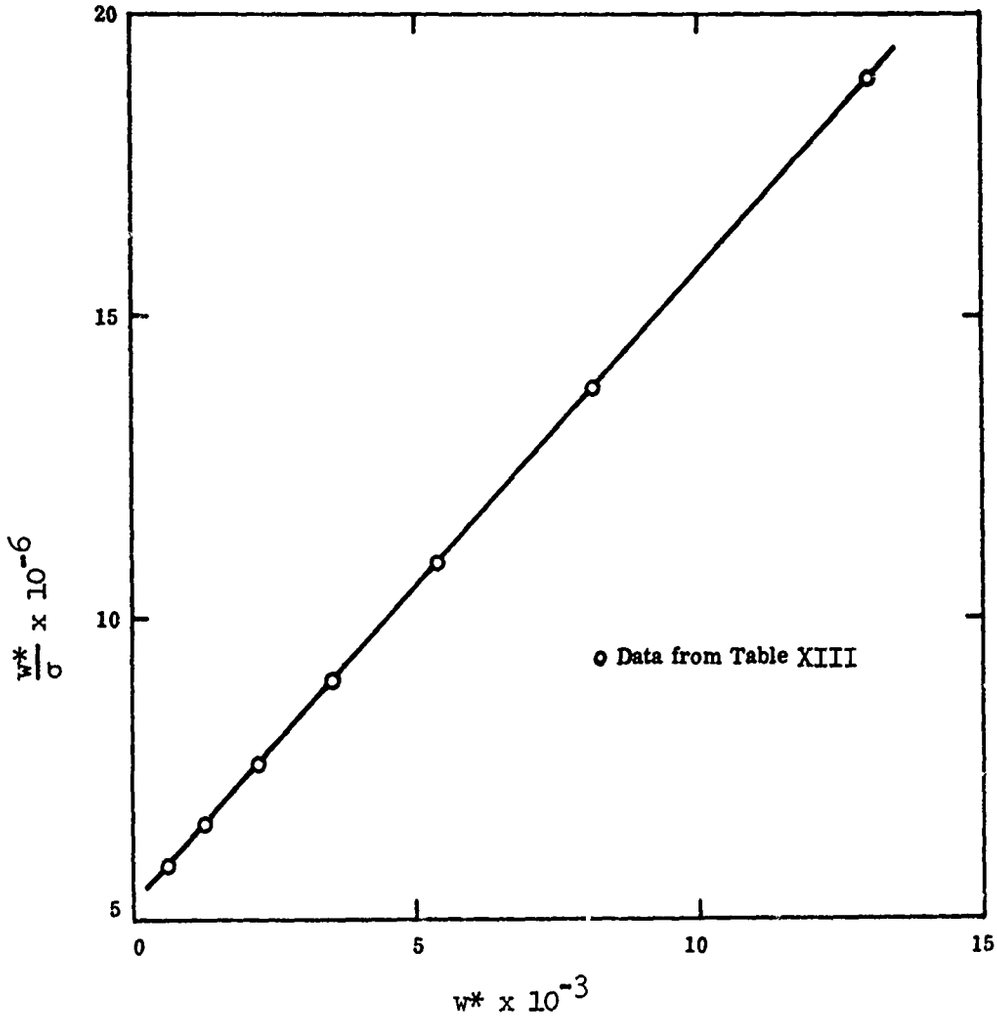

Figure 42. Southwell Plot for Biaxially Loaded Plate. Computed Data Points From Reference 31.

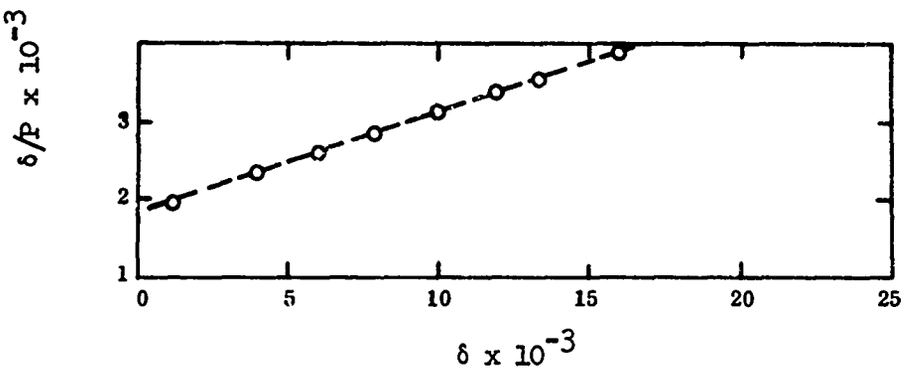

Figure 43. Southwell Plot of Nonuniformly Loaded Plate as Given by Walker[32].

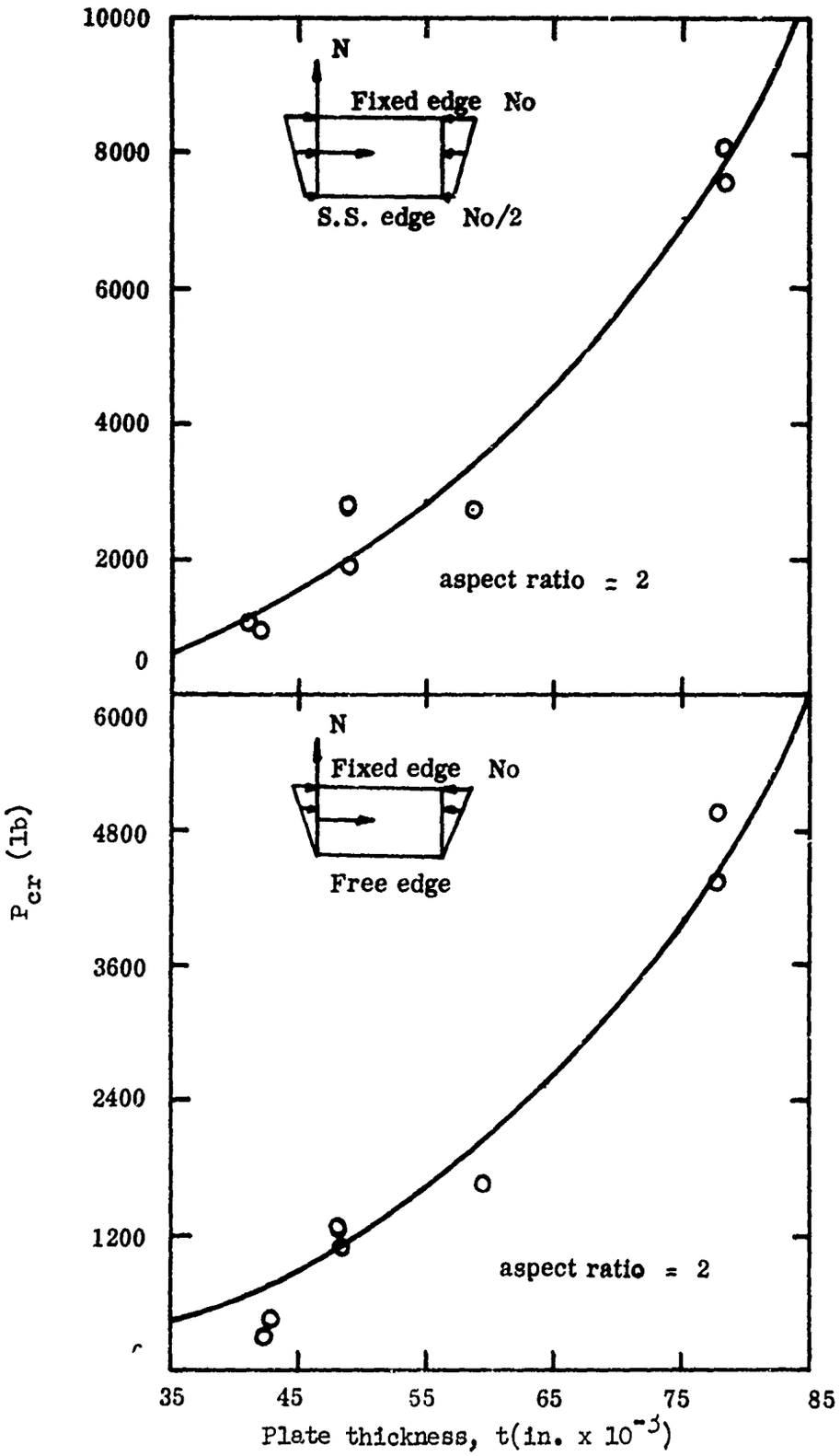

Figure 44. Comparison of Experimental Results and Theory. Data Points Depict the Critical Load Determined From Southwell Plots From Reference 32.

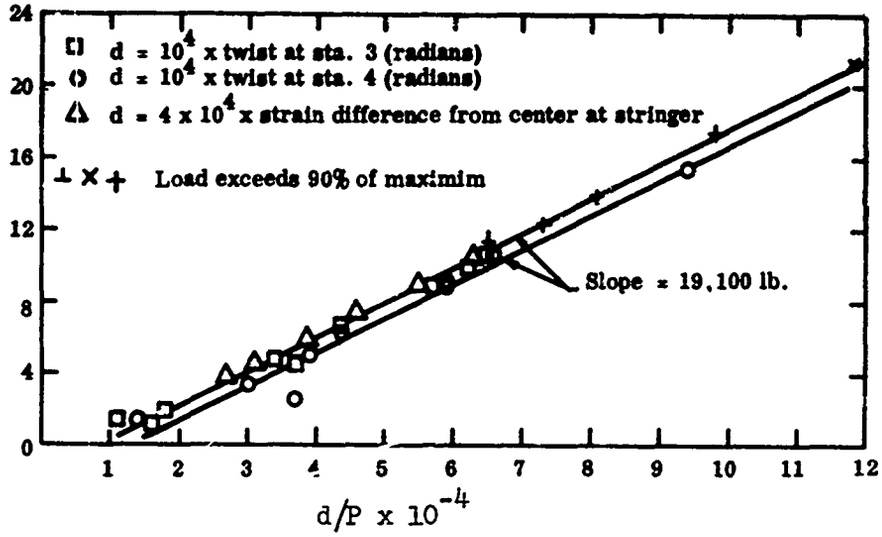

Figure 45. Southwell Plot of Twisting Instability of Short Z-Type Stringer From Reference 33.

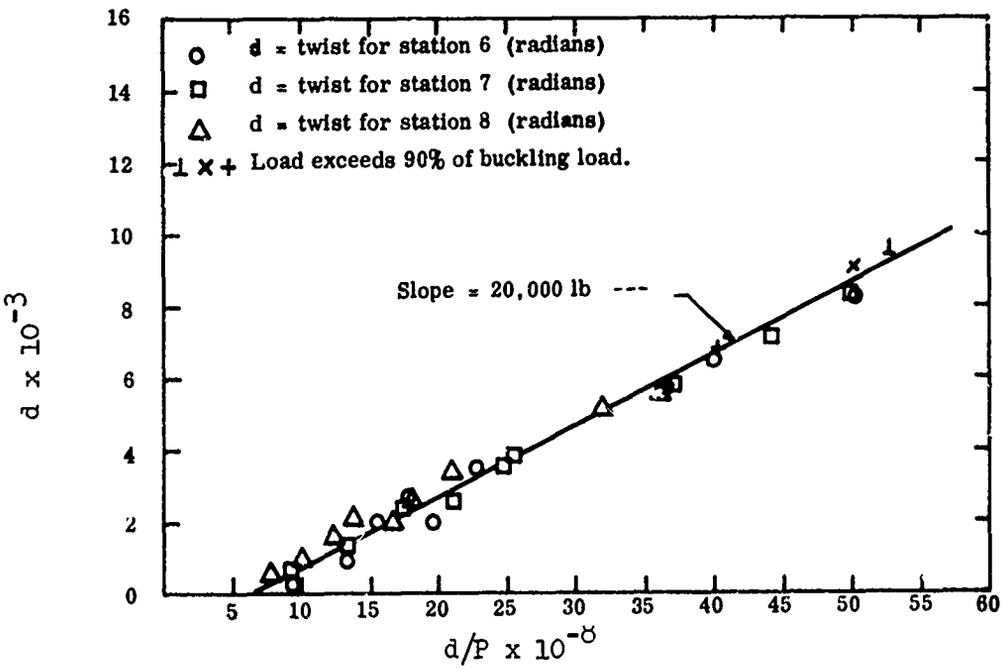

Figure 46. Southwell Plot of Twisting Instability of Stringer of Specimen 6 From Reference 33.

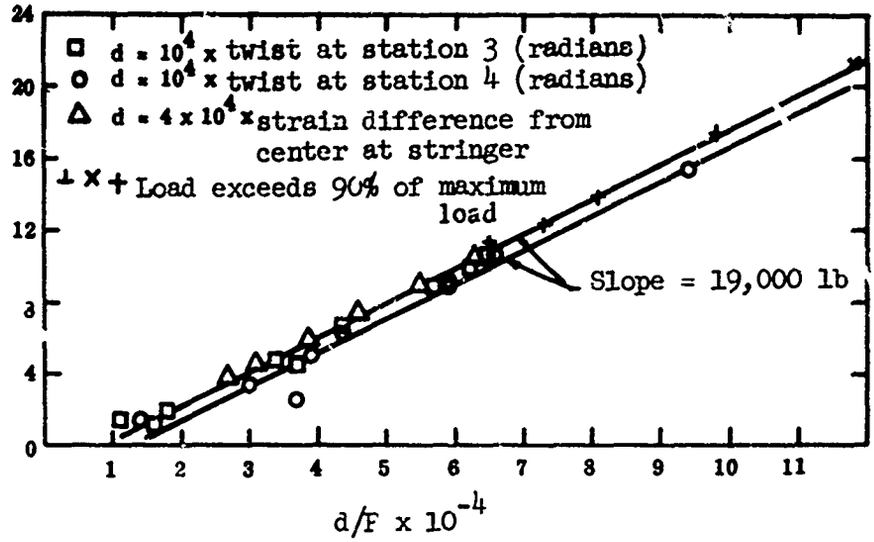

Figure 47. Southwell Plot for Stringer Instability From Reference 33.

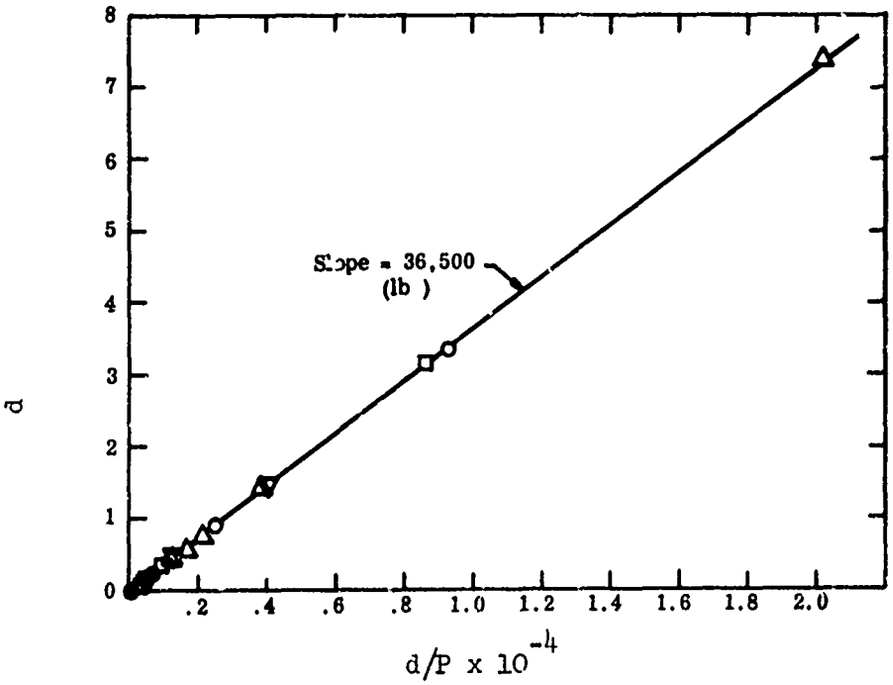

Figure 48. Southwell Plot for Stringer A of Specimen 1 of Reference 33.

Generally speaking, references to the Southwell Plot define the displacement parameter as a motion normal to the direction of loading. However, it is relatively simple to demonstrate that there is a one-to-one correspondence between this deflection and some strain parameter in the plane of the body. The first report to utilize this point was that of Tuckerman.[15] Indeed, in the harmonic test previously discussed with respect to his report, the determination of the Southwell Plots was made using strains on the surface of the column. The linear relationship between normal displacement and elastic bending component strains for flat plates is demonstrated here in Figure 49 from tests made in conjunction with the flat plate studies conducted at Stanford University and those previously mentioned. The use of the Southwell Plots based upon strain measurements also has been outlined and verified by Gregory [34,35,36,37] for application to struts.

Thus, concern has been mainly with elastic structural instabilities which have been produced by usual force systems. However, in 1961 Queinec[38] analytically studied the behavior of a centrally heated "flat" circular plate with free edges and checked these results experimentally. In the course of his work, he treated the problem using both the linear and nonlinear theories. A most important step was taken when the author correlated the test results with theory. He revealed, on the basis of linear plate theory which included the possibility of a constant initial geometric imperfection, the validity of the Southwell Plot for this particular loading. Also, a deflection-squared law (δ^2) was derived using the large displacement analysis and this was correlated with some experimental data.

The basis of Queinec's analyses is as follows. The temperature distribution and edge conditions were assumed to be perfectly axisymmetric. The plate was considered to be of uniform thickness, at uniform temperature, and free from stresses in its initial state. The temperature variation through the thickness was neglected, as was the effect of gravity forces. The usual bending theory assumptions were made.

The general equations of plate bending (Kármán equations) modified for temperature effects were used.

$$\frac{D}{t}\nabla^2\nabla^2 w = \frac{\partial^2 U}{\partial y^2}\frac{\partial^2 w}{\partial x^2} + \frac{\partial^2 U}{\partial x^2}\frac{\partial^2 w}{\partial y^2} - 2\frac{\partial^2 U}{\partial x \partial y}\frac{\partial^2 w}{\partial x \partial y}$$

$$\nabla^2\nabla^2 U = -\nabla^2 E\,\epsilon_T + E\left[\left(\frac{\partial^2 w}{\partial x \partial y}\right)^2 - \frac{\partial^2 w}{\partial x^2}\frac{\partial^2 w}{\partial y^2}\right] \qquad (74)$$

These equations, transformed into polar coordinates and reduced for the axisymmetric case, are

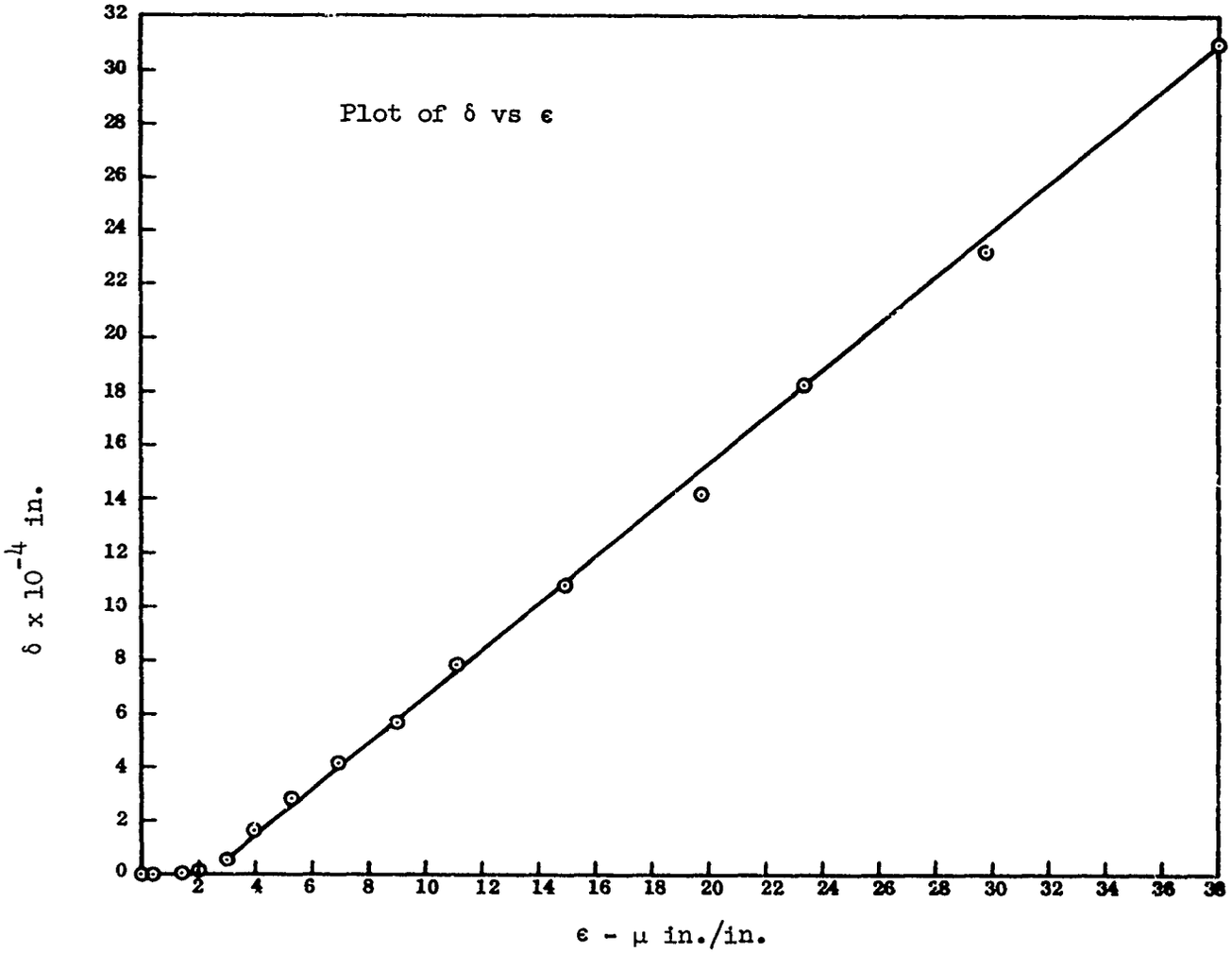

Figure 49. Central Lateral Deflection vs Bending Strain of Square Fiberglas Plate Under Uniaxial Compression.

$$\frac{D}{t}\nabla^2\nabla^2 w = \frac{1}{r}\frac{d}{dr}\left(\frac{dU}{dr}\frac{dw}{dr}\right)$$

$$\nabla^2\left[\nabla^2 U + E\,\epsilon_T\right] + E\,\frac{1}{r}\frac{dw}{dr}\frac{d^2w}{dr^2} = 0 \qquad (75)$$

or these two equations can be written as

$$\frac{1}{r}\frac{d}{dr}\left\{r\frac{d}{dr}\left(\nabla^2 U + E\,\epsilon_T\right)\right\} + \frac{E}{r}\frac{d}{dr}\left\{\frac{1}{2}\left(\frac{dw}{dr}\right)^2\right\} = 0$$

$$\frac{1}{r}\frac{d}{dr}\left\{\frac{dU}{dr}\cdot\frac{dw}{dr}\right\} - \frac{D}{t}\cdot\frac{1}{r}\cdot\frac{d}{dr}\left\{r\frac{d}{dr}\left(\nabla^2 w\right)\right\} = 0 \qquad (76)$$

where

U = the usual Airy stress function for circular plates[39]

D = flexural stiffness $\dfrac{Et^3}{12(1-\mu^2)}$

w = lateral deflection

t = plate thickness

∇^2 = $\dfrac{\partial^2(\ )}{\partial x^2} + \dfrac{\partial^2(\ )}{\partial y^2} = \dfrac{1}{r}\dfrac{d}{dr}\left[r\dfrac{d(\ )}{dr}\right]$

ϵ_T = αT, the thermal strain.

Unfortunately, these coupled nonlinear differential equations have no closed form solutions except for very special cases; i.e.

$\sigma r = 0$ (no membrane stresses) or

$\dfrac{dw}{dr} = 0$ (plane stress problem).

So Queinec utilized the well-known energy method for determining the approximate critical temperature for both the linear and nonlinear theories.

Because his experiments revealed that lateral deflections occur well below the critical value of temperature, he realized that these plates were not absolutely flat. Hence, Queinec considered the effect of initial imperfections. The initial deflection was assumed to be axisymmetric and was defined by $w_i(r)$. When the initial temperature is uniform and the initial state is free from stresses, the additional deflection $w(r)$ is a solution of the differential equation

$$\frac{d}{dr}\left[\frac{1}{r}\frac{d}{dr}\left(r\frac{dw}{dr}\right)\right] = \frac{\sigma r^{t}}{D} \cdot \frac{d}{dr}(w + w_i) \qquad (77)$$

where

σr = stress due to temperature rise $T(r) = T_o(\theta)$

and this equation is valid for small deflections. Equation (76) is no longer homogeneous. When the initial imperfection is proportional to the elastic deflection, the following expression is obtained from equation (77):

$$\frac{T_{crit}}{T_o} = 1 + \frac{w_{io}}{w_o}$$

This relationship can also be written as

$$w_o\left[\frac{T_{crit}}{T_o} - 1\right] = w_{io} \qquad (78)$$

which of course has the identical graphical form of the Southwell Plot. This researcher was probably the first to investigate the case when the imperfection and the additional deflection were not of the same form. Using the energy equation, he derived the following expression:

$$\frac{T_{crit}}{T_o} = 1 + \frac{\int_o^1 \theta \frac{dw_o}{dr}\frac{dw_{io}}{dr} \cdot \rho \cdot d\rho}{\int_o^1 \theta \left(\frac{dw_o}{dr}\right)^2 \cdot \rho \cdot d\rho} \qquad (79)$$

where $\rho = r/a$ (a = radius of plate)

$$\theta = \frac{1}{\rho^2}\int_o^{\rho} \frac{T}{T_o} \cdot \rho \cdot d\rho - \int_o^1 \frac{T}{T_o} \cdot \rho \cdot d\rho \qquad (80)$$

The subscripts denote particular radial positions; thus, T_o is the temperature at $r = 0$. Queinec then showed that this equation reduces to

$$\frac{T_{crit}}{T_o} = 1 + K_1 \cdot \frac{w_{io}}{w_o} \qquad (81)$$

where the coefficient K_1 depends only on the initial shape. Equation (81) reduces once again to

$$w_o \left[\frac{T_{crit}}{T_o} - 1\right] = K_1 \cdot w_{io} \tag{82}$$

This equation then is similar to equations (78) and (14). All three are equal to constants.

The central temperature versus the central deflection or specimens numbers one and two is plotted in Figure 50. The corresponding Southwell Plots are illustrated in Figure 51. The critical temperature for the center of the plate determined from this Southwell Plot is $T_{o_{crit}} = 59^\circ F$. This shows a 7.8-percent difference from the value determined from the energy approximation which is normally unconservative. Therefore, this percent of difference should actually be smaller when compared to an exact solution.

The author appears to have been the first to realize that it was possible to develop a relationship between the postbuckling deformations and the initial buckling load. For the problem which he considered, he derived the following equation:

$$\frac{T_o - T_{crit}}{T_{crit}} = K_2 \left[\frac{w_o}{t}\right]^2 \tag{83}$$

where T_o and w_o are the midpoint temperature and displacement, respectively, T_{crit} is the critical temperature and K_2 is a constant.

In a report published in 1962 by Fernandez-Sintes, Horton, and Hoff,[40] dealing with the thermal buckling of annular plates, the Southwell plot was used to correlate the derived theoretical results with the test data.

Moiré fringe techniques were used to measure the lateral deflections when the plate was heated in an axisymmetric manner. The test setup is shown in Figures 52, 53, and 54.

The relationship derived by Queinec and just discussed, equation (82), was utilized by these researchers to compare the experimental results. Figures 55, 56, and 57 show the curves of central edge temperature and central edge deflection versus time for the three test specimens. The corresponding Southwell plots are shown in Figures 58, 59, and 60. The values of critical temperature determined from these graphs were, respectively,

$$(T_{crit})_1 = 127^\circ F$$

$$(T_{crit})_2 = 120^\circ F$$

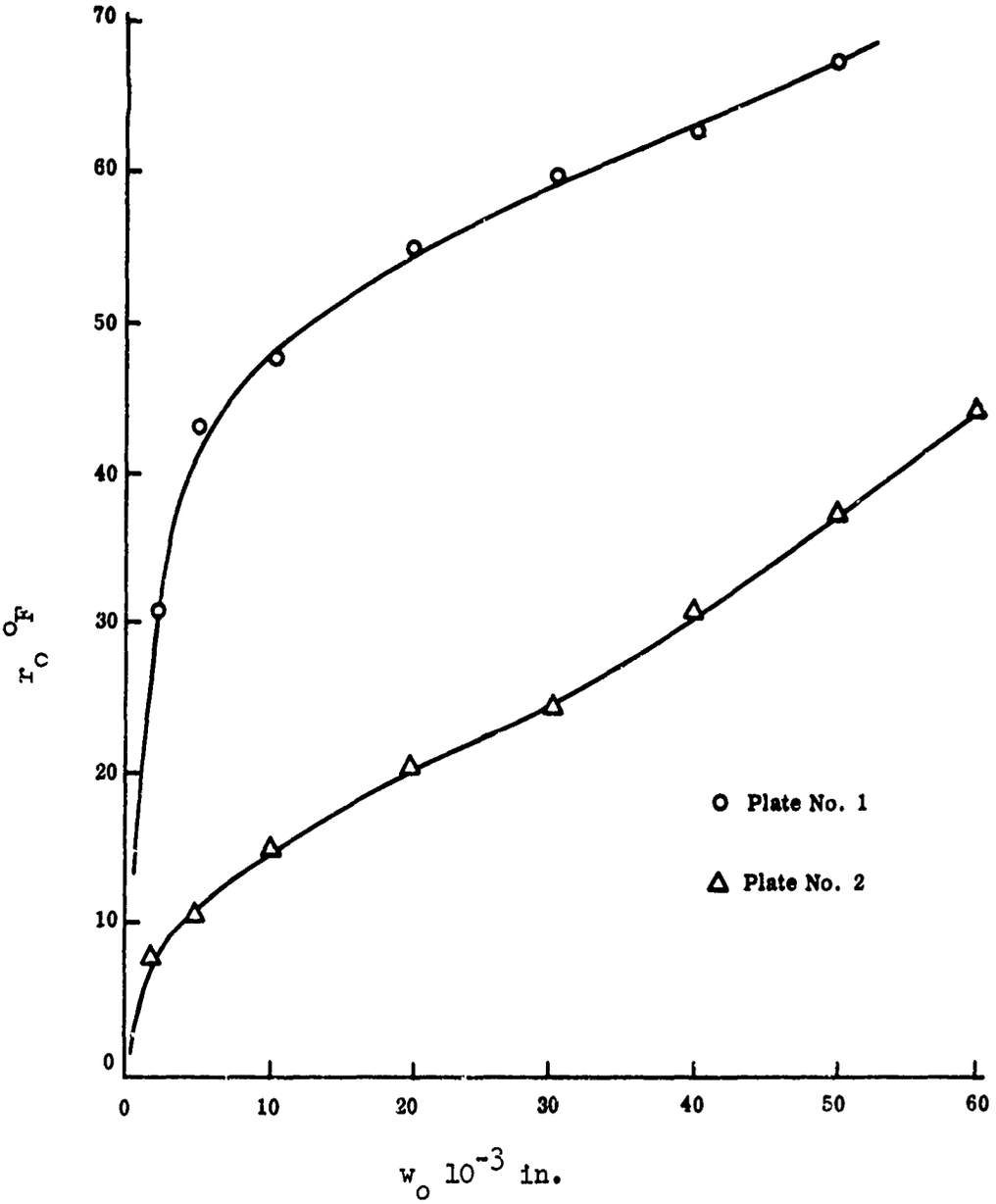

Figure 50. Plot of Central Temperature vs Central Deflection for Specimens One and Two From Reference 38.

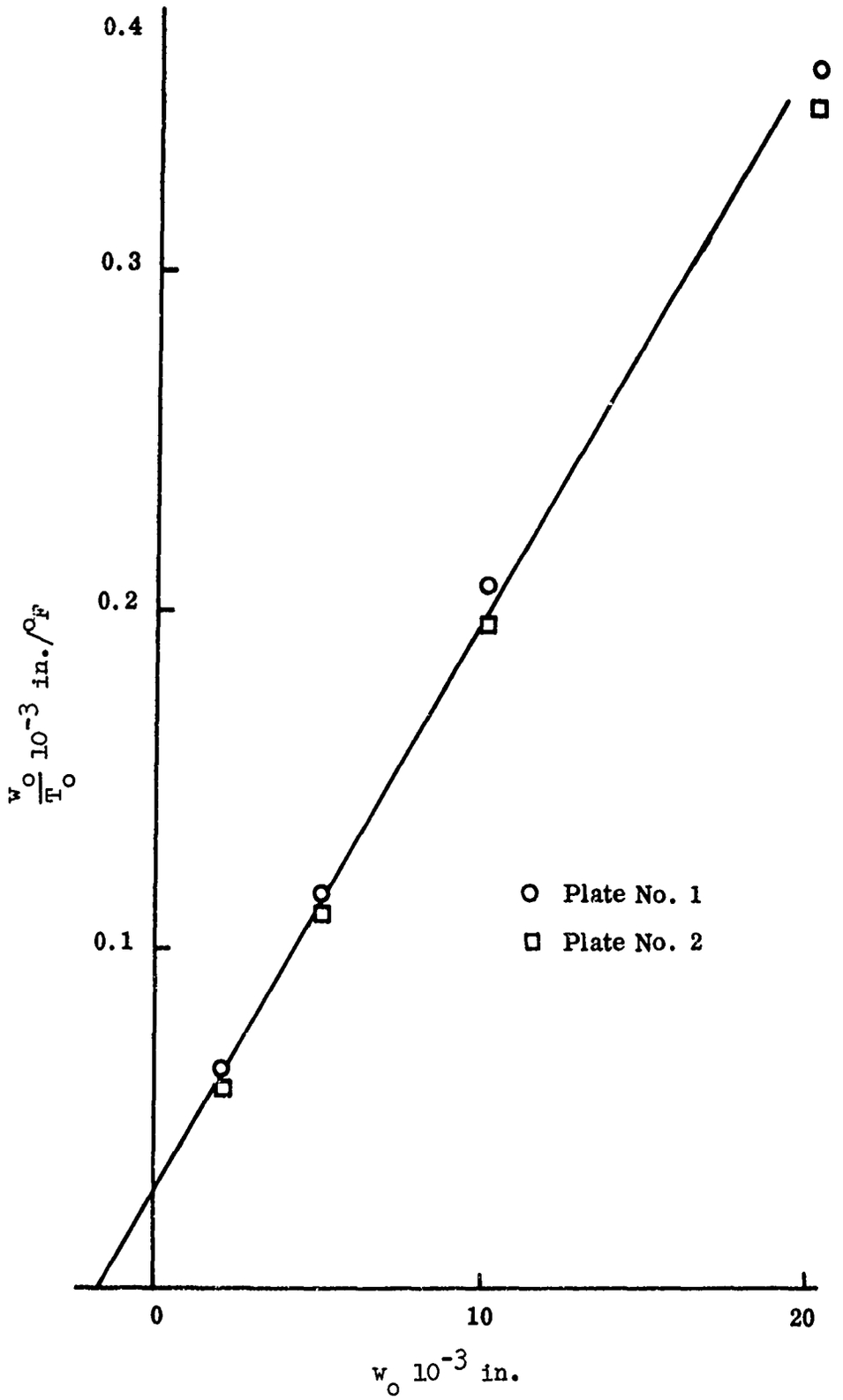

Figure 51. Southwell Plot of Data Given in Figure 50 From Reference 38.

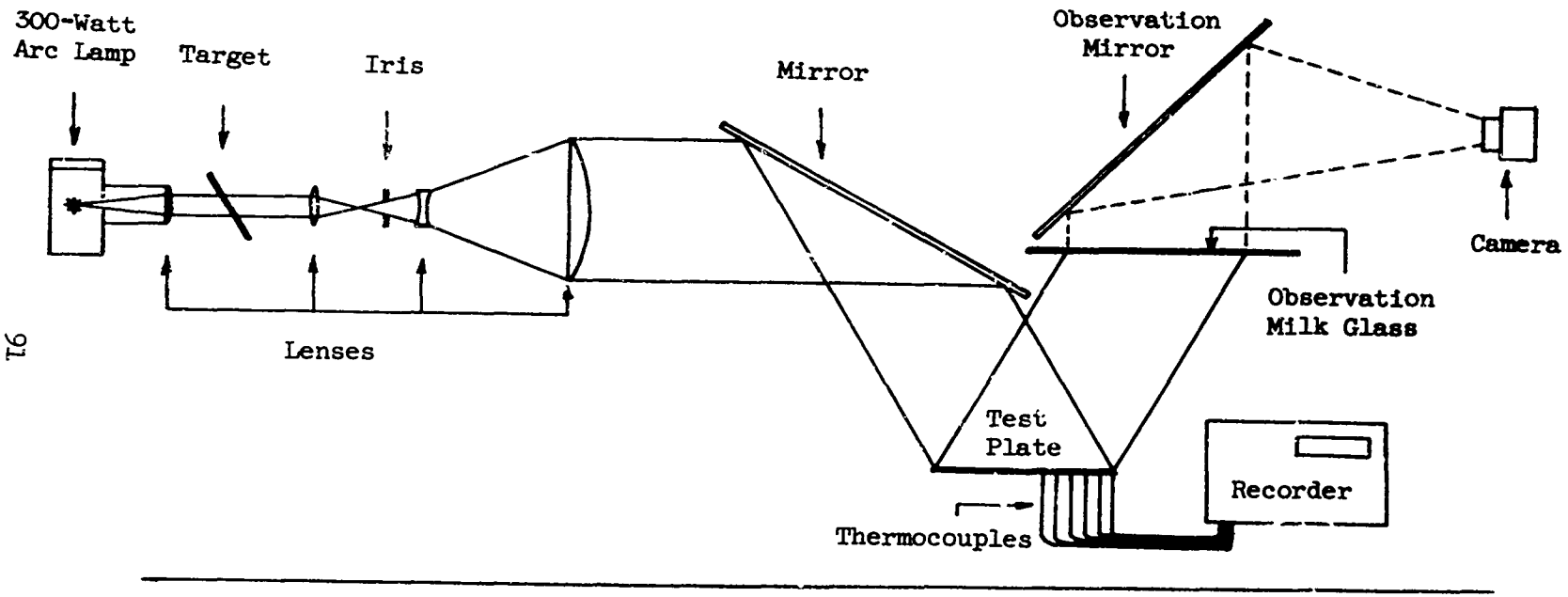

Figure 52. Schematic of Moiré Fringe Equipment From Reference 40.

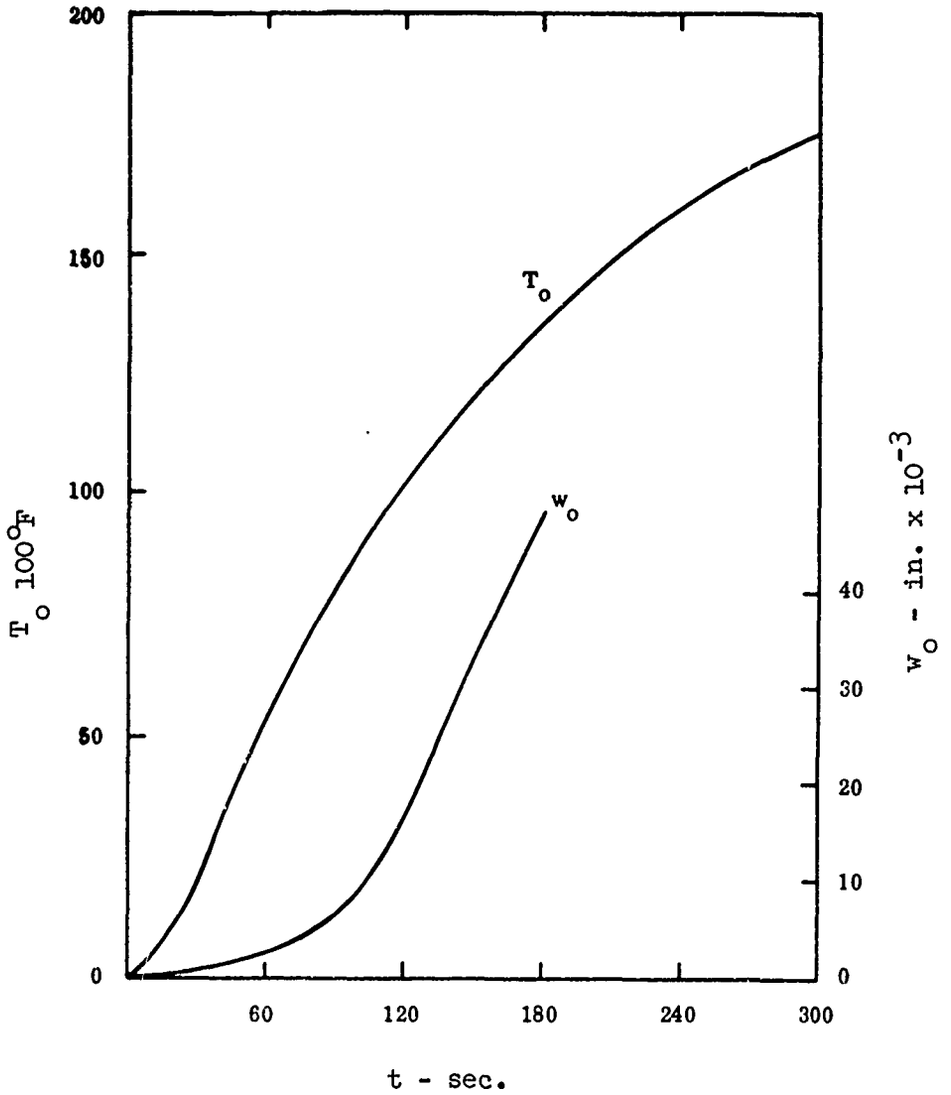

Figure 53. Central Edge Temperature and Central Edge Deflection vs Time for Test No. 1 From Reference 40.

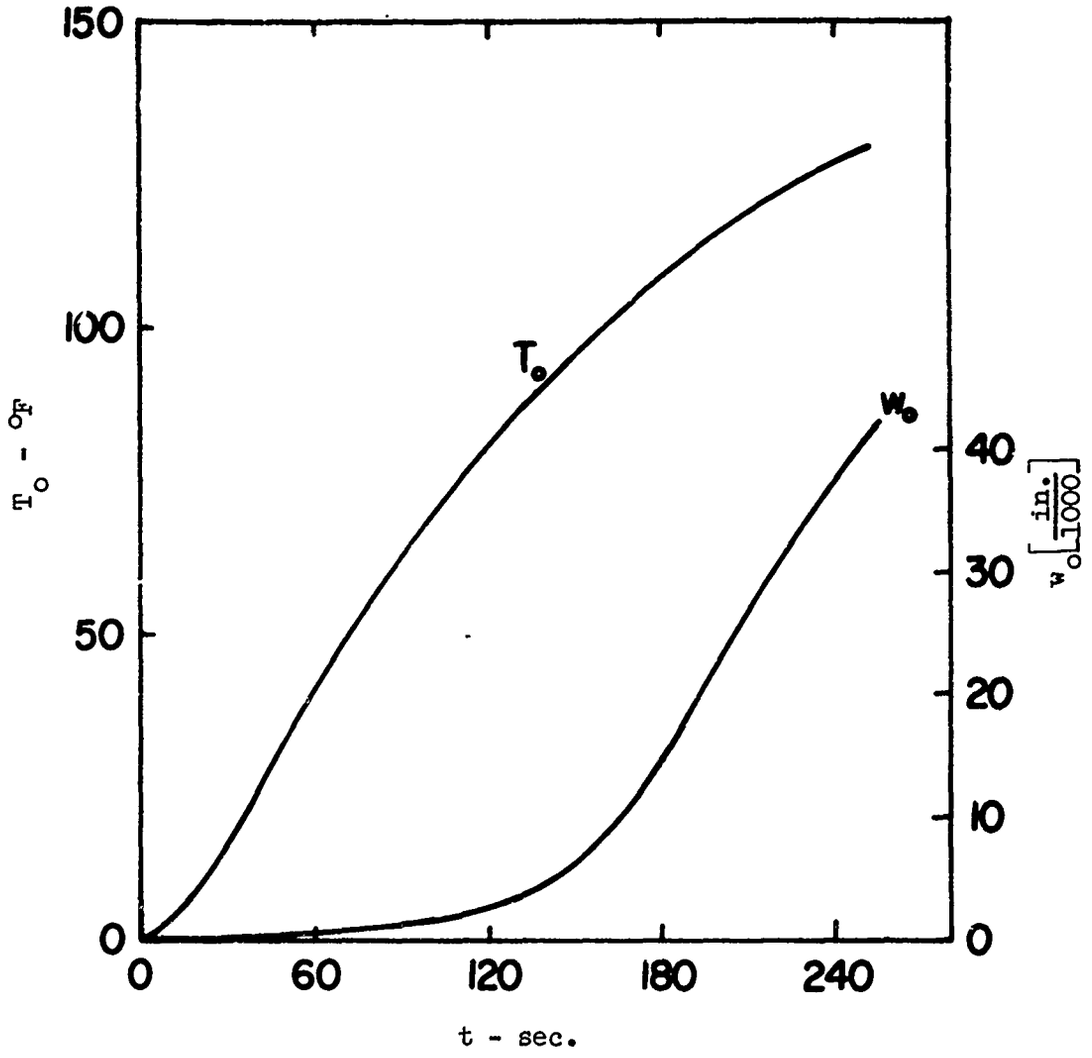

Figure 54. Central Edge Temperature and Central Edge Deflection vs Time for Test No. 2 From Reference 40.

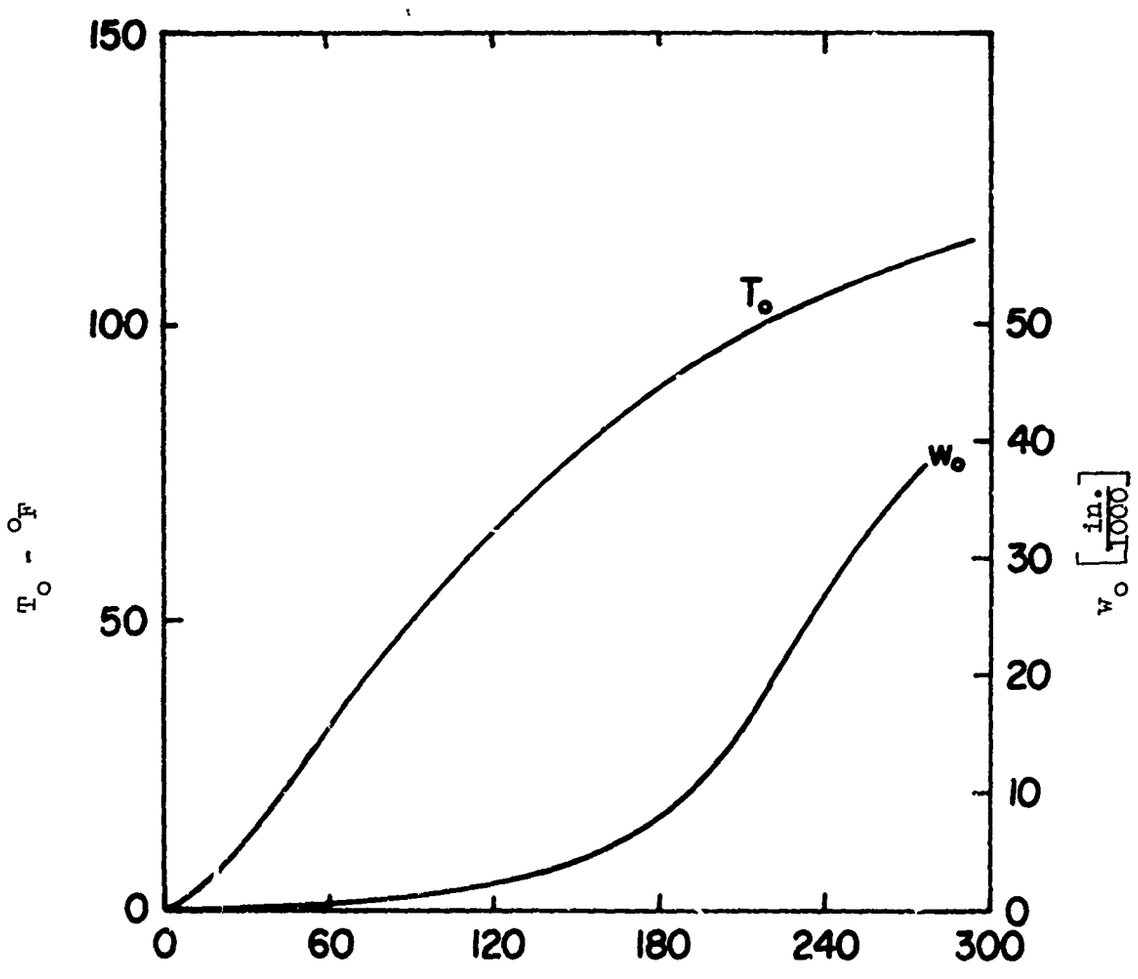

Figure 55. Central Edge Temperature and Central Edge Deflection vs Time for Test No. 3 From Reference 40.

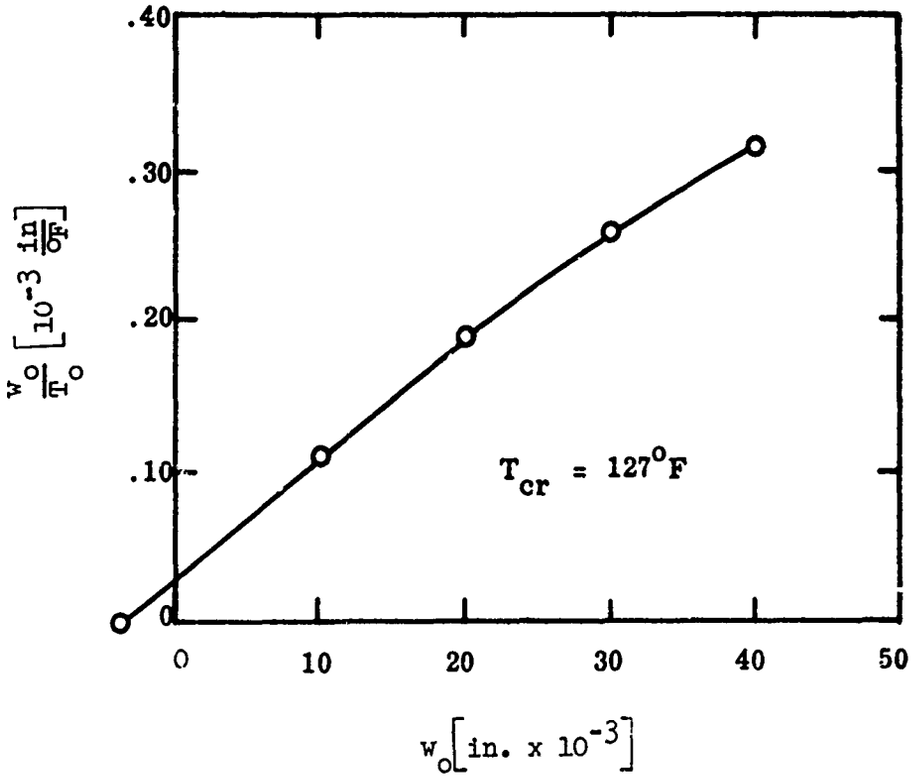

Figure 56. Southwell Plot for Test No. 1 From Reference 40.

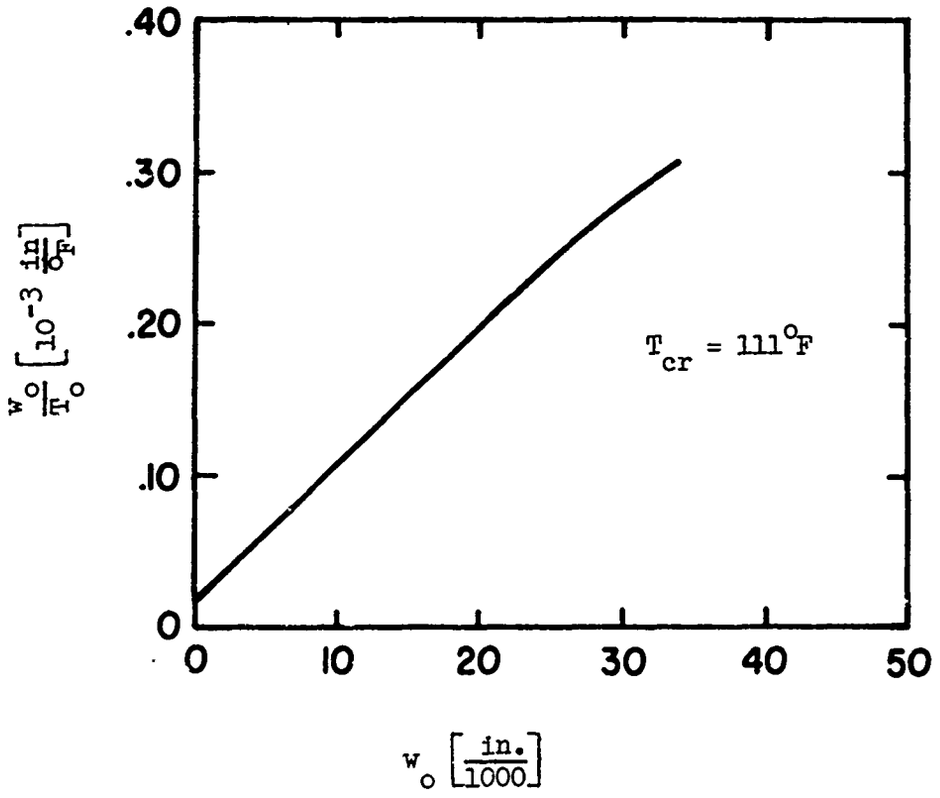

Figure 57. Southwell Plot for Test No. 2 From Reference 40.

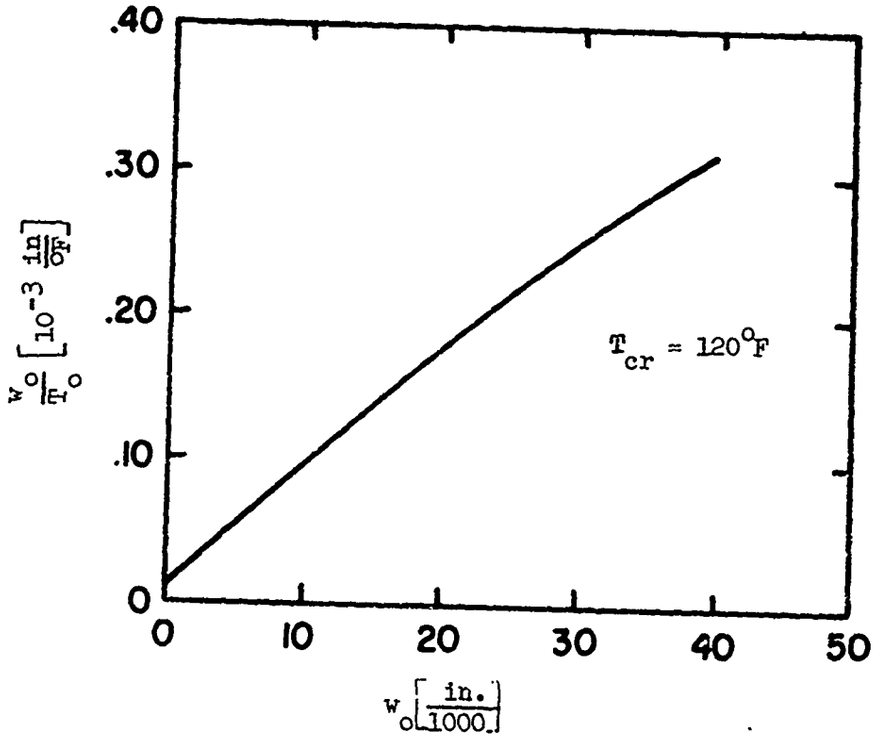

Figure 58. Southwell Plot for Test No. 3 From Reference 40.

$$(T_{crit})_3 = 111^\circ F$$

The comparative theoretical values were, respectively,

$$(T_{crit})_1 = 119.5^\circ F$$

$$(T_{crit})_2 = 111^\circ F$$

$$(T_{crit})_3 = 102^\circ F$$

The differences of these results were all within the order of accuracy predicted for the particular test equipment.

Once again the value of the Southwell plot for correlation of a theory has been shown. The accuracy of these results most certainly will be improved with the intended implementation of noncontacting measurement devices of high sensitivity and accuracy.

This general process for correlating experiment and theory can also be applied to the case of the lateral instability of the deep beam under the action of a concentrated force applied in the vertical plane. Such a beam when simply supported in two planes is shown in Figures 61 and 62. In this type of structure, where the t/h ratio is small, bending takes place in the plane of the greatest flexural rigidity, and lateral buckling may occur at a certain critical value of the applied load. Both bending and twisting must be considered.

The Rayleigh-Ritz method is applied to the total potential energy to determine the relationships between the load and both the elastic lateral deformation and the elastic torsional deformation for a deep beam with initial imperfections simply supported in two planes.

As the beam buckles laterally, the strain energies of lateral bending and twist about the longitudinal axis increase while, at the same time, a certain amount of work results from the movement of the point of application of the concentrated load. Assuming that the small change in the strain energy of bending in the plane of the beam during buckling is negligible, we find that the change in the strain energy due to the lateral buckling is

$$\Delta U = \frac{EI}{2} \int_0^1 \left[\frac{d^2w}{dx^2}\right]^2 \cdot dx + \frac{G\bar{J}}{2} \int_0^1 \left[\frac{d\varphi}{dx}\right]^2 \cdot dx \qquad (84)$$

Where

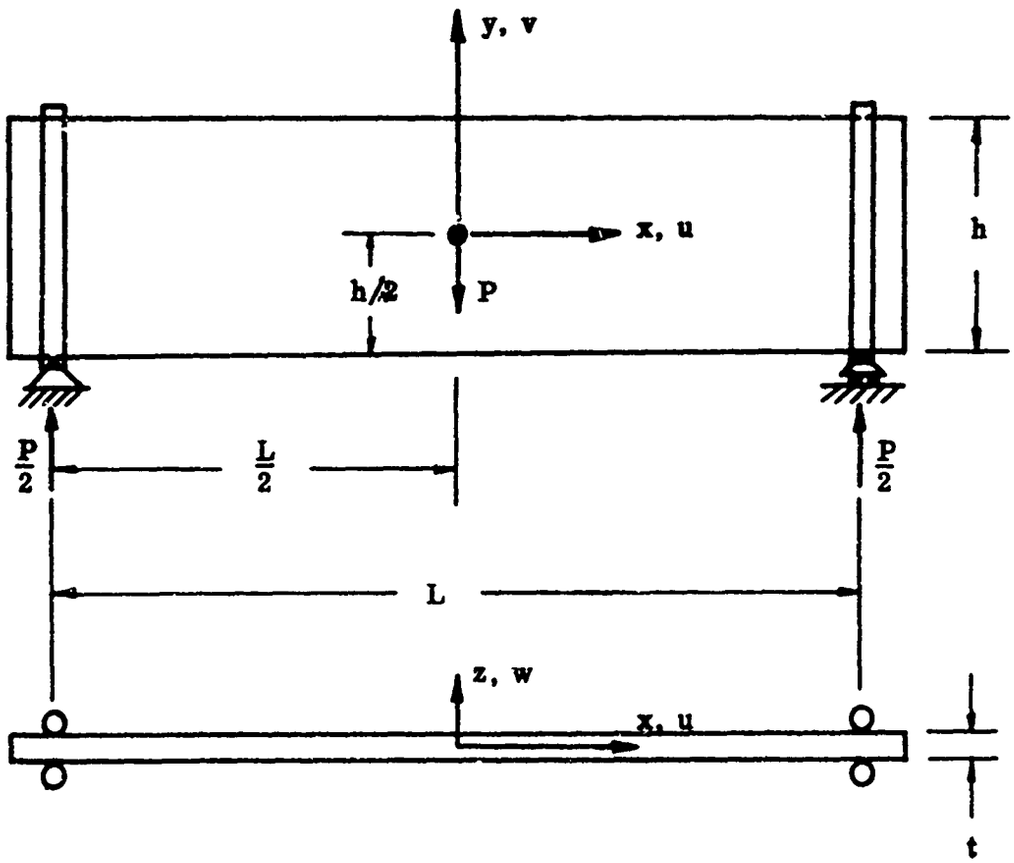

Coordinate axes are x, y, z

Respective displacement is u, v, w

Figure 59. Deep Beam Simply Supported in Two Planes With a Concentrated Load at the Centroid.

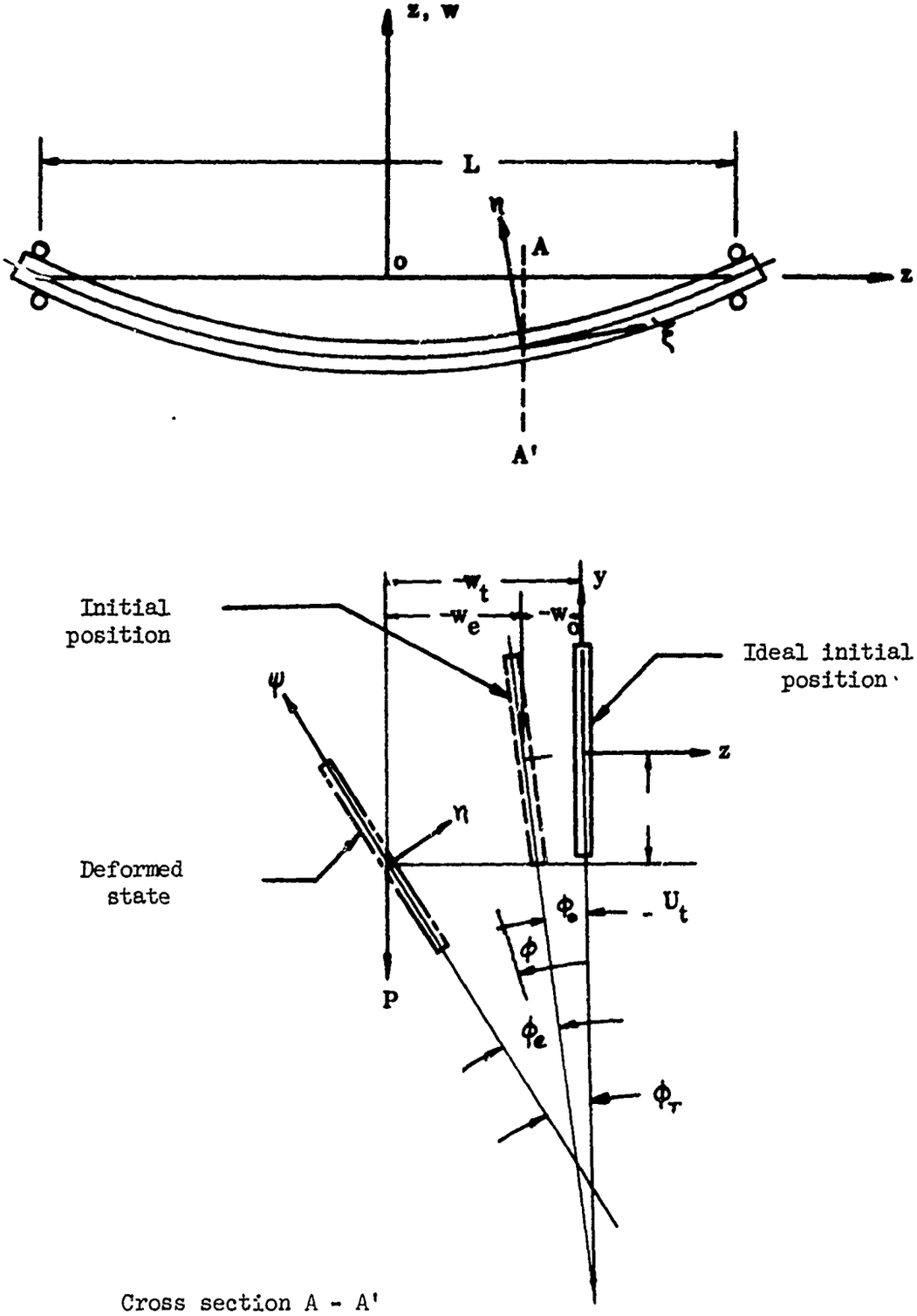

Figure 60. Deformed Elemental Cross Section of Deep Beam Simply Supported in Two Planes With a Concentrated Load at the Centroid.

E = the modulus of elasticity

G = the modulus of elasticity in shear ($G = \frac{E}{2(1+\mu)}$)

I = I_{ψ} = second moment about ψ axis

J = polar second moment

μ = Poisson's ratio

w = the lateral deflection

φ = the angle of rotation of the cross section.

When the symmetry of the buckled shape is considered, equation (84) may be written as

$$\Delta U = EI \int_0^{\frac{L}{2}} \left[\frac{d^2w}{dx^2}\right]^2 \cdot dx + GJ \int_0^{\frac{L}{2}} \left[\frac{d\varphi}{dx}\right]^2 \cdot dx \qquad (85)$$

Now the work done by the applied load during buckling is

$$\Delta W = P \int_0^{\frac{L}{2}} \varphi \cdot \left[\frac{d^2w}{dx^2}\right] \left(\frac{L}{2} - x\right) \cdot dx \qquad (86)$$

The term

$$\frac{d^2w}{dx^2}\left[\frac{L}{2} - x\right] \cdot dx$$

is the infinitely small arc described by the end of the beam with respect to the elemental cross section. It is caused by the bending of the element in the $\eta\xi$ plane. The vertical component of this arc when the angle of rotation, φ, is small is

$$\varphi \cdot \frac{d^2w}{dx^2}\left[\frac{L}{2} - x\right] \cdot dx$$

This, then, is the small distance through which the applied force moves. The total work done is one-half the summation across the beam of these elemental vertical components multiplied by the applied load. When symmetry of the deformed shape is assumed, this total work of buckling is as given in equation (86).

The total potential energy is

$$V = \Delta U - \Delta W$$

or

$$V = EI \int_o^{\frac{L}{2}} \left[\frac{d^2w}{dx^2}\right]^2 \cdot dx + GJ \int_o^{\frac{L}{2}} \left[\frac{d\varphi}{dx}\right]^2 \cdot dx$$

$$- P \int_o^{\frac{L}{2}} \varphi \left[\frac{d^2w}{dx^2}\right] \left(\frac{L}{2} - x\right) \cdot dx \qquad (87)$$

when small imperfections of both the twist and the lateral deflection are considered; the total deformations are the sum of the initial and elastic components

$$\left.\begin{aligned} w_t &= w_e + w_o \\ \varphi_t &= \varphi_e + \varphi_o \end{aligned}\right\} \qquad (88)$$

where

w_e = elastic lateral deflection

w_o = initial lateral deflection

φ_e = elastic angle of rotation

φ_o = initial angle of rotation.

Now equation (87) becomes

$$V = EI \int_o^{\frac{L}{2}} \left[\frac{d^2(w_t - w_o)}{dx^2}\right]^2 \cdot dx + GJ \int_o^{\frac{L}{2}} \left[\frac{d(\varphi_t - \varphi_o)}{dx}\right]^2 \cdot dx$$

$$- P \int_o^{\frac{L}{2}} \varphi_t \left[\frac{d^2(w_t - w_o)}{dx^2}\right] \left(\frac{L}{2} - x\right) \cdot dx \qquad (89)$$

For the simply supported case in question, the total deformations may be represented by

$$\varphi_t = \sum_{n=1}^{\infty} \alpha_n \cos \frac{n\pi x}{L}$$

$$w_t = \sum_{m=1}^{\infty} A_m \cos \frac{m\pi x}{L} \qquad (90)$$

and the initial imperfections may be chosen as

$$\varphi_o = \sum_{n=1}^{\infty} \beta_n \cos \frac{n\pi x}{L}$$

$$w_o = \sum_{m=1}^{\infty} B_m \cos \frac{m\pi x}{L} \tag{91}$$

It has been shown[20] that the resulting critical load is within 1.5 percent of the exact solution when only the first term of equation (90) is used. Therefore, this simplification is utilized here also. Moreover, the same simplification is applied to the initial deformations. These first terms of equations (90) and (91) are substituted into equation (89). This total potential must be minimized with respect to the unknown amplitudes of the total deflections. Then

$$\frac{\partial V}{\partial A_1} = 0 \text{ and } \frac{\partial V}{\partial \alpha_1} = 0$$

yield

$$P \left[B_1 - A_1 \right] = \frac{2GJ}{L} \cdot \left[\beta_1 - \alpha_1 \right] \cdot \frac{1}{K} \tag{92}$$

and

$$2EI \left[\frac{\pi}{L} \right]^2 \cdot \left[B_1 - A_1 \right] = PI\alpha_1 \cdot K \tag{93}$$

where

$$K = 0.351$$

This factor is the result of performing the prescribed integrations.

If the amplitudes of the elastic lateral deflection and of angle of elastic rotation are denoted by δ and Φ, respectively, and substitution for the total deformation amplitudes is made in equations (92) and (93), the following relationships are obtained:

$$P\ L\ K\ \delta = 2\ G\ J\ \Phi \tag{94}$$

$$2EI \left[\frac{\pi}{L} \right]^2 \cdot \delta - P\ L\ K\ (\Phi + \beta) = 0 \tag{95}$$

Equations (94) and (95) are algebraic relationships coupled in δ and Φ. If the expression for δ, as obtained from equation (94), is substituted into equation (95), it yields

$$\Phi\left[\frac{4EIGJ\pi^2}{P^2L^4K^2} - 1\right] = \beta \tag{96}$$

But

$$\sqrt{\frac{4\pi^2}{K^2}} \cdot \sqrt{\frac{EIGJ}{L^2}} = P_{cr} \tag{97}$$

and thus

$$\Phi\left[\frac{P_{cr}^2}{P^2} - 1\right] = \beta \tag{98}$$

It is not immediately apparent that this expression can be transposed into the Southwell form. However, if β is much less than Φ, so that powers of β/Φ greater than the first can be ignored, we may write

$$\frac{P_{cr}^2}{P^2} = 1 + \beta/\Phi \tag{99}$$

and so it follows that

$$\frac{P_{cr}}{P} - 1 = \beta/2\Phi \tag{100}$$

which is a relationship of the Southwell type.

A search of the literature did not reveal any existing experimental data on this subject. Thus, a special series of tests was made to check the process. The experimental setup less the displacement transducer is depicted in Figures 61 and 62. The deformation mode of the beam is clearly seen in this picture. The concentrated load was applied via a dowel and yoke system which is readily seen in the figure. The dimensions of the beam together with the deformations under load are given in Table XIV. The resulting Southwell Plot is given in Figure 63. The critical load deduced from this curve is 21.4 pounds and is in excellent agreement with the theoretical value of 22.1 pounds. Additional tests made with a small spring providing some side restraint, show that under these conditions there is an increase in buckling load just as was demonstrated by Hayashi and Kihira for the strut supported in the same manner. Full details of this test series are given in Reference 41.

The presentation so far has been concerned mainly with the use of the Southwell technique in interpreting data obtained from uniform x-section members tested as individual items. It must not be inferred, however, that the process is not applicable to structures fabricated from such elements. The first application to a member in a realistic structure appears to have been made by Lundquist[42]. In 1939 he analytically formulated a method for determining the critical loads for the displacement variable, normally the mid-

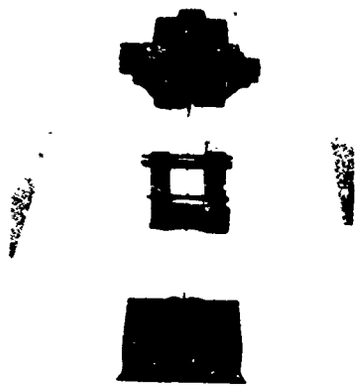

Figure 61. Beam Loaded Below Critical Load - Lateral Movement of Load Point Possible.

Figure 62. Buckling Mode - Lateral Movement of Load Point Possible.

TABLE XIV. LATERAL INSTABILITY OF DEEP BEAM (Ref. 41)

P lb	δ in.	δ/P
0.0	0.0	-
7.70	0.001	1.30×10^{-4}
12.17	0.006	4.93×10^{-4}
14.59	0.001	7.55×10^{-4}
15.85	0.016	9.47×10^{-4}
17.10	0.021	12.29×10^{-4}
17.85	0.026	14.58×10^{-4}
18.28	0.031	16.97×10^{-4}
18.70	0.036	19.25×10^{-4}
19.11	0.041	21.45×10^{-4}
19.32	0.046	23.80×10^{-4}
19.64	0.051	26.00×10^{-4}
19.79	0.056	28.30×10^{-4}
19.90	0.061	30.65×10^{-4}
20.05	0.066	32.92×10^{-4}
20.11	0.071	34.80×10^{-4}
20.25	0.076	37.50×10^{-4}
20.32	0.081	39.90×10^{-4}
20.42	0.086	42.10×10^{-4}
20.50	0.091	44.40×10^{-4}
20.55	0.096	46.80×10^{-4}
20.58	0.101	49.10×10^{-4}
20.60	0.106	51.50×10^{-4}
20.65	0.111	53.80×10^{-4}
20.67	0.116	56.20×10^{-4}
20.69	0.121	58.50×10^{-4}
20.71	0.126	60.90×10^{-4}
20.77	0.131	63.10×10^{-4}
20.79	0.137	66.00×10^{-4}
20.80	0.141	67.80×10^{-4}
20.81	0.151	72.50×10^{-4}
20.84	0.161	77.30×10^{-4}
20.89	0.171	81.90×10^{-4}
20.90	0.181	86.70×10^{-4}
20.92	0.191	91.40×10^{-4}
20.93	0.201	96.00×10^{-4}
20.93	0.211	100.9×10^{-4}
20.97	0.221	105.3×10^{-4}
20.99	0.231	110.0×10^{-4}
21.01	0.241	114.7×10^{-4}
21.02	0.261	124.0×10^{-4}

Beam Dimensions	Thickness	t = 0.059 in.
	Depth	d = 1.953 in.
	Length	L = 30.69 in.

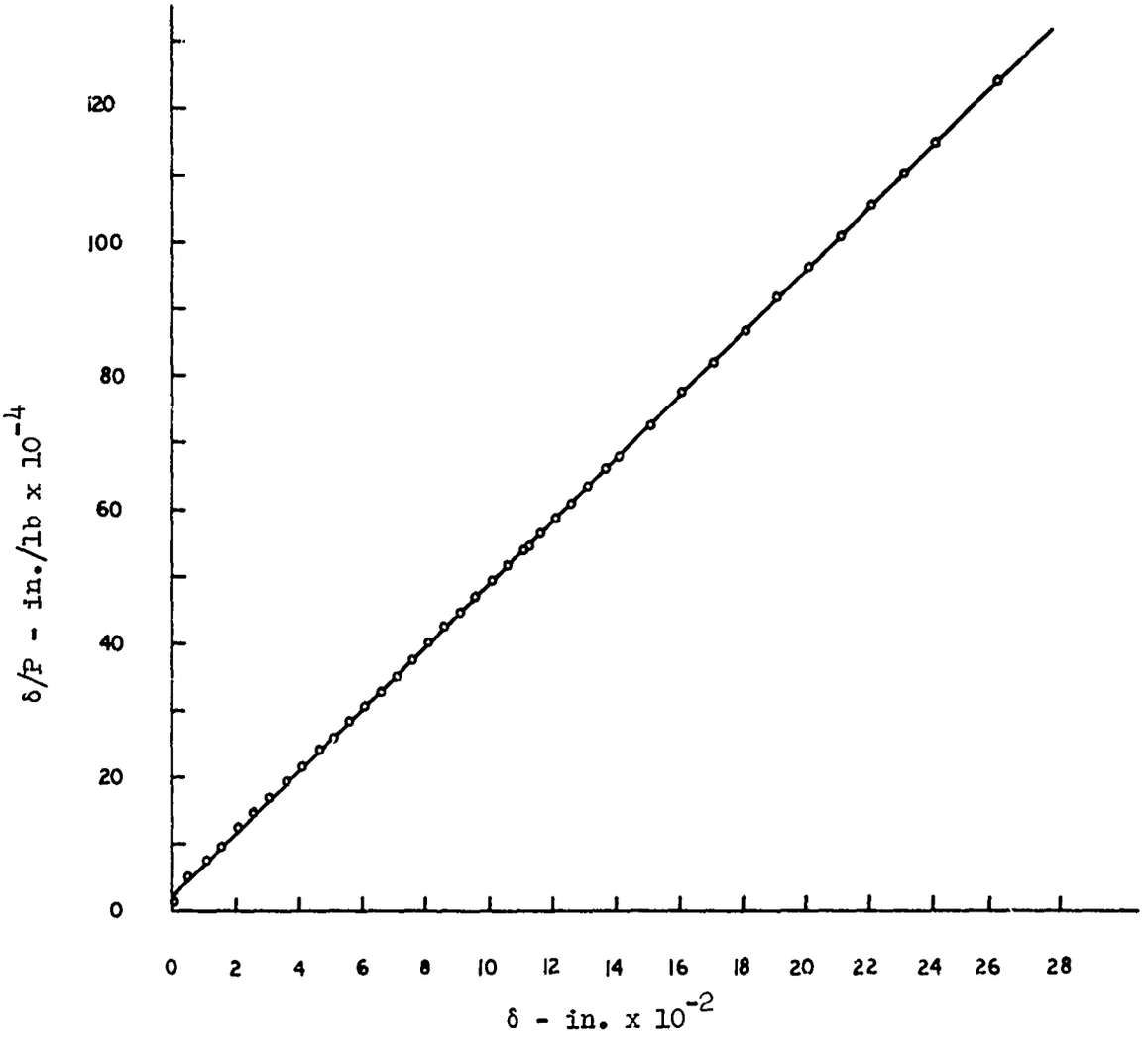

Figure 63. Southwell Plot From Test of Lateral Instability of Deep Beam From Reference 41.

point lateral deflection, used for the Southwell representation could equally well be chosen as the angle of end rotation. In 1960, Gregory[35,36] applied the technique to frame structures under torsion and bending. He was able to use the procedure to develop a design system for lattice girders liable to lateral buckling.[34] The routine followed was to load the member in question to a load value less than that required to precipitate instability and, from the load-displacement relationship thus established, to determine the effective initial imperfection and the theoretical critical moment. From these two experimentally established parameters, he then predicted the probable buckling moment for this real structure.

Ariaratnam[13] theoretically established the validity of the Southwell type linear relationship for struts having a variable flexural rigidity and various end conditions and for plane frameworks subjected to both flexural and torsional buckling. In 1963 Stevens and Schmidt[43] proposed a design scheme for frameworks. In this plan they combined the Southwell formulation with an iteration procedure. Thus, they were able to predict the critical loads in the compression components of the structure.

It is clear from the discussion already given that the key to the correlation of experiment and theory lies, in all cases, in the treatment of a slightly imperfect system. From this presentation it might be inferred that Ayrton and Perry were the first to realize that initial and elastic deformations of a strut could be associated with the Euler load and the actual load. This is not so. Admittedly, Euler himself appears to have given consideration to the initially straight column only. However, an awareness of the influence of initial curvature has existed since the beginning of the nineteenth century. Young,[44] in his course of Lectures on Natural Philosophy and the Mechanical Arts published in 1807, gave a theorem with regard to this question. This theorem, theorem 323 in his Magnum Opus, states:

"If a beam is naturally of the form which a prismatic beam would acquire, if it were slightly by a longitudinal force, calling its depth, b, its length, e, the circumference of a circle of which the diameter is unity, c, the weight of the modulus of elasticity, m, the natural deviation from rectilinear form, d, and a force applied at the extremities of the axis, f, the total deviation from the rectilinear form will be

$$A = \frac{bbccdm}{bbccm - 12eef}$$ "

If Young's equation is rewritten in present-day language, we obtain the formulation

$$w_t = \frac{w_o}{1 - \frac{P}{P_E}}$$

where

w_t = the total deflection

w_o = the initial deflection

P_E = Euler Load $\frac{EI^2}{L^2}$

P = axial load applied

This is identical with the Southwell formulation, equation (11), provided it is realized that in his time Young perpetrated Jacob Bernoulli's error in determining the expression for the second moment ("Moment of Inertia") for the cross-sectional area. Bernoulli had fixed this for a rectangular section as

$$\frac{bh^3}{3},$$

instead of the presently acceptable relationship of

$$\frac{bh^3}{12}.$$

There is little in the literature between 1807 and 1886 to indicate that engineers had taken note of Young's contribution, but it seems clear that many were aware of the lack of agreement between the Euler theory for a perfect body and reality. Smith,[45] a contemporary of Ayrton and Perry, was certainly cognizant of the importance of initial curvature and eccentric loading prior to 1886. He recognized, about this time too, that the load displacement curves for struts subjected to axial compression were hyperbolic. This is evidenced from a footnote to Ayrton and Perry's report[5] and also from Reference 45.

That the leaders in the field of engineering mechanics of this era recognized the problem and were acquainted with the mathematical relationship of equation (14) is clear from T. Claxton Fidler's text.[46] In this treatise of 1887 he wrote: "Let R denote the resilient force of the ideal column, equal to EI^2/L^2, and let Δ denote the initial deflection, and δ the elastic deflection, then

$$P = R \cdot \frac{\delta}{\Delta + \delta}$$

and

$$\delta = \Delta \cdot \frac{P}{R - P}" \qquad (101)$$

Claxton Fidler's equation (99) is identical to Southwell's equation (14). Therefore, the deflection will now have a certain assignable value depending on the load P; and if the load is gradually increased the column will exhibit an increasing deflection, or, in other words, it will always be in

a condition of stable equilibrium; and looking at formula (99) it is evident that when the load P is increased to within a little of the fixed quantity, R, the factor P/R - P will be a very large multiple, and a very small initial curvature (Δ) will then be sufficient to produce a comparatively large deflection of the column.

Without doubt, there were other derivations of this basic equation which we have not been able to trace, but few, if any, could be more general than that of Westergaard.[16] In 1922, this author made a very detailed study of the buckling of elastic structures. Where most previous and contemporary analyses dealt with buckling from the point of view of the differential equations of equilibrium, Westergaard's analysis was based upon the use of a generalized Lagrangian analysis. He made, of course, the usual assumptions with regard to linearity of stress-strain relationships and considered only deflections which were small. In this manner, he was able to show that the relationship was by no means restricted to the simple column. Unfortunately, like his predecessors, Fidler,[46] Smith,[45] and Young,[44] he did not recognize the potential of his formula for correlating theory and experiment. Neither, of course, did other engineers.

From analysis and by reference to tests made on virtually all practical cases of tubes, braced structures, and flat plates subjected to in-plane loadings, it has been established in this report that the simple Southwell[6] formula

$$\delta \left(\frac{P}{P_{cr}} - 1 \right) = \text{constant}$$

is absolutely general and is of great importance in interpreting experimental data in all these areas.

Its equal applicability in the area of shell structures is asserted. This question is discussed in another report.[29] The large displacement analysis briefly mentioned for flat plates under compression and for the circular disc with a central hot spot is also a method of wide generality and is discussed further in a paper to be published shortly.[47]

It is to be emphasized that the Southwell method calls for diligence in measurement of the displacements and for care in interpretation of the results. It can be a dangerous practice, for example, to use a least-squares-fit method in constructing the line.

REFERENCES

1. Euler, L.: METHODUS INVENIENDI LINEAS CURVAS MAXIMI MINIMIVE PROPRIETATE GAUDENTES, SIVE SOLUTIO PROBLEMATIS ISOPERIMETRICI LATISSIMO SENSU ACCEPTI, Additamentum 1, De curvis elasticis; Marcus-Michaelus Bousquet, p. 267, Lausanne and Geneva, 1744.

2. Hodgkinson, E.: EXPERIMENTAL RESEARCHES ON THE STRENGTH AND OTHER PROPERTIES OF CAST IRON, (Forming a second part to the 4th edition of Tredgold's "Practical Essay on the Strength of Cast Iron and other Metals"), Vol. II, 4th Ed., John Weale, London, 1842.

3. Euler, L.: SUR LA FORCE DES COLONNES, Mémoires de L'Académie de Berlin, XIII, 1759.

4. Poisson, M.: TRAITÉ DE MÉCHANIQUE, Vol. I, 2nd Ed., 1833.

5. Ayrton, W. E., and Perry, John: ON STRUTS, The Engineer, Vol. 62, December 10, 1886, pp. 464-465, and December 24, 1886, pp. 513-515.

6. Southwell, R. V.: ON THE ANALYSIS OF EXPERIMENTAL OBSERVATIONS IN PROBLEMS OF ELASTIC STABILITY, Proceedings of the Royal Society, A, Vol. 135, 1932, pp. 601-616.

7. Donnell, L. H.: ON THE APPLICATION OF SOUTHWELL'S METHOD FOR THE ANALYSIS OF BUCKLING TESTS, Stephen Timoshenko 60th Anniversary Volume, McGraw-Hill Book Company, 1938, pp. 27-38.

8. von Kármán, Theodore: UNTER SUGHUNGER UBER KNICK FEST IG KEIT, MITTEL UNGER UBER FORSCHUNGSARBEITEN AUF DEM GEBEITE DES INGENIEURWESENS, Vol. 81, 1960.

9. Lundquist, E. E.: GENERALIZED ANALYSIS OF EXPERIMENTAL OBSERVATIONS IN PROBLEMS OF ELASTIC STABILITY, NACA TN-658, 1938.

10. Fisher, H. R.: NOTE OF A METHOD OF REPRESENTING SPAR TESTS, A.R.C. Vol. II, R and M no. 1437, February 1933, p. 497.

11. Fisher, H. R.: AN EXTENSION OF SOUTHWELL'S METHOD OF ANALYZING EXPERIMENTAL OBSERVATIONS IN PROBLEMS OF ELASTIC STABILITY, Proceedings of the Royal Society, A, Vol. 144, 1934, pp. 609-630.

12. Hayashi, T., and Kihira, M.: ON A METHOD OF EXPERIMENTAL DETERMINATION OF THE BUCKLING LOAD OF AN ELASTICALLY SUPPORTED COLUMN, Paper presented at Japan Congress on Testing Materials, Kyoto, Japan, September 1966.

13. Ariaratnam, S. T.: THE SOUTHWELL METHOD FOR PREDICTING CRITICAL LOADS OF ELASTIC STRUCTURES, The Quarterly Journal of Mechanics and Applied Mathematics, Vol. XIV, 1961, pp. 137-153.

14. Hill, H. N.: NOTE ON THE ANALYTICAL TREATMENT OF LATERAL DEFLECTION MEASUREMENTS FROM TESTS INVOLVING STABILITY PROBLEMS, Unpublished Alcoa Report.

15. Tuckerman, L. B.: HETEROSTATIC LOADING AND CRITICAL ASTATIC LOADS, National Bureau of Standards Research Paper RP 1163, Journal of Research NBS, Vol. 22, January 1939, pp. 1-18.

16. Westergaard, H. M.: BUCKLING OF ELASTIC STRUCTURES, Transactions of the American Society of Civil Engineers, Vol. 85, 1922, pp. 576-654.

17. Bridget, F. J., Jerome, C. C., and Vosseller, A. B.: SOME NEW EXPERIMENTS ON THE BUCKLING OF THIN WALL CONSTRUCTION, Transactions of the American Society of Mechanical Engineers, Vol. 56, 1934.

18. Gough, H. J., and Cox, H. L.: SOME TESTS ON THE STABILITY OF THIN STRIP MATERIAL UNDER SHEARING FORCES, Proceedings of the Royal Society, A, Vol. 137, 1932, pp. 145-157.

19. Southwell, R. V., and Skan, Sylvia W.: ON THE STABILITY UNDER SHEARING FORCES OF A FLAT ELASTIC STRIP, Proceedings of the Royal Society, A, Vol. 105, 1924, p. 582.

20. Timoshenko, S. P., and Gere, J. M.: THEORY OF ELASTIC STABILITY, 2nd Ed., McGraw-Hill Book Co., 1961.

21. Donnell, L. H.: A NEW THEORY FOR THE BUCKLING OF THIN CYLINDERS UNDER AXIAL COMPRESSION AND BENDING, Transactions of the American Society of Mechanical Engineers, Vol. 56, AER-56-12, November 1934, pp. 795-806.

22. von Kármán, Theodore: ENCLYKLOPEADIE DER MATHEMATISCHEN WISSENSCHAFTEN, IV, ART. 27, 1910, p. 349.

23. Yoshiki, M.: A NEW METHOD OF DETERMINING THE CRITICAL BUCKLING POINTS OF RECTANGULAR PLATES IN COMPRESSION, Journal of the Society of Applied Mechanics of Japan, Vol. 3, No. 1, 1947.

24. Yoshiki, M., Fujita, Y., and Yoshida, K.: PLASTIC DESIGN IN STEEL STRUCTURES (6th Report) - COMPRESSIVE STRENGTH OF STRUCTURAL ELEMENTS IN PLASTIC RANGE, Journal of the Society of Naval Architecture of Japan, No. 118, July 1965.

25. Yoshiki, M., and Fujita, Y.: A NEW METHOD TO DETERMINE THE PLASTIC BUCKLING LOAD OF AXIALLY COMPRESSED PLATE FROM EXPERIMENTAL DATA, American Society for Testing and Materials, 69th Annual Meeting, Paper No. 210, 1966.

26. Coan, J. M.: LARGE DEFLECTION THEORY FOR PLATES WITH SMALL INITIAL CURVATURE LOADED IN EDGE COMPRESSION, Journal of Applied Mechanics, June 1951, pp. 143-151.

27. Hoff, N. J., Bolay, B. A., and Coan, J. M.: THE DEVELOPMENT OF A TECHNIQUE FOR TESTING STIFF PANELS IN EDGEWISE COMPRESSION, Proceedings of the Society for Experimental Stress Analysis, Vol. V, No. II, pp. 14-24.

28. Loo, T. C., and Evan-Iwanowski, R. M.: DEFORMATIONS AND COLLAPSE OF SPHERICAL DOMES SUBJECTED TO UNIFORM PRESSURE AND NORMAL CONCENTRATED LOADS AT THE APEX, Proceedings of the World Conference on Shell Structures, San Francisco, 1962.

29. Horton, W. H., and Cundari, F. L.: ON THE APPLICABILITY OF THE SOUTHWELL PLOT TO THE INTERPRETATION OF TEST DATA OBTAINED FROM INSTABILITY STUDIES OF SHELL BODIES, SUDAAR No. 290, Department of Aeronautics and Astronautics, Stanford University, August 1966.

30. Turner, M. J., Martin, H. C., and Weikel, R. C.: FURTHER DEVELOPMENT OF THE STIFFNESS METHOD, AGARD Structures and Materiel Panel, Paris, France, July 1962, Agardograph 72, New York, Pergamon Press, The MacMillan Co., 1964.

31. Martin, H. C.: LARGE DEFLECTION AND STABILITY ANALYSIS BY THE DIRECT STIFFNESS METHOD, NASA-JPL Technical Report no. 32-931, August 1, 1966, in which reference is made to the possible application of the Southwell plot to square panels under biaxial load.

32. Walker, A. C.: LOCAL INSTABILITY IN PLATES AND CHANNEL STRUTS, Journal of the Structural Division, Proceedings of the American Society of Civil Engineers, Vol. 92, No. ST 3, June 1966, pp. 38-55.

33. Ramberg, W., McPherson, A. E., and Levy, S.: EXPERIMENTAL STUDY OF DEFORMATION AND OF EFFECTIVE WIDTH IN AXIALLY LOADED SHEET-STRINGER PANELS, NACA Technical Note 684, February 1939.

34. Gregory, M. S.: THE USE OF MEASURED STRAINS TO OBTAIN THE CRITICAL LOAD OF A STRUT, Civil Engineering and Public Works Review, London, Vol. 55, No. 642, January 1960, pp. 80-82.

35. Gregory, M. S.: THE USE OF THE SOUTHWELL PLOT ON STRAINS TO DETERMINE THE FAILURE LOAD OF A LATTICE GIRDER WHEN LATERAL BUCKLING OCCUR, Australian Journal of Applied Science, Vol. 10, No. 4, December 1959, pp. 371-376.

36. Gregory, M. S.: THE BUCKLING OF AN EQUILATERAL TRIANGULAR FRAME IN ITS PLANE, Australian Journal of Applied Science, Vol. 10, No. 4, December 1959, pp. 367-387.

37. Gregory, M. S.: THE APPLICATION OF THE SOUTHWELL PLOT ON STRAINS TO PROBLEMS OF ELASTIC INSTABILITY OF FRAMED STRUCTURES, WHERE BUCKLING OF MEMBERS IN TORSION AND FLEXURE OCCURS, Australian Journal of Applied Science, Vol. II, No. 1, March 1960, pp. 49-64.

38. Queinec, A.: THERMAL BUCKLING OF CENTRALLY HEATED CIRCULAR PLATES, SUDAER No. 106, Department of Aeronautics and Astronautics, Stanford University, June 1961.

39. Timoshenko, S., and Goodier, J. N.: THEORY OF ELASTICITY, 2nd Ed., McGraw-Hill Book Co., 1951.

40. Fernandez-Sintes, J., Horton, W. H., and Hoff, N. J.: THERMAL BUCKLING OF ANNULAR PLATES, SUDAER No. 143, Department of Aeronautics and Astronautics, Stanford University, December 1962.

41. Way, E.: AN EXPERIMENTAL STUDY OF THE INSTABILITY OF DEEP BEAMS, Engineer's Thesis, under preparation.

42. Lundquist, E. E.: A METHOD OF ESTIMATING THE CRITICAL BUCKLING LOAD FOR STRUCTURAL MEMBERS, NACA Technical Note 717, July 1939.

43. Stevens, L. K., and Schmidt, L. C.: DETERMINATION OF ELASTIC CRITICAL LOADS, Journal of the Structural Division, Proceedings of the American Society of Civil Engineers, Vol. 89, No. ST 6, Part 1, December 1963, pp. 137-158.

44. Young, T.: A COURSE OF LECTURES ON NATURAL PHILOSOPHY AND THE MECHANICAL ARTS, Vol. II, 1st Ed., Sect. IX, London, 1807, p. 47.

45. Smith, R. H., Wheatley, and Wood: STIFFNESS OF STRUTS, The Engineer, Vol. LXV, January 6, 1888, p. 1.

46. Fidler, T. C.: A PRACTICAL TREATISE ON BRIDGE CONSTRUCTION, 1st Ed., London, 1887.

47. Horton, W. H., Tenerelli, D., and Willey, B. A.: A COMPARISON OF SMALL AND LARGE DISPLACEMENT METHODS.